University of the Witwatersrand, Johannesburg

MASTER'S DISSERTATION


# Investigating the Effects of Altitude (Air Density) on the HVDC Breakdown Voltage of Small Rod-Plane Air Gaps

*Author:* Tatenda Gora

A dissertation submitted to the Faculty of Engineering and the Built Environment, University of the Witwatersrand, in fulfilment of the requirements for the degree of Master of Science in Engineering.

Johannesburg, 2016

# DECLARATION

I declare that this dissertation is my own unaided work. It is being submitted for a Degree of Master of Science to the University of the Witwatersrand, Johannesburg. It has not previously been submitted for any degree or examination to any other university.

**Signature:**

# ABSTRACT

The validity of the atmospheric correction method presented in the IEC 60060-1 (2010) standard is analysed and evaluated by means of theoretical and laboratory work. In order to understand the problem, the evolution of the atmospheric correction methods, from as early as 1914, has been presented. A procedure (Calva prediction method) for predicting the direct current (DC) breakdown voltage for an air gap at any altitude was discovered and was also analysed along with the IEC 60060-1 (2010). A critique of some of the atmospheric correction methods commonly used standards was also done. Experiments were carried out at altitudes of 1 740 m (Wits University), 130 m (UKZN HVDC centre) and at less than 2 m above sea level (Scottburgh beach, Clansthal). More tests were conducted using a pressure vessel where high altitude relative air density was simulated. All tests were conducted on rod-plane air gaps using a 15 mm diameter flat tip rod. Test results from Scottburgh beach were used as the standard breakdown voltages of the air gaps tested since the environmental conditions were the closest to the conventional standard conditions (stp). The test results obtained were compared with predictions using the Calva method in order to validate the method. The test results were also corrected according to IEC 60060-1 (2010) and compared to the standard breakdown voltages obtained at Scottburgh beach. It was shown that the IEC 60060-1 (2010) is quite suitable for atmospheric correction for data obtained at low altitudes (about 130 m). When applied to high altitude (1 740 m) data, the correction method is accurate and suitable for very small air gaps less than 0.1 m. As the air gap length increased, the corrected results began to deviate from the expected standard voltage. The same trend was shown with the corrected results from the pressure chamber tests. The prediction method by Calva was accurate when compared to the experimental data from the high altitude and low altitude test results. When compared to the data from the pressure chamber, the prediction method had a linear error factor which was different for each gap length. It was concluded that the IEC 60060-1 (2010) is not only unsuitable for atmospheric correction for data at relative air densities below 0.8, but also that the correction method is prone to an increase in error as the air gap length increases when the relative air density is higher than 0.8. The Calva prediction method was found to be suitable to use after additional factors are added when applied to high altitude conditions.

# ACKNOWLEDGEMENTS

The author would like to acknowledge with gratitude the mentorship and aid provided by professor Cuthbert Nyamupangedengu, professor Ian Jandrell and Mr. Nishanth Parus. The author would also like to sincerely acknowledge the ISH2009-SAIEE Postgraduate Research Scholarship in High Voltage Engineering for directly funding the research. Gratitude is also extended to Dr. Andrew Swanson and the UKZN HVDC centre for providing some equipment and their laboratory for experimental work. Gratitude is given to Eskom for their support of the High Voltage Engineering Research Group at Wits University through TESP. The author would also like to express gratitude to the Department of Trade and Industry (DTI) for THRIP funding and to thank the National Research Foundation (NRF) for direct funding of the research group.

# Contents

# List of Figures

# List of Tables

# Abbreviations

| | |
|---|---|
| **asl** | **A**bove **S**ea **L**evel |
| **Cigré** | International Council on Large Electric Systems |
| **DC** | **D**irect **C**urrent |
| **HVDC** | **H**igh **V**oltage **D**irect **C**urrent |
| **IEC** | **I**nternational **E**lectrotechnical **C**ommission |
| **RAD** | **R**elative **A**ir **D**ensity |
| **WG** | **W**orking **G**roup |

# Chapter 1

# Introduction

The development of high voltage power system schemes has significantly improved with higher voltage levels being used and longer distances being covered by the transmission lines. As these longer distances are achieved, high voltage direct current (HVDC) becomes more and more favourable and necessary given that load centres are located further away from the source [1]. As the transmission lines traverse to the load centres, they pass through different altitudes. This has major implications on the insulation coordination of the line as is evidenced in countries like South Africa where the altitude varies from sea level to approximately 3 450 m (peaks along the Drakensburg range) [2]. By so doing, much attention is required on the selection of appropriate insulators and air gap clearances for the transmission lines.

It is already known that changes in environmental conditions (temperature, humidity and air pressure) affect the dielectric strength of an air gap, and these conditions change with altitude. Standards have been put in place to facilitate the correction of voltages to standard conditions (20°C temperature, 11 g/m$^3$ humidity and 1013 mbar pressure). This helps in the standardisation of equipment and derivation of rating/de-rating factors to be applied to the equipment and calculation of clearances for high voltage structures if used at different altitudes.

The standardisation procedure used for voltage correction however does not apply to data obtained at altitudes above 2 000 m, especially for DC voltages [3]. This problem has led to the International Council on Large Electric Systems (Cigré) creating a study

Working Group (WG D1.50) to develop new methods for altitude correction for air gaps and equipment for installation at altitudes above 6 000 m above sea level (asl).

In combating the same problem, China has set up an HVDC research facility in Tibet, at an approximate altitude of 4 400 m. It is at this facility that most of the high altitude data for the Cigré WG D1.50 is obtained. In South Africa, possibilities of increased HVDC transmission are a reality. Plans have also been put in place for the country to draw power from the Congo and this will also require the use of HVDC transmission for it to be feasible [1]. In order to develop the HVDC transmission schemes within South Africa, a lot of research is being carried out as the initial step towards these developments. Among some of the research topics proposed in their initiative towards strategic research into HVDC transmission, Eskom proposed that research be conducted on the insulation strengths of basic air gaps in the altitude range of 1 200 m to 1 600 m ~[4]. Some work has been done in South Africa under the proposed strategic research [5].

This dissertation presents the investigation carried out on the effects of altitude (specifically relative air density) on the HVDC breakdown of small rod-plane air gaps. The research details explanations of the observations noted during the experimental work along with a critical analysis of the existing correction methods.

The structure of this dissertation is as follows:

- **Chapter 2** presents the evolution of the atmospheric correction methods. This chapter goes through the history of and the research taken to develop atmospheric correction procedures.
- **Chapter 3** is a theoretical section on the mechanisms of the breakdown processes of an air gap.
- **Chapter 4** describes the experimental set up in the laboratory and the procedure followed.
- **Chapter 5** presents the results obtained and a discussion and analysis of the results.
- **Chapter 6** concludes the dissertation and presents recommendations for future work.

- **Appendix A** contains the tables of all the experimental test data.
- **Appendix B** is a copy of a discussion paper presented at the SAUPEC 2015 by the author. The paper constitutes a significant part of **Chapter 2.**
- **Appendix C** is a copy of a paper published in the proceedings of the International Symposium on High Voltage Engineering (ISH) in 2015. Part of the findings highlighted in this paper are portions of **Chapter 5**.
- **Appendix D** is a report submitted as a contribution to the Cigré WG D1.50 task force on short air gaps.

# Chapter 2

# Historical evolution of Altitude Correction Methods

---

*Opening Summary*

---

Work to create a way of correcting voltages for insulators began as far back as 1914 when Peek investigated altitude effects on flashover voltages of insulators [6]. Ever since, a lot of work has been done to develop a standard procedure of atmospheric correction. This chapter looks at the evolution of knowledge in the creation of the commonly used IEC 60060-1(2010) and also critically analyses how atmospheric correction is done in the commonly used international standards. The knowledge gaps are identified and the research questions of the present work are developed. A summary of the development of the IEC 60060-1 standard is given in Figure 2.1. Further work has been done after the development of the IEC 60060-1 standard and the work is also highlighted in this chapter.

## 2.1 Peek Model

The effect of altitude on the breakdown voltage of insulators was noted as early as 1914 by Peek [6]. A significant amount of research has been done since then with regard to air density effects on the breakdown voltage of air gaps and external insulation, and

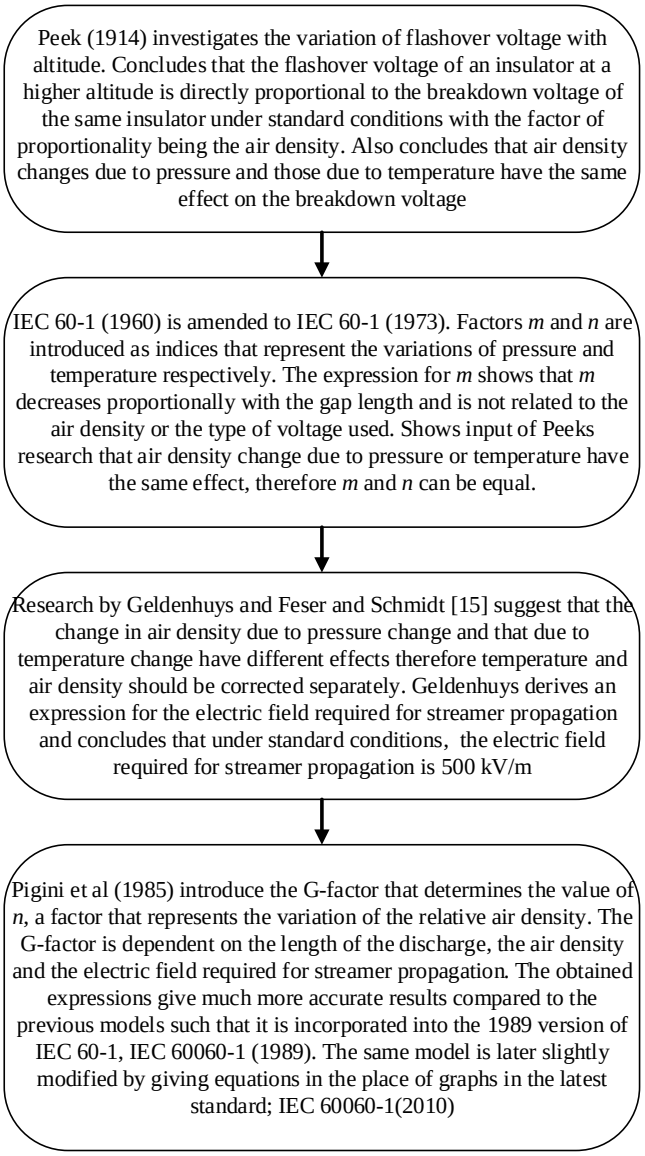


FIGURE 2.1: Summary of the development of altitude correction methods in IEC 60060-1(2010)

more recently air gaps under DC voltage stress [5, 7–12]. Peek [6] investigated the effect of altitude on the spark-over voltages of bushings and insulators by placing them in a wooden cask and conducting breakdown tests under variable pressure. Pressure was varied to obtain relative air densities between 0.5 and 1.0 while the temperature variations due to the pressure changes were recorded. In his research, Peek [6] was able to produce tables of correction factors to be used on specific insulators by reading off the relative air density. From the obtained results, the correction factors for insulators were different from those of bushings and leads under the same relative air density [6]. Peek attributed these to the uniformity of the field suggesting that the flashover voltage for a

uniform field decreases directly with relative air density (RAD), whereas for non-uniform fields, the flashover voltage decreases at a smaller rate than the RAD [6]. Peek therefore concluded that, given that the flashover voltage of an insulator at sea level ($\delta$=1) is $v_1$, then the breakdown voltage $v$ at $\delta$=$x$ was given by

$$v = xv_1 \tag{2.1}$$

where $\delta$ is the relative air density at a specific altitude and read from the tables derived from empirical test results by Peek [6].

Peek's method for atmospheric correction did not incorporate vital factors to be considered when it comes to the breakdown of air gaps. The method did not include factors like the length of the discharge path and the variation of the electric field under different environmental conditions and different voltage types. Therefore, this method was not robust enough to be used as the standard atmospheric correction procedure.

## 2.2 IEC 60-1 (1973)

In 1973, the existing altitude correction standard then, IEC 60-1, was amended such that the breakdown voltage of an air gap or insulator at relative air density $\delta$, $u_\delta$ is related to the breakdown voltage of the same air gap or insulator under standard conditions, $u_0$ by [13]

$$u_\delta = \frac{k_d}{k_h} u_0 \tag{2.2}$$

where $k_d$ is the air density correction factor defined as

$$k_d = (\frac{P}{P_0})^m (\frac{T_0}{T})^n \tag{2.3}$$

and $k_h$ is the humidity correction factor defined as

$$k_h = k^w \tag{2.4}$$

In equation 2.3, $P$ and $P_0$ are the pressure and standard pressure, in mbar, respectively while $T$ and $T_0$ are the temperature and standard temperature, in °C, respectively. In equation 2.4, $k$ is the humidity correction factor given in a graph as a function of

absolute humidity and $w$ is an exponent that defines the humidity factor depending on the test type voltage and electrode arrangement [14].

The exponents $m$ and $n$ are the variations of pressure and temperature respectively that are supposed to be determined before $k_d$ is evaluated. Since the air density is dependent on pressure, the determination of the exponent $m$ became the area of concern regarding atmospheric corrections. The exponent $m$ was defined in IEC 60-1 (1973) as

$$m = \begin{cases} 1.0 & \text{for } d \leq 1, \\ -0.12d + 1.12 & \text{for } 1<d<6, \\ 0.4 & \text{for } d \geq 6. \end{cases} \tag{2.5}$$

where $d$ is the air gap length. The factor $m$ in this standard implied that pressure variation was linearly dependent on the length of the air gap. Compared to the model proposed by Peek, the model in the IEC 60-1 does not give a linear relationship between the flashover voltage and the relative air density. However, the standard suggests that the effect of pressure varies at a quicker rate with the increase in gap length. For short gaps (less than 1 m long) and large gaps (above 6 m), $m$ is considered constant and the gap sizes between 1 m and 6 m are where linearity was observed for $m$. For all voltage types of either polarity, the standard specifies that $m$ and $n$ can be considered equal despite the geometry of the electrodes. Some of the electrode geometries for some voltage types have the exponents $m$ and $n$ set to a value of 1.0 while other geometries refer to equation 2.5. Some geometries did not have enough data when the standard was put together, therefore $m$ and $n$ were set as 0. Three electrode geometries (sphere-sphere, rod-rod and rod-plane) were used in the standard. If any electrode geometry besides the three geometries mentioned earlier was used, $m$ and $n$ were set to 1.0 and there was no humidity correction to be applied.

The evaluation of $m$, $n$, $w$ and the restriction of the correction method to specific electrode arrangements made the standard undergo revision and new correction methods were to be introduced. This led to the development of the IEC 60060-1(1989) discussed in the next section.

## 2.3 IEC 60060-1:1989(Pigini Model)

During his research, Geldenhuys [15], was able to derive the approximate expression of the average electric field required for positive streamer propagation as given in equation (2.6).

$$E_s^+ = 425\delta^{1.5} + (4 + 5\delta)H \tag{2.6}$$

where $H$ is the absolute humidity and $\delta$ is the relative air density. By varying the humidity, the average electric field required for streamer propagation under standard conditions was determined to be 500 kV/m. The findings achieved by Geldenhuys [15] gave way for the determination of the breakdown voltage of an air gap in terms of the electric field of the leader zone of the discharge ($E_l$), the length of the leader ($l_l$), the electric field of the streamer zone ($E_s$) and the length of the streamer ($l_s$) as given by equation (2.7) [16].

$$U = E_l l_l + E_s l_s \tag{2.7}$$

If breakdown occurs purely due to the streamer mechanisms (without any leader formation), the leader terms $E_l$ and $l_l$ are set to zero leaving the breakdown voltage to be dependent only on the streamer field $E_s$ and streamer length $l_s$. With this information, Pigini et al [16] were able to derive a factor $G$ to be used to determine the index of the relative air density correction factor by incorporating the discharge mechanism used and the relative air density. To correct the voltage, a similar expression to equation (2.2) was used but modified as follows,

$$U_{50} = U_{50(std)}(\delta.K)^n \tag{2.8}$$

where $K$ is the humidity correction factor graphically determined, $n$ is the air density correction factor and $U_{50(std)}$ and $U_{50}$ are the 50% probability breakdown voltage under standard and non-standard conditions respectively. To determine $n$ in equation (2.8), the G factor, equation (2.10), was used and $n$ took the following values [16] depending on the range of values of G

$$n = \begin{cases} \frac{G(G-0.2)}{0.8} & \text{for } 0.3 \leq G \leq 1, \\ \frac{3-G}{2G} & \text{for } 1 \leq G \leq 2, \end{cases} \tag{2.9}$$

where $G$ is the G factor under standard conditions ($\delta$ and $k$=1). The factor G was defined as in equation 2.10 and was determined on the assumption that the major process during the breakdown of the gap was streamers [16].

$$G = \frac{U_{50}}{500\delta k d} \tag{2.10}$$

where $d$ is the length of the discharge gap in metres and $k$ is a factor dependent on the type of voltage used and $\delta$ is defined as:

$$\delta = \frac{P}{P_0}\left(\frac{273 + t_0}{273 + t}\right) \tag{2.11}$$

where $t_0$ and $t$ are the standard temperature and actual temperature in °C respectively and $P_0$ and $P$ are the standard pressure and actual pressure in mbar respectively. The results by [16] were incorporated into the IEC 60060-1 (1989), including the graphs of equation (2.9) as the air density correction factors [17]. The final correction procedure in IEC 60060-1(1989) was as follows:

$$U_0 = \frac{U}{k_t} \tag{2.12}$$

where $U$ is the non-standard breakdown voltage in kV, $U_0$ is the standard breakdown voltage in kV and $k_t$ is the atmospheric correction factor defined as

$$k_t = k_1 k_2 \tag{2.13}$$

where $k_1$ is the air density correction factor and $k_2$ is the humidity correction factor. The air density correction factor is defined as

$$k_1 = \delta^m \tag{2.14}$$

where $\delta$ is defined according to equation 2.11. The humidity correction factor is defined as

$$k_2 = k^w \tag{2.15}$$

where k is a parameter that takes into account the type of test voltage used and is graphically defined for each test voltage as a function of the ratio of the absolute test humidity to the relative air density. It is at this point that the type of voltage is taken

into consideration during the correction procedure. The G factor is then calculated as

$$g = \frac{U}{500L\delta k} \tag{2.16}$$

where $U$ is as earlier defined, $L$ is the length of the air gap in metres, $\delta$ is defined in equation 2.11 and $k$ is the parameter described above.

The exponents $m$ and $w$ in equations 2.14 and 2.15 respectively were determined using the value of $g$. Once $g$ was determined, the values of $m$ and $w$ were then read of a graph that relates $g$ to $m$ and $w$. Thereafter, $k_1$ and $k_2$ can be determined and the standard voltage $U_0$ can be calculated.

The procedure in the IEC 60060 (1989) standard still plays a major role in the recent IEC 60060-1(2010) which, instead of using graphs for determining $m$ and $w$ as in IEC 60060-1(1989), uses equations that are similar to equations (2.9) [3]. It is important to note that the model derived by Pigini et al takes into account the voltage type through the factor $k$ in equation (2.10) whereas IEC 60-1 (1973) did not include any factor that took into account the type of voltage used. Since the standard was produced from the work conducted by Pigini et al, the standard is limited to an altitude of 1 800 m. Given that the only difference in the altitude correction procedures highlighted in the current version of IEC 60060-1 (2010) with those of IEC 60060-1 (1989) is the use of equations to determine the index $n$ instead of graphs, it therefore holds that the current version of IEC 60060-1 is also limited to an altitude of 1 800 m.

Due to the altitude limit of the work done by Pigini et al, extra work by Ramirez [18] was done in an attempt to modify the procedure to cover altitudes up to 3 000 m asl. This results of the work are described in the following section.

## 2.4 Ramirez Model

A year after IEC 60060-1 (1989) was published, Ramirez and his counterparts [18] proposed a model claimed to be more accurate than the one incorporated in IEC 60060-1(1989) and takes account of the influence of air density on rod-plane gaps. The model

is expressed in equation (2.17)

$$\frac{U}{U_0} = \frac{0.8[1 + T(1 - \delta)](\delta - 0.2G_0')}{(1 - 0.2G_0')} + 0.2 \tag{2.17}$$

where $\delta$ is the relative air density calculated using equation (2.11) and

$$T = 1.4\frac{1 - 0.8G_0'}{1 - 0.2G_0'} \tag{2.18}$$

with $G'_0$ defined as

$$G_0' = \frac{U_0}{500[\frac{1+(F_0-1)}{3}D]} \tag{2.19}$$

where $F_0$ is the gap factor and $D$ is the gap length. This proposed model satisfies corrections for altitude up to 3000 m for positive impulse voltages [18].

The method proposed by Ramirez et al was not a full correction in that the effects of humidity were not yet incorporated in the method. The derivation of the method was done using the fundamentals used by Pigini et al and using positive impulse voltages. Therefore, the correction procedure is questionable as there are a number of missing factors which are critical in the breakdown process. The search for improved correction factors continued with one of the notable efforts being contributed by Calva et al [9] as discussed in the next section.

## 2.5 Calva Model

Calva et al [9] proposed a model to use for altitude correction for gaps under DC voltage stress. This model determines the breakdown voltage $V_b$ as

$$V_b = E_{so}d[k_1 + k_2]S \tag{2.20}$$

where $k_1$ is the air density correction factor

$$k_1 = \delta^m \tag{2.21}$$

and $m$=1.4 for positive polarity and 0.44 for negative polarity and $\delta$ is as in equation 2.11. $k_2$ is the humidity correction factor

$$k_2 = 1.3\delta^{-0.83}\left(\frac{h-11}{100}\right) \tag{2.22}$$

and S is the gap factor. $E_{so}$ is the electric field required for streamer propagation and considered to be 500 kV/m for positive polarity and for negative polarity is given by equation (2.23)

$$E_{so} = 1476.4 \times 1121.91d \tag{2.23}$$

The models presented by Ramirez et al [18] and Calva et al [9] were not considered as inputs to the latest version of the IEC 60060-1(2010) and it would therefore be of interest to compare these models. It is now generally agreed that there are shortfalls in the IEC 60060-1(2010) standard with regard to altitude correction factors. In that regard, a Cigre work group (WG D1.50) "Atmospheric and altitude correction factors for air gaps and clean insulators" has been established to coordinate further studies and investigations on altitude correction. It has also been proven by [5, 10] that the IEC 60060-1 is still inconsistent in its calculated results compared to the experimental results obtained as altitude increases for air gaps under DC voltage stress and that the model proposed by Calva et al yields better accuracy in results than the IEC 60060-1(2010).

It has been observed that when the models by Ramirez, Pigini and Calva were derived, there were inconsistencies in the type of voltage used. It is suspected that the inconsistency in the voltage type used to derive the models could be among the causes of the variations in the models. IEC 60060-1 was derived from empirical results conducted on switching and lightning impulse voltages only [15, 16, 19]. The model presented by Ramirez was also derived using switching and lightning impulse voltages but the data was limited to only the rod-plane electrode configuration and could not be extended into a general method as the IEC 60060-1. Finally, the model presented by Calva et al [9] was developed using DC voltage conditions. This procedure is currently unique in literature and further work regarding this procedure is still under way.

## 2.6 Some Irregularities In The Commonly Used Standards

There is a fair number of standards used internationally that entail atmospheric correction voltages. The three notable standards widely used are the IEC 60060-1(2010) [3], IEC 60071-2 (1996) [20] and IEEE Std 4 (2013) on high voltage testing techniques [14]. In as much as these standards are widely used, the standards have notable irregularities regarding atmospheric corrections that are highlighted in the following subsections.

### 2.6.1 IEC 60060-1 (2010)

The most commonly used standard is the IEC 60060-1 (2010), largely based on Pigini et al [16] and discussed previously in Section 2.3. The standard defines two methods of atmospheric correction:

(i) The standard procedure; This procedure is used to correct voltages from non-standard conditions to standard conditions using the relationship,

$$U_0 = \frac{U}{K_t} \tag{2.24}$$

where $U_0$ is the disruptive-discharge voltage under standard conditions, $U$ is the measured disruptive-discharge voltage under non-standard conditions and $K_t$ is the atmospheric correction factor [3]. The derivation of this procedure was covered in Section 2.3.

(ii) The converse procedure; This is an iterative method used to predict breakdown voltages at non-standard conditions using equation (2.24) applied on known breakdown voltage at standard atmospheric conditions.

The determination of $K_t$ in [3] involves the calculation of the g-factor to determine the exponents $m$ (exponent $n$ in Section 2.3) and $w$ (exponent used for humidity correction). The function that relates $m$ to the g-factor is derived from a curve that averages the results obtained during the work done by [16] of different gap geometries and positive polarities of different impulse shapes [21]. This gives rise to the possibility of over-correction or under-correction of the voltage [21]. With regards to negative polarity impulses, the value $m$=1 was assumed by [16] and incorporated into the standard. This

implies that the value of $m$ for negative impulses is independent of the air density. Since the variation of air density has an effect on the breakdown voltage, the assumption of a constant value of $m$ is an approximation that cannot be considered accurate.

The relationship between $m$, $w$ and $g$ in [3] is only valid when $\delta \times \mathrm{k} \approx 1$ [22]. This condition is valid for high voltage laboratories located at altitudes near sea level. For laboratories at much higher altitudes however, $\delta \times \mathrm{k} < 1$ [22] implying that the application of the correction method in [3] becomes invalid for results obtained in such laboratories.

For one to be able to use the g-factor, the $U_{50}$ of the apparatus/gap is assumed to be known. However, for high voltage apparatus, the type test withstand voltage (the specified prospective value that characterises an insulator [3]) is the one known and cannot be assumed to be the $U_{50}$ of the apparatus [22]. Therefore the g-factor calculated using the type test withstand voltage can be invalid. Also, as mentioned earlier, the g-factor is defined with the assumption that streamer propagation is the dominant discharge mechanism and that the discharge is directly proportional to the relative air density. Therefore for streamer dominant discharges, the g-factor remains accurate but cannot be trusted to be accurate for other types of discharges especially in larger air gaps.

These irregularities make the IEC 60060-1 standard be deemed unreliable for correction of voltages at altitudes greater than 1 800 m and for discharges that are not streamer dominated.

### 2.6.2 IEC 60071-2 (1996)

The IEV 60071-2 (1996) standard was based on the same data used to develop IEC 60060-1 and therefore by default, makes the standard to be valid only up to 1 800 m, although it is used for higher altitudes [20]. The relationship between the required withstand voltage ($U_{rw}$) and the co-ordination withstand voltage ($U_{cw}$) is given by equation (2.25)

$$U_{rw} = U_{cw} \times K_a \tag{2.25}$$

where $K_a$ is the atmospheric correction factor given by equation (2.26)

$$K_a = e^{m(\frac{H}{8150})} \tag{2.26}$$

where H is the altitude in m. In this standard, the value of $m$ is defined as 1 for lightning impulses and short duration AC voltage tests. For switching impulses, the value of $m$ is taken from a plot of curves that relate $m$ to $(U_{cw})$. However, $(U_{cw})$ is defined as the 10% probability breakdown voltage therefore, when designing insulation for a lower breakdown voltage probability, the value of $(U_{cw})$ cannot be used [22]. The curves relating $m$ and $(U_{cw})$ in the standard are for phase-to-earth insulation, longitudinal insulation, phase-to-phase insulation and rod-plane gap. These cannot fully describe the dielectric strength and and discharge characteristics of different gap configurations, rod-to-rod for instance. Also, a value for $m$ to be used for AC voltages is recommended but no recommendation is given for DC voltage.
Even though this standard is assumed to be able to correct for altitudes greater than 1 800 m, there are irregularities in the determination of $m$ and no recommendation for DC voltages is given.

### 2.6.3 IEEE Std 4

The IEEE Std 4 standard has two methods for atmospheric correction [14]:

1. Method 1- This method uses the factor $K$ and similar as the one used in IEC 60060-1

2. Method 2- This method uses the factors $k_d$ (air density correction factor) and $k_h$ (humidity correction factor) for correction and is applicable to gaps less than 1 m.

Since Method 1 is similar to the one presented in IEC 60060-1, it will not be discussed again in this section. Method 2 states the following relationship,

$$U = \frac{k_d}{k_h} U_0 \tag{2.27}$$

where $U_0$ and $U$ are the standard voltage and non-standard voltage respectively.

The values of $m$ and $n$ used for evaluating $k_d$ are assumed in the standard to be the same irrespective of the gap geometry and RAD . For other electrode configurations and voltage types, the values of $m$, $n$ and $w$ are determined from a graph that relates the three variables to the gap length [14]. The values of $m$, $n$ and $w$ will also be the same

(that is, $m$=$n$=$w$) for the same gap length, configuration. This does not agree with the variation of the air density correction factor with the type of discharge that governs breakdown in the air gap.

---

*Closing Summary*

---

The atmospheric correction method stated in IEC 60060-1 (2010) is derived from data based on empirical work conducted up to an altitude of 1 800 m. This makes the method unsuitable for use when applied to altitudes higher than 1 800 m. Literature has shown discrepancies in the factors $m$ and $w$ thereby suggesting changes in breakdown mechanisms since the factors are dependent on the dominant breakdown mechanism. A prediction method proposed by Calva et al for DC voltages has been discovered and will be investigated. With the evolution history discussed in the previous pages, the problem statement and the research question were put together as follows:

## The Problem

As altitude increases, air density decreases and air breakdown mechanisms change. The IEC 60060-1 (2010) standard has been found to cover only a limited altitude range. Some models that can possibly extend the altitude correction factors to cover a higher altitude range have been suggested in the literature but are not yet incorporated into the standards. Very little knowledge is available in literature regarding the variation in breakdown mechanisms under HVDC with altitude, leading to limited knowledge on the correction methods. Also, the currently used standard, IEC 60060-1(2010) is built on the empirical results of impulse tests over a limited altitude range. No empirical data on AC and DC voltages was used towards the establishment of the standard. Further verification of the proposed models is required, especially for DC voltages, and the reliability of IEC 60060-1 (2010) needs to be tested.

## Research Question

It is known that the breakdown voltage of an air gap is dependent on pressure. However, the altitude correction factors given by the current version of IEC 60060-1 (2010) (based on the model proposed by Pigini et al) are not reliable for higher altitudes. A procedure proposed by Cavla et al, described in the Chapter 2, has not been incorporated into the current standard even though they have been suggested to be more accurate at higher altitudes. The following questions therefore arise:

*"What are the similarities and differences between the different altitude correction models (IEC 60060-1 (2010) and Calva procedure) when tested on the same experimental data set?"*

and

*"Out of the two procedures, which one can be recommended for current use and is there any possible modification that will give more accurate correction factors for wider altitude ranges?"*

By answering these questions, it is hoped that insight into a more informed approach to altitude correction will be established. The first step towards understanding altitude correction is a study into the electrical breakdown mechanisms in air. This is discussed in the next chapter.

# Chapter 3

# Breakdown Mechanisms in Air

---

*Opening Summary*

---

The electrical breakdown of air is governed by processes that include corona, streamer development and propagation, leader development and propagation and then the breakdown arc. The detailed explanation of each of these processes are laid out in the following sections. The process is explained by considering the rod-plane geometry as it gives a typical non-uniform field profile compared to other geometries. By studying the breakdown mechanisms, one can understand altitude correction factors from first principle since environmental conditions (which strongly influence the breakdown mechanisms), especially pressure, vary with altitude.

## 3.1 Non-Uniform Field Breakdown

Rod-plane electrode configurations are commonly used as they give electric field profiles common in high voltage electric equipment. The voltage breakdown mechanism for a rod-plane short gap under positive DC stress is dominated by the streamer process [23, 24]. In a rod-plane gap with voltage applied, a divergent field is created between the rod and the plane. This field is stronger around the tip of the rod and weaker towards the plane as illustrated in Figure 3.1. When breakdown of a rod-plane air gap occurs, the processes in Figure 3.2 occur. In larger gaps, streamer-leader transition can occur

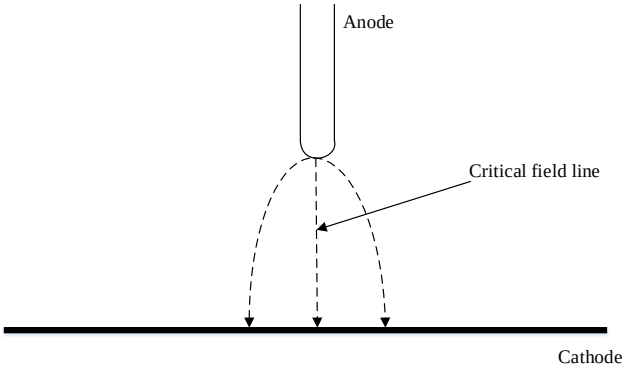


FIGURE 3.1: Electric field distribution in a rod-to-plane gap

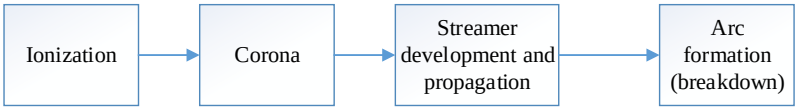


FIGURE 3.2: Processes that occur leading to breakdown in a short gap

before arc formation and streamer propagation [25].

### 3.1.1 Ionization

The process in which a neutral molecule loses an electron thereby gaining a positive net charge is called ionization [26]. The process of ionization is the first step towards breakdown of air. Ionization can be achieved by the process of collision, photo-ionization and secondary ionization [26].

Ionization by collision occurs when a free electron or metastable collides with a neutral molecule causing the neutral molecule to release an electron. The process of dislodging an electron from a neutral molecule by collision requires that the energy being transferred during the collision be greater than the ionization energy of the molecule [26]. In the case where the energy transferred during collision is greater than the ionization energy, the process can be represented by equation (3.1).

$$e^- + M \rightarrow 2e^- + M^+ \tag{3.1}$$

where $e^-$ is an electron, M is the molecule and $M^+$ is the produced positive ion. In a given electric field, the ability of an electron to gain enough energy to dislodge an electron from the molecule is dependent on the spacing between the molecules (mean free path, $\tau$). Generally, further apart the molecules are, the more energy gained by the electron during acceleration (because of the surrounding electric field), whereas if the molecules are close together, there will not be enough space between the molecules for the electrons to gain enough energy to dislodge an electron. Therefore, the ionization of molecules is highly dependent on the "mean free path" between molecules. This means that ionization by collision can be easily achieved in a gas under low pressure compared to that under higher pressure. Ionization by collision is the most common form of ionization processes in gases, therefore making the air breakdown mechanism highly dependent on the air pressure.

Ionization of gases can also occur through the process of photo-ionization. This process is achieved by the molecule or atom being able to absorb radiation energy that exceeds the ionization energy of the molecule or atom [26]. Other secondary processes like electron emission due to positive ion impact with the cathode, emission of electrons due to photons and electron emission due to metastable and neutral atoms also occur during the ionization process of gases [26]. For this research, ionization due to molecular collisions is of most relevance as this process is directly linked to atmospheric pressure. Electrical breakdown of a gas is through electron avalanches as reviewed in the next section.

### 3.1.2 Electron Avalanche Mechanisms

If a free electron appears between the cathode and anode with a voltage applied, the electron accelerates towards the anode due to the electric field. While the electron accelerates towards the anode, it collides with molecules along the way and therefore initiating ionization in accordance with equation (3.1). One collision adds a free electron to the system, therefore as the initial electron propagates through the gap, the number of electrons in the system increases exponentially causing an avalanche of electrons. The number of electrons ($n_d$) reaching the anode a distance $d$ from cathode can be calculated by

$$n_d = n_0 e^{\int_{x=0}^{x=d} \alpha dx} \tag{3.2}$$

where $n_0$ is the initial number of electrons emitted from the cathode and $\alpha$ (Townsend's first ionization coefficient) is the average number of ionizing collisions made per electron per unit distance travelled in the direction of the field [26]. The ions produced from the process propagate towards the cathode. This leads to a charge separated system with the electrons travelling towards the anode and ions towards the cathode. Since electrons are lighter than the ions, the electrons get to travel a greater momentum compared to the ions therefore reaching the anode before the ions reach the cathode. The initial avalanche propagation towards the anode is mainly driven by the potential difference between the electrodes. In the presence of secondary ionisation mechanisms, the overall number of secondary electrons produced per incident positive ion, photon, excited particle or metastable particle is a function of the secondary ionisation coefficient ($\gamma$) [26]. As the voltage is increased, the avalanche will transform into a streamer. The development and propagation of a streamer is discussed in the next section.

### 3.1.3 Streamer Development and Propagation

In a rod-plane electrode configuration, a non-uniform electrical field is produced in the air gap. The maximum electric field *($E_{max}$)* for a gap length of $d$ and rod tip radius $r$ can be calculated by equation (3.3) [27].

$$E_{max} = \frac{2V}{rln(1 + \frac{4d}{r})} \tag{3.3}$$

The non-uniformity of the field leads to the first ionization coefficient varying across the gap [26, 28] resulting in the breakdown criterion as given in equation (3.5). In order to initiate a streamer, the charge in the avalanche head should have reached a critical value of

$$n_0 e^{\alpha x_c} \approx 10^8 \tag{3.4}$$

where $x_c$ is the length of the path taken by the avalanche in the direction of the electric field. In order for breakdown to occur, the criterion in equation 3.5 should be met.

$$\int_0^{x_c} \alpha dx = lnN_{cr} \approx 18 - 20 \tag{3.5}$$

where $N_{cr}$ is the critical charge in the avalanche. For the criterion in equation (3.5) to be met, it was empirically discovered that at standard atmospheric pressure, the electrical

field should be ≈2.5 kV/mm for a very small (few mm) streamer length within the range $\ln(N_{cr})$≈9-21 [25]. Since the field will be non-uniform, streamer inception occurs in the areas of the highest electric field. When the electric field strength reaches approximately 2.5 kV/mm the breakdown criterion is met and the air around the rod begins to breakdown. The breakdown of the air occurs around the rod tip and is usually accompanied by a cracking noise and is known as corona [26, 28]. Since the field is non-uniform, the electric field strength varies from a maximum at the rod tip to a minimum at the plane electrode.

As the streamer propagates across the gap, the streamer head distorts the background electric field thus producing a resultant electric field modified by the space charge. The resultant electric field, partially, drives the process of self-sustained ionization and growth of avalanches [25] as depicted in Figure 3.3. Having the resultant field at the

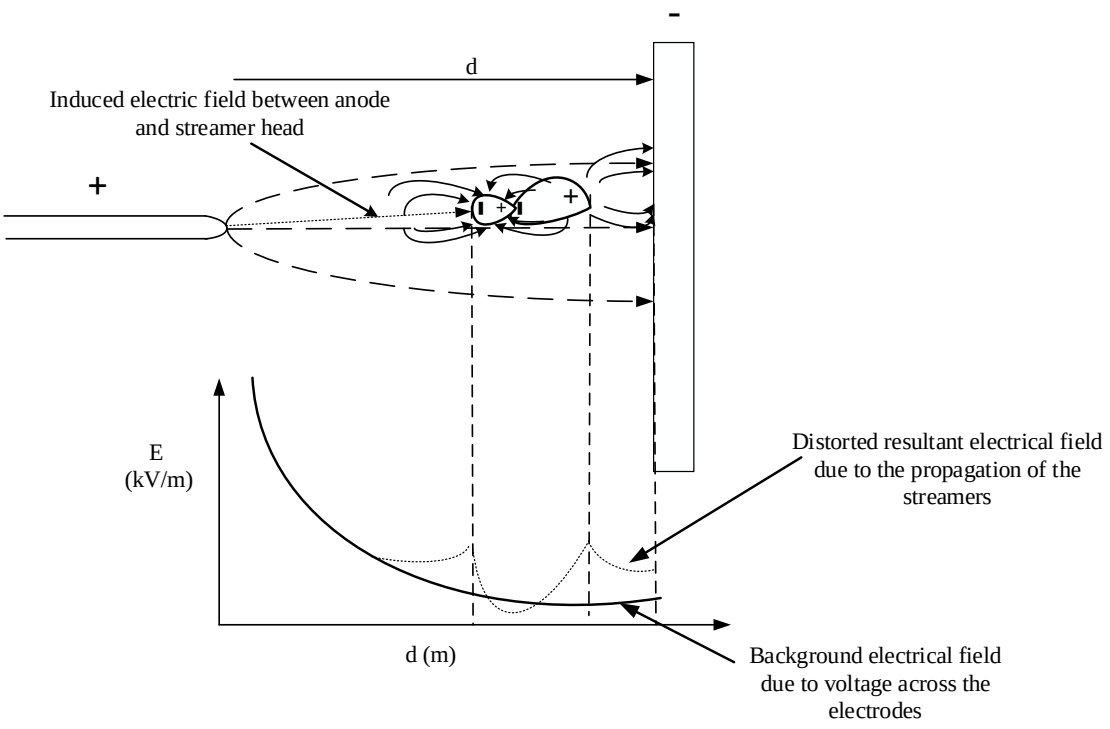


FIGURE 3.3: Streamer propagation in electric field

head of the streamer of approximately 2.5 kV/mm or more allows for the streamer to be sustained. Due to the photo-ionization process that drives the streamer propagation, the path which the streamer takes is probabilistic. Therefore a bundle of streamers can be formed due to the creation of two differently directed avalanches as the streamer

propagates. When the main stem of the streamer has enough current to achieve a temperature above 5000 K (4726.85 $^0$C), then the streamer transforms to a leader (if the gap is more than 2 m long) [25]. Once the leader bridges the gap, it creates a conductive path and the gap breaks down.
It is important to note that there are four possible outcomes when voltage is applied across a rod-plane air gap. These outcomes are highly dependent on the applied voltage and gap length.

1. The voltage is applied and the avalanches propagate towards the anode. However, along the way the avalanches are unable to initiate the self propagation process and the streamer breakdown criterion is not met. This scenario occurs if the gap is weakly stressed therefore there will not be enough energy for the streamers to propagate. In such a case, the field is so weak such that the streamers produced do not cross the whole gap.

2. The streamers propagate across the gap and are able to lead to breakdown without any leader formation. This usually happens to air gaps between 5 cm and 2 m [25].

3. For gaps bigger than 2 m, streamers develop into leaders and breakdown occurs through the leader.

---

*Closing Summary*

---

In order to understand and develop altitude correction methods, the study of breakdown mechanisms is essential. it has been noted that the atmospheric pressure has great influence on the ionisation process, which is the backbone of the electrical breakdown process. In the next chapter, the experimental set-up and procedure used in the research on the effect of altitude (pressure) on air gap breakdown voltage are introduced.

# Chapter 4

# Experimental Set-Up

---

*Opening Summary*

---

This chapter highlights the experimental set-up and procedures for the experiments conducted to investigate the effect of altitude on the DC breakdown voltage of rod-plane air gaps. Four sets of experiments were conducted and are categorised as open air tests and pressure vessel tests. The open air tests were conducted at three different altitude locations while the pressure vessel was used to simulate higher altitudes that are not physically easily accessible. The following sections give detailed descriptions of the set-ups and procedures followed.

## 4.1 The Tests

The work done in the laboratory included two types of tests; open air tests and the pressure vessel tests.

### 4.1.1 Open Air Tests

The open air tests carried out in this project were conducted in three different locations. These locations were selected according to a criteria whereby a high voltage DC supply kit is available and the altitude of the locations is at either end of the altitude extremities

that are easily accessible in South Africa. The result of the selection criteria left two possible locations, Wits University($\approx$ 1 800 m asl) and the University of KwaZulu-Natal (UKZN) Westville Campus DC Centre ($\approx$ 130 m asl). The third test was conducted less than 2 m asl at Scottburgh beach, Clansthal. These tests were conducted in order to obtain results closest to the standard breakdown voltage. These results are used for comparison with the results from the high altitude and low altitude tests.

By conducting the tests at the above mentioned locations, data was captured at both low altitude and high latitude. The data was then used in producing standard condition breakdown voltages by being corrected according to IEC 60060-1 and was also compared to the prediction method proposed by Calva et al [9]. For higher altitudes greater than that at Wits University, the tests were conducted in a variable pressure vessel.

### 4.1.2 Pressure Vessel Tests

The pressure vessel tests were conducted at Wits University using a cylindrical pressure vessel borrowed from the UKZN. Due to the locking mechanism of the top cover of the vessel, air was only drawn out of the vessel to simulate high altitudes (low pressure) since pumping air in (high pressure) would cause structural damage to the vessel. Further physical details of the pressure vessel are presented in the next section. A maximum of 300 mbar was able to be drawn from the ambient pressure within the chamber. This resulted in a relative air density (RAD) of 0.53, corresponding to an altitude of $\approx$ 5200 m. The results obtained from this test were compared to the prediction method proposed by Calva et al [9] and were also used to evaluate the applicability of the IEC 60060-1 standard on altitudes greater than 1 800 m asl (RADs lower than 0.8).

## 4.2 Laboratory test configuration and Equipment

### 4.2.1 Test configurations

The same set-up in Figure 4.1 was used in the tests in UKZN. For the sake of consistency, the exact same rod was also used in the tests in UKZN and at sea level.

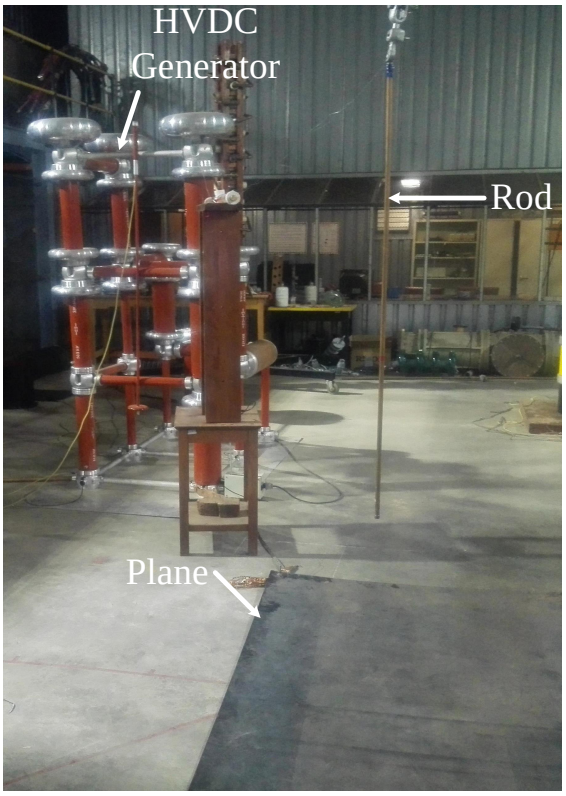


FIGURE 4.1: Open air test set-up in the HV lab at Wits University

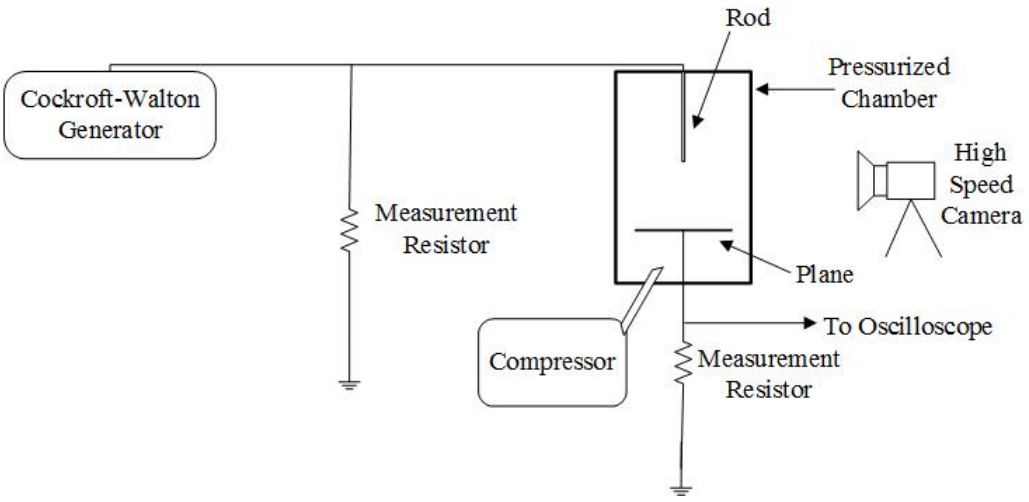


FIGURE 4.2: Pressure vessel test set-up

### 4.2.2 Equipment Used in the Tests

#### The DC Generators

The two generators used for the tests are shown in Figures 4.6 and 4.7.

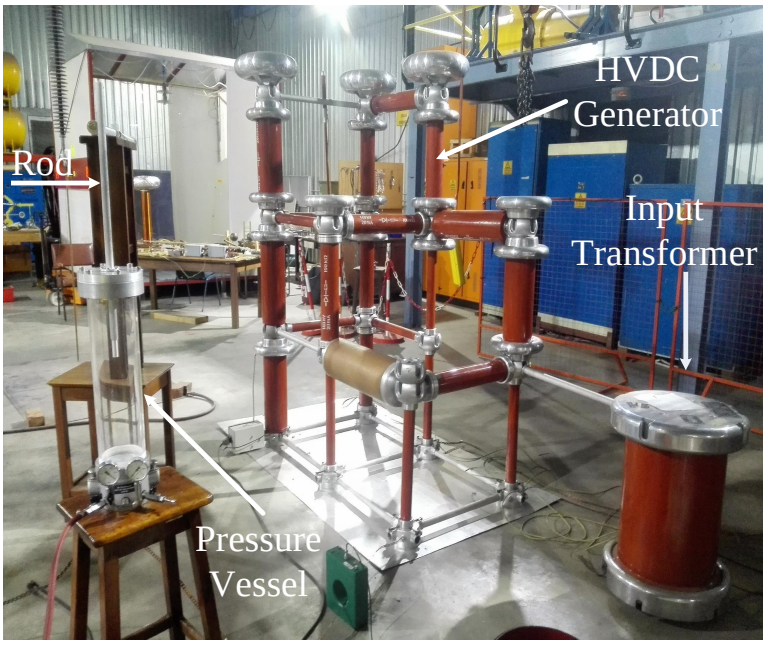


FIGURE 4.3: Pressure vessel test set-up in the HV lab at Wits University


FIGURE 4.4: Test site for sea level tests

The generator at Wits University (Figure 4.6) is a 400 kV rated 3 stage Cockroft-Walton DC unit which can reach a maximum of 325 kV due to high altitude effects. The generator at UKZN (Figure 4.7) is a 2 stage Cockroft-Walton DC unit rated at 500 kV. The generator can only operate at a maximum voltage of approximately 250 kV due to clearance limitations in the lab, as can be seen in Figure 4.7. The generators

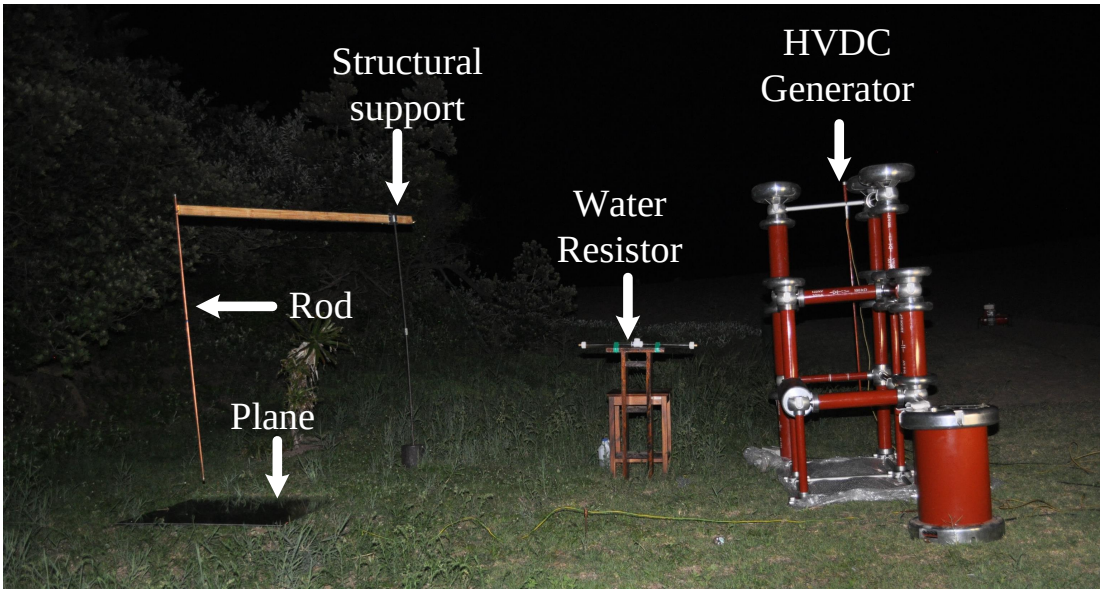


FIGURE 4.5: Experimental set-up for sea level tests

FIGURE 4.6: 400 kV DC Generator at WITS

are equipped with a stack of resistors at the output end. These resistors form a voltage divider and a panel on the control board displays the output voltage read from the voltage divider. The output of the divider was compared to an already resistive potential divider calibrated at NETFA and the readings fell within a 2% error. The voltage divider

FIGURE 4.7: 500 kV DC Generator at UKZN

on the generator was therefore deemed accurately calibrated and usable for the project.

### Rod and Plane Electrode Set-Up

A rod-plane electrode configuration was used for the tests conducted because this geometry is widely used in literature and the results can be comparable to other similar work done in South Africa [5]. For the open air tests, a copper rod 1.5 m long and with a 15 mm diameter was used as the rod electrode. The rod dimensions and electrode set up is commonly used in other research centres around the world that are taking part in the round robin tests for the Cigré D1.50 working group. The end of the rod was fitted with an end cap that was smoothly soldered for contact purposes and to avoid electric field distortions around the end cap. The rod was suspended from the roof by a nylon rope pulley system in order to maintain clearances. A 1.8 m by 2 m steel plate was used as the grounded plane.

The rod used in the pressure vessel experiment was a 0.7 m aluminium rod 15 mm in diameter. The rod was machined at the Wits Genmin laboratory to have the same tip profile as the copper rod used in the open air experiments. A circular plate 112 mm in

diameter was machined in the Genmin laboratory and was used as the ground plane for the experiment.

### The Pressure Vessel

The pressure vessel used in the experiment was a 0.55 m long cylindrical tube with a 0.12 m inner radius borate glass wall. A picture of the pressure vessel is shown in Figure 4.8. The pressure vessel had two valves that were used to control the inlet and outlet of

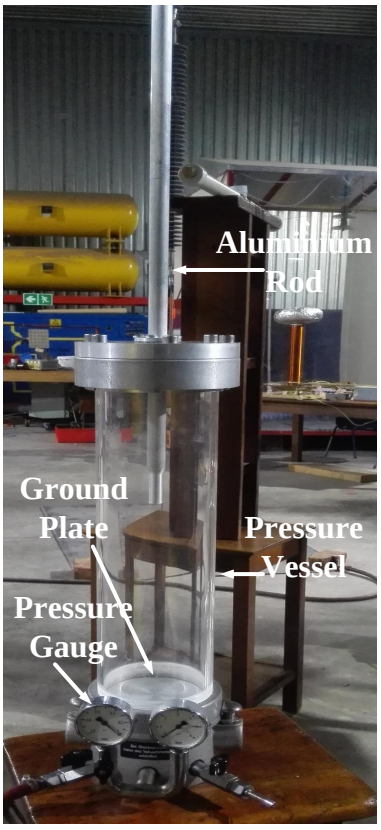


FIGURE 4.8: Picture of pressure vessel used in the experiment

the air. A new top cap for the chamber was machined in the Genmin laboratory. The top cap was designed such that the rod electrode can go through the cap. A clamping mechanism to hold the rod in place after setting the gap length was designed on the top cap. The design of the top cap came with the constraint that the pressure vessel could only be used under ambient and low pressure conditions. If pressure was increased, the top cap would have been blown off.

Furthermore, due to the dimensions of the chamber and the design of the top cap, only gap sizes up to 0.3 m could be tested. These two limitations meant that only high altitude RADs could be simulated. In order to verify whether the gas laws could affect the experiment due to drawing pressure, a pilot test was carried out. By drawing pressure in the vessel with a digital thermometer inside, the temperatures in Table 4.1 were recorded. The external temperature at the beginning of the test was the same as the

TABLE 4.1: Variation of temperature due to pressure in the chamber

| **Pressure** | **Temperature ($^0$C)** |
|---|---|
| Ambient | 22.2 |
| Ambient-100 mbar | 22.0 |
| Ambient-150 mbar | 22.0 |
| Ambient-200 mbar | 21.9 |
| Ambient-250 mbar | 22.0 |
| Ambient-300 mbar | 22.0 |
| Ambient-350 mbar | 21.9 |

initial temperature inside the vessel. At the end of the test, the external temperature was 22.4 $^0$C. Therefore, the temperature variations inside the chamber were not significant during the pressure vessel tests as the temperature was approximately the same as outside the chamber. Therefore all temperature readings during the tests were taken outside the chamber.

## 4.3 Test Procedure

### 4.3.1 Open Air Experiments

The following procedure was used in conducting the open air tests:

1. Set gap length to 0.1 m
2. Record temperature, pressure and humidity
3. Slowly increase the voltage at approximately 3 kV/sec until breakdown occurs and record the breakdown voltage. Breakdown would have occurred when an arc completely bridges the air gap.
4. Observe 5 minute waiting period to allow dissipation of any accumulated space charge

5. Repeat 3 and 4 until 5 breakdowns have been recorded. 5 breakdowns were used because it was discovered that the breakdown of an air gap under HVDC stress is repeatable and there is not much scatter in the results.

6. Increase gap length by 0.05 m

7. Repeat 2 to 6 until readings for 0.4 m air gap have been recorded.

### 4.3.2 Pressure Vessel Experiments

The pressure vessel tests were similar to those of the open air experiments. Due to limitations in the size of the pressure vessel, gap sizes that were tested were 0.1 m, 0.2 m and 0.3 m. Starting at ambient pressure, a set of 5 breakdowns were recorded for each gap length per pressure level. The pressure was decreased in the chamber by 100 mbar using an Edwards$^{TM}$ pump once 5 breakdowns were recorded for the current pressure level. Tests were done until tests on a pressure level 300 mbar below the ambient were conducted. Due to the confined space in the chamber, a 10 minute waiting period was observed between breakdowns to allow adequate dispersion of accumulated space charge. Environmental conditions were recorded for each gap length and each pressure level tested.

In the next chapter, the test results, analysis and discussion are presented.

# Chapter 5

# Experimental Results, Analysis and Discussion

---

*Opening Summary*

---

This chapter lays out the results obtained from the tests conducted at high altitude, low altitude, sea level and in the variable pressure vessel. All experiments were conducted using a rod-plane air gap with a 15 mm flat tip diameter rod. All the results, except the sea level results, were corrected according to IEC 60060-1 (2010) and were also compared to predictive calculations using the Calva prediction method. Corrected IEC 60060-1(2010) results were compared to the sea level results as they should ideally be similar. Trends in the results were analysed and functions were derived to modify the Calva model for improved accuracy.

## 5.1 Open Air Gap Breakdown Experiments

### 5.1.1 Sea Level Tests

The results of the sea level tests are shown in Figure 5.1 (average of 5 breakdowns per air gap length) and Table 5.1 shows the environmental conditions during the tests.

TABLE 5.1: Environmental conditions during sea level experiments

| **Gap length (m)** | **Temp. (°C)** | **Hum. (%)** | **Press. (mbar)** | **Breakdown Voltage(kV)** | **Std Deviation(%)** |
|---|---|---|---|---|---|
| 0.10 | 23.6 | 89 | 1012.4 | 63.6 | 0.8 |
| 0.15 | 23.5 | 89 | 1012.4 | 87.4 | 0.6 |
| 0.20 | 23.4 | 90 | 1012.5 | 112.0 | 0.6 |
| 0.25 | 23.4 | 90 | 1012.6 | 139.8 | 0.3 |
| 0.30 | 23.3 | 92 | 1012.8 | 164.2 | 0.2 |
| 0.40 | 23.3 | 92 | 1012.7 | 218.0 | 0.6 |

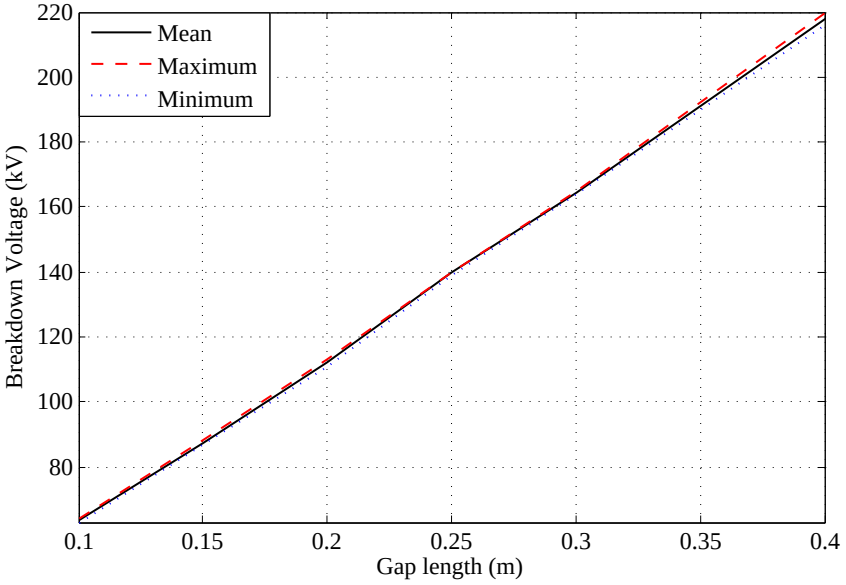


FIGURE 5.1: Sea level test results

Figure 5.1 shows the deviation of the results from the mean. The results had a maximum deviation of 1% from the mean. The small variation shows that the results obtained were precise and instils confidence that they are accurate. The environmental conditions during the tests were the closest to the defined standard conditions in IEC 60060-1, therefore the results will be used as the reference standard breakdown voltages.

### 5.1.2 Low Altitude Tests (UKZN) (≈ 130 m asl)

The results obtained during the tests at UKZN are in Figure 5.2 and the recorded environmental conditions during the test are in Table 5.2.

Figure 5.2 is a plot of the average voltage of 5 breakdowns per each gap length and shows how the breakdown voltages per each gap length varied in range and how the maximum and minimum breakdown voltages vary from the mean.

TABLE 5.2: Environmental conditions during low altitude tests

| **Gap length (m)** | **Temp. ($^0$C)** | **Hum. (%)** | **Press. (mbar)** | **Breakdown Voltage (kV)** | **Std Deviation (%)** |
|---|---|---|---|---|---|
| 0.10 | 27.6 | 49 | 987.8 | 56.9 | 1.2 |
| 0.15 | 26.2 | 56 | 986.3 | 82.2 | 0.6 |
| 0.20 | 27.8 | 52 | 986.1 | 107.6 | 0.2 |
| 0.25 | 26.5 | 55 | 985.4 | 131.5 | 0.1 |
| 0.30 | 27.2 | 55 | 985.2 | 157.1 | 0.3 |
| 0.35 | 21.9 | 56 | 985.8 | 174.9 | 0.1 |
| 0.40 | 25.5 | 46 | 985.5 | 196.8 | 0.1 |

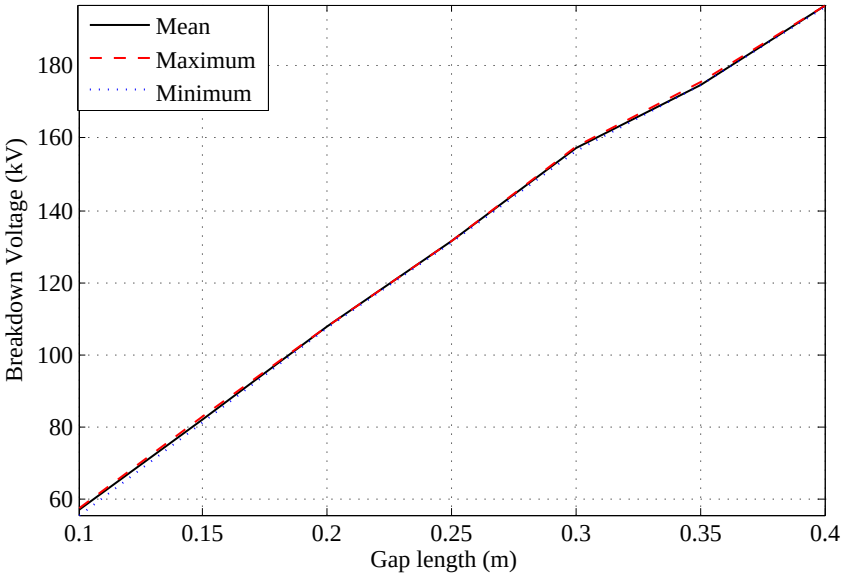


FIGURE 5.2: Low altitude (130 m asl)rod-plane breakdown voltages showing scatter

A maximum deviation of 2.4% from the mean breakdown voltage was observed for the entire data set. This occurred at the 0.1 m air gap length results. Therefore, the rest of the 5 individual breakdown voltages obtained per each gap length falls within 2.4% of the mean breakdown voltage of each gap length. This is an acceptable error value and therefore the data set gives high confidence in its accuracy.

The low altitude results are plotted against the predicted results using the Calva method in equation 5.1 where $d$ is the gap length, $k_1$ and $k_2$ are defined in equations

$$V_b = 500d(k_1 + k_2)S \tag{5.1}$$

5.3 and 5.3 respectively and $S$ is the gap factor and is dependent on the rod electrode geometry and polarity [9]. $S$ was defined as $1.01\mathrm{d}^{-0.10}$ and in equation 5.3, $m$ was

defined as 1.4 for positive polarity [9].

$$k_1 = \delta^m \tag{5.2}$$

$$k_2 = (1.3\delta^{-0.83})\left(\frac{h-11}{100}\right) \tag{5.3}$$

TABLE 5.3: Comparison of test results and Calva prediction

| **Gap size (m)** | **Breakdown Voltage (kV)** | **Calva Prediction (kV)** | **(%) Difference** |
|---|---|---|---|
| 0.10 | 56.9 | 59.0 | 3.7 |
| 0.15 | 82.2 | 86.3 | 5.0 |
| 0.20 | 107.6 | 111.1 | 3.2 |
| 0.25 | 131.5 | 136.3 | 3.6 |
| 0.30 | 157.1 | 161.0 | 2.5 |
| 0.35 | 174.9 | 184.2 | 5.3 |
| 0.40 | 196.8 | 202.1 | 2.7 |

Figure 5.3 shows the plot of the comparison of the obtained low altitude experimental results and the predicted results while Table 5.3 shows the tabulated data. The plot in

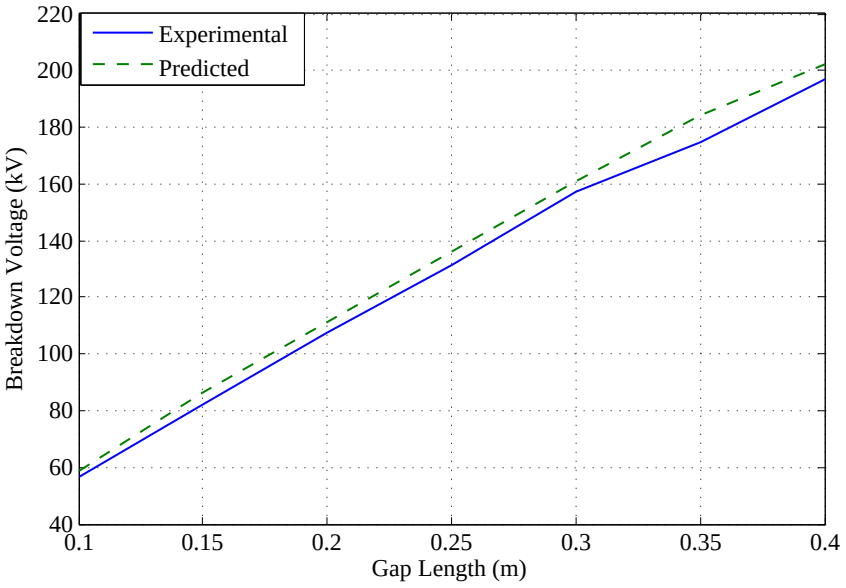


FIGURE 5.3: Comparison of low altitude test results and predicted results

Figure 5.3 shows that the prediction method proposed by Calva provides fairly accurate results since the average error for the low altitude test results is 3.7%. The maximum error when considering individual air gaps is 5.3% observed for the 0.35 m air gap. By observing the trend of the predicted and experimental results, it can be noted that the

Calva prediction method over estimates the breakdown voltage by an average of 3.7% (obtained error). This error is advantageous when considering clearances during design as it will naturally add in an extra safety factor. It is deduced that the Calva prediction method is therefore reasonably accurate for gaps in the range 0.1 m - 0.4 m at an altitude of ≈ 200 m asl.

### 5.1.3 High Altitude Tests (Wits University)(≈ 1 740 m asl)

High altitude tests were conducted at Wits University at an altitude of ≈1 740 m asl. The corresponding relative air density at this altitude is 0.82 and is close to the IEC 60060-1 limit of $\delta$=0.8. The plot of the results is shown in Figure 5.4. Table 5.4 presents the conditions under which the results were obtained.

TABLE 5.4: Environmental conditions the high altitude tests

| **Gap length (m)** | **Temp. ($^0$C)** | **Hum. (%)** | **Press. (mbar)** | **Breakdown Voltage (kV)** | **Std Deviation (%)** |
|---|---|---|---|---|---|
| 0.10 | 15.3 | 41 | 844.7 | 52.5 | 1.9 |
| 0.15 | 14.4 | 45 | 841.7 | 67.8 | 1.1 |
| 0.20 | 15.4 | 34 | 840.2 | 81.2 | 0.3 |
| 0.25 | 14.9 | 42 | 841.1 | 100.2 | 0.4 |
| 0.30 | 15.1 | 46 | 842.3 | 118.2 | 0.7 |
| 0.35 | 15.8 | 33 | 839.7 | 129.9 | 0.3 |
| 0.40 | 14.8 | 47 | 842.3 | 156.8 | 0.2 |

The results shown in Figure 5.4 are an average of 5 breakdowns per each gap length. Figure 5.4 also shows the breakdown range observed for each air gap and how they vary from the mean breakdown voltage. Out of this set of data, a maximum variation of 3.2% was observed between the maximum breakdown voltage and the mean breakdown voltage during the 0.1 m test. With this, the results pose high confidence in their accuracy.

As done for the low altitude test results, the plot for the results of the high altitude test compared to the predicted results is shown in Figure 5.5. Table 5.5 shows the tabulated data for Figure 5.5.

Unlike the low altitude results, it is observed that the Calva prediction method under-predicts the breakdown voltage of the 0.1 m and 0.15 m air gaps, then over-predicts (as expected) for the bigger air gaps. This trend is approximately the same trend observed

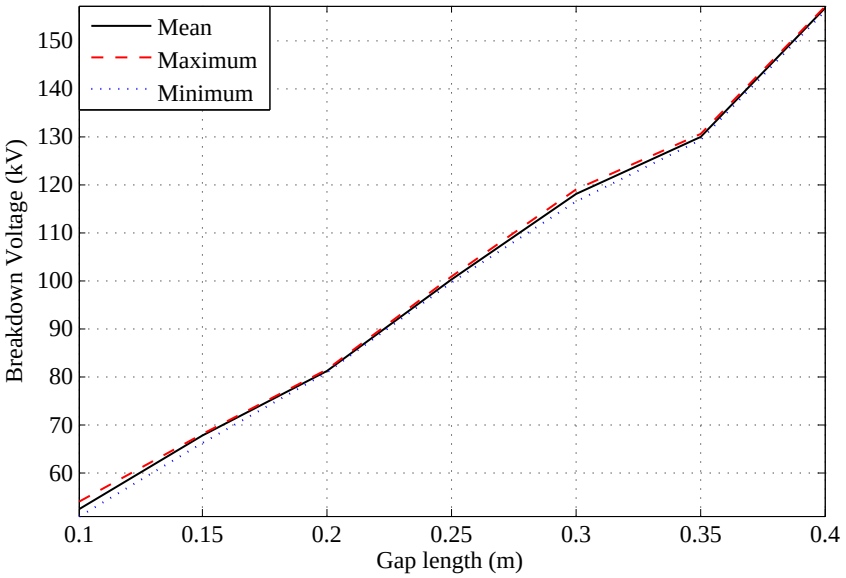


FIGURE 5.4: High altitude (1 740 m asl)rod-plane breakdown voltages showing scatter

TABLE 5.5: Comparison of test results to the Calva prediction at 1 740 m asl

| **Gap size (m)** | **Breakdown Voltage (kV)** | **Calva Prediction (kV)** | **(%) Difference** |
|---|---|---|---|
| 0.10 | 52.5 | 46.3 | 11.8 |
| 0.15 | 67.75 | 67.0 | 1.1 |
| 0.20 | 81.18 | 83.7 | 3.1 |
| 0.25 | 100.15 | 105.0 | 4.8 |
| 0.30 | 118.2 | 126.8 | 7.3 |
| 0.35 | 129.9 | 134.8 | 3.8 |
| 0.40 | 156.8 | 162.2 | 3.4 |

by [5] at an altitude of 1 880 m asl. However, the crossing point of their results and the Calva prediction method occurs between 0.3 m and 0.4 m, whereas in Figure 5.5 the crossing point occurs at an approximate 0.19 m gap length. This trend seems to suggest that as the altitude increases, the Calva prediction method under-predicts for smaller gaps and as the altitude increases, the method over-predicts.

However, the comparison of the results show that the Calva prediction is reasonably accurate as the average error between the two sets of data is 5.0%. This error falls within the generally allowed 5% error, therefore the Calva prediction is proven to be reasonably accurate at an altitude of 1 740 m asl for air gaps ranging in size between 0.1 m to 0.4 m.

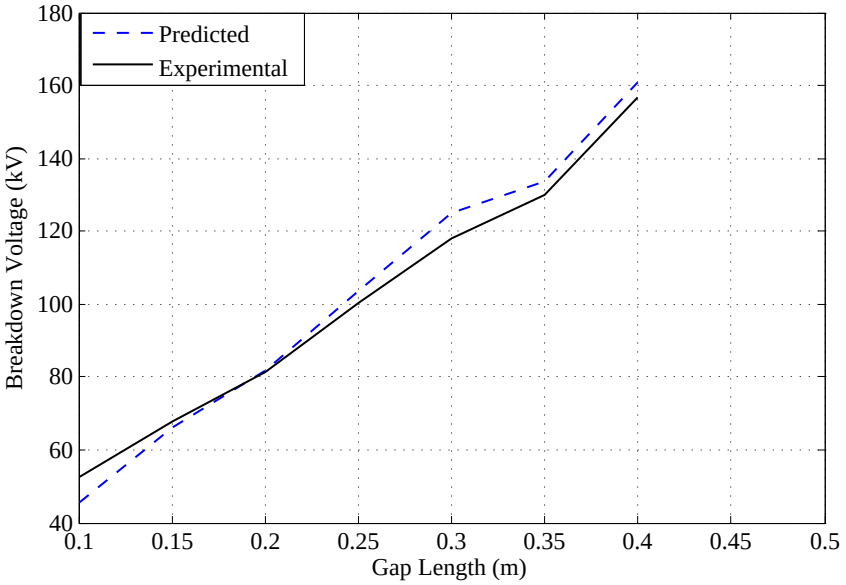


FIGURE 5.5: Comparison of high altitude test results and predicted(Calva) results

### 5.1.4 IEC 60060-1 Correction of Low Altitude and High Altitude Results

Since IEC 60060-1 standard correction method serves to correct voltages to standard conditions, both sets of data were corrected according to the standardised method. The IEC 60060-1 standard has been described in Chapter 2. Table 5.6 shows the tabulated comparison of the high altitude and low altitude corrected results.

TABLE 5.6: Comparison of high altitude and low altitude IEC 60060-1 (2010) corrected results

| **Gap Length (m)** | **High Altitude Corrected Voltage (kV)** | **Low Altitude Corrected Voltage (kV)** | **% Difference** |
|---|---|---|---|
| 0.10 | 64.4 | 59.6 | 8.1 |
| 0.15 | 82.8 | 84.9 | 2.5 |
| 0.20 | 102.8 | 111.6 | 7.9 |
| 0.25 | 122.9 | 136.1 | 9.7 |
| 0.30 | 140.3 | 162.0 | 13.4 |
| 0.35 | 163.0 | 181.9 | 10.4 |
| 0.40 | 187.1 | 210.2 | 11.0 |

The plot of the corrected data is shown in Figure 5.6. IEC 60060-1 states that the correction methods are applicable and accurate when applied to results obtained between $0.8<\delta<1$. Therefore, if the same electrodes are used to conduct experiments for the same gap lengths in different altitude locations within the $\delta$ range stated in the standard,

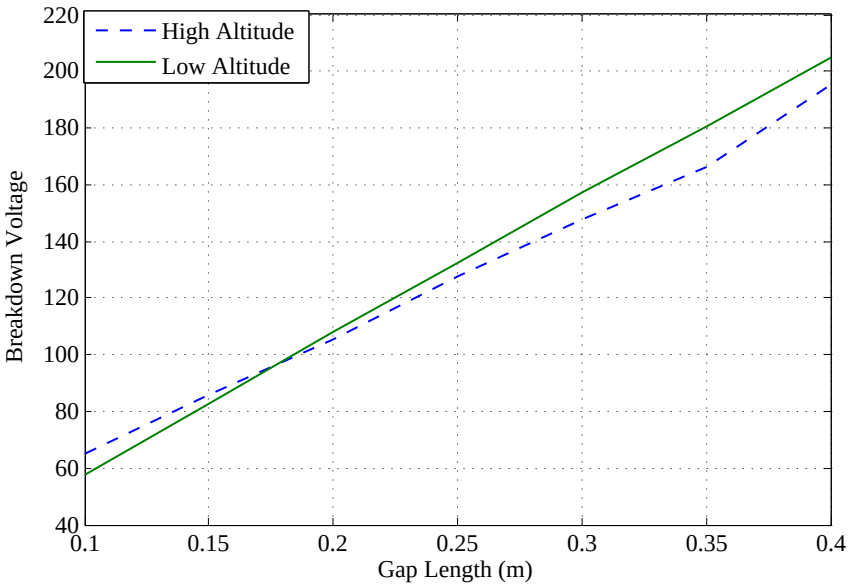


FIGURE 5.6: Comparison of IEC 60060-1 corrected low altitude and high altitude test results

then the corrections should converge to the same values. That is, in the figure showing the comparison of the two tests corrected according to IEC 60060-1 (Figure 5.6), it is expected that the two trend lines overlap but this is not the case. Below the gap length of 0.155 m, the corrected values are an average of 4.1% above the low altitude corrected values whereas above 0.155 m they are an average 9.2% below the low altitude corrected values.

Work also done in South Africa by Parus et al [5] shows that the IEC 60060-1 correction does not correct the breakdown voltages obtained at different altitudes to the same value. In their work, Parus et al compared IEC 60060-1 corrected results obtained at altitudes of 822 m, 1 500 m and 1 880 m asl. It was also observed that the corrected results at these three different altitudes do not converge to the same value as they should if the corrections methods were correct. In order to verify the above mentioned claims regarding the standard, tests were carried out at sea level. The comparison of the low altitude and high altitude corrected voltages to that of the sea level tests are shown in Figure 5.7. The environmental conditions during the sea level tests were not exactly as the conventional standard conditions mentioned in IEC 60060-1 (2010) (20°C, 1 013 mbar and 11 g/m$^3$). The temperature, pressure and humidity during testing averaged approximately 23°C, 1 012.8 mbar and 18 g/m$^3$m. The humidity was higher than the standard whereas the other parameters were comparable to the standard conditions.

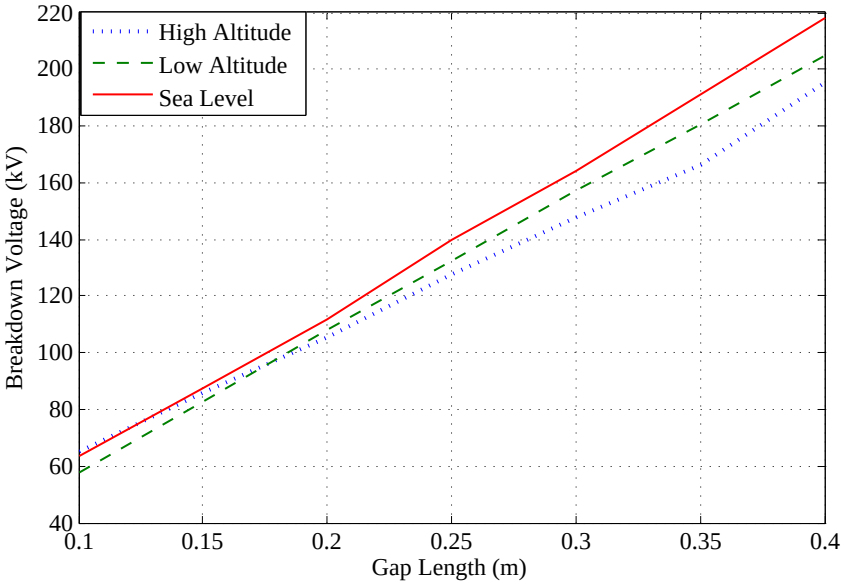


FIGURE 5.7: Comparison of IEC 60060-1 corrected low altitude and high altitude test results to sea level results

However, the conditions at sea level were the closest to the actual standard conditions, therefore the results are taken as the standard voltages. The low altitude data has an average error of 5.6% compared to the standard results, whereas the high altitude data has an average error of 7.1%. The high altitude data shows that as the gap length increases, the corrected voltage begins to deviate from the standard breakdown voltage. Both high altitude and low altitude corrections deviate from the sea level data by more than the acceptable 5% measurement error. However, the data shows that the corrections of low altitude data are more accurate than that of high altitude data.

Rickmann et al [22] state that in order to use the IEC 60060-1 correction, the relationship between $m$, $w$ and $g$ should be valid and this is when $(\delta \times k) \approx 1$. This condition can be confirmed by the Cigré brochure [11] used to determine the IEC 60060-1 correction. The brochure states that the standardized procedure was between $0.9 < (\delta \times k) < 1.1$. From the available data, this criteria is only met by the low altitude data as shown in Table 5.7.

This confirms the corrected data closest to the actual standard breakdown voltages is that of the low altitude tests as the results show.

TABLE 5.7: Table of $\delta \times k$ values

| | **Gap Length (m)** | $\delta$ | $\boldsymbol{k}$ | $\delta \times \boldsymbol{k}$ |
|---|---|---|---|---|
| Low Altitude | 0.10 | 0.95 | 1.03 | 0.98 |
| | 0.15 | 0.95 | 1.05 | 1.00 |
| | 0.20 | 0.95 | 1.05 | 0.99 |
| | 0.25 | 0.95 | 1.04 | 0.99 |
| | 0.30 | 0.95 | 1.05 | 1.00 |
| | 0.35 | 0.97 | 1.00 | 0.97 |
| | 0.40 | 0.95 | 1.01 | 0.96 |
| High Altitude | 0.10 | 0.85 | 0.93 | 0.79 |
| | 0.15 | 0.85 | 0.93 | 0.79 |
| | 0.20 | 0.84 | 0.91 | 0.77 |
| | 0.25 | 0.85 | 0.93 | 0.79 |
| | 0.30 | 0.85 | 0.94 | 0.80 |
| | 0.35 | 0.84 | 0.91 | 0.77 |
| | 0.40 | 0.85 | 0.94 | 0.80 |

## 5.2 Pressure Vessel Results

Since pressure was drawn from ambient in the pressure vessel, it was difficult to do a test at precisely the same pressure level for different gap lengths. Therefore, in order to have comparable data sets, the results were plotted against the relative air density due to the drawn vacuum for each test. By varying the relative air density, different altitudes were simulated. Table 5.8 shows the different relative air densities and the corresponding altitudes calculated as per equation 5.4 that were simulated during the experiments.

$$p = 1013.e^{\left(\frac{-H}{8150}\right)} \tag{5.4}$$

Where $H$ is the height above sea level in metres. Due to the limitation in gap length

TABLE 5.8: Approximate altitudes simulated during the tests

| $\delta$ | $\approx$ **Altitude (m)** |
|---|---|
| 0.82 | 1 600 |
| 0.77 | 2 100 |
| 0.72 | 2 700 |
| 0.67 | 3 200 |
| 0.62 | 3 800 |
| 0.57 | 4 500 |
| 0.53 | 5 200 |

because of the size of the chamber, only gaps up to 0.3 m were tested and the results are shown in Figure 5.8.

TABLE 5.9: Pressure Vessel Test Results

| Gap Length (m) | RAD | Average Breakdown (kV) | Std Deviation (%) |
|---|---|---|---|
| 0.1 | 0.82 | 49.7 | 1.7 |
| | 0.77 | 49.8 | 1.7 |
| | 0.72 | 47.5 | 5.9 |
| | 0.67 | 48.4 | 3.7 |
| | 0.57 | 55.6 | 1.0 |
| 0.2 | 0.82 | 99.6 | 4.3 |
| | 0.72 | 94.6 | 0.8 |
| | 0.63 | 86.9 | 1.4 |
| | 0.58 | 78.0 | 2.5 |
| | 0.53 | 85.9 | 2.2 |
| 0.3 | 0.82 | 155.9 | 7.0 |
| | 0.72 | 148.2 | 1.1 |
| | 0.62 | 129.8 | 2.8 |
| | 0.53 | 115.8 | 2.4 |

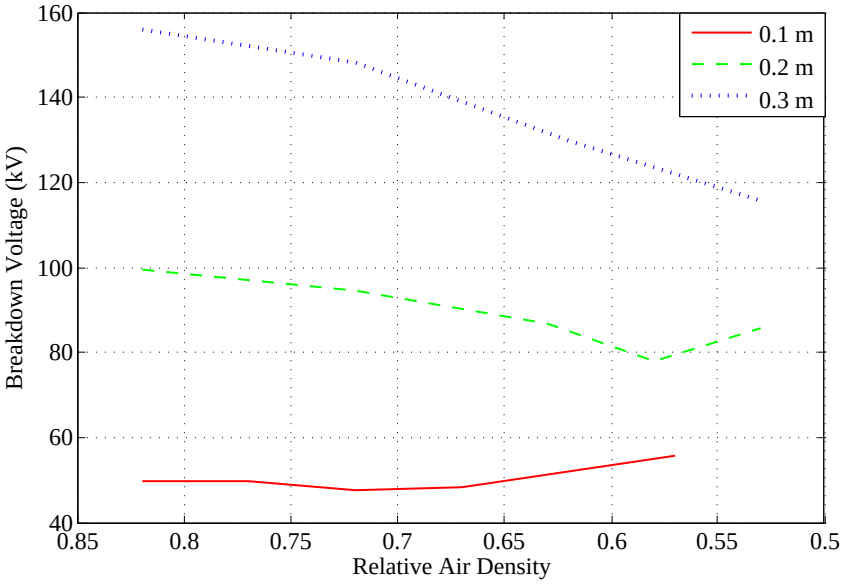


FIGURE 5.8: Results of breakdown voltage against relative air density in a variable pressure vessel

The results of the pressure vessel tests are shown in Table 5.9 and Figure 5.8 is a plot of the mean of 5 breakdowns per air gap per relative air density. The results obtained followed the expected trend of the breakdown voltage decreasing with a decrease in relative air density. However, it was observed that the breakdown voltage would start increasing with further decrease in relative air density after a certain threshold relative

air density. This trend was observed for the 0.1 m air gap and, more clearly, for the 0.2 m air gap.

Plots showing the statistical deviations about the mean of the recorded voltage data (5 breakdowns per air gap) are shown in Figure 5.9 to Figure 5.11.

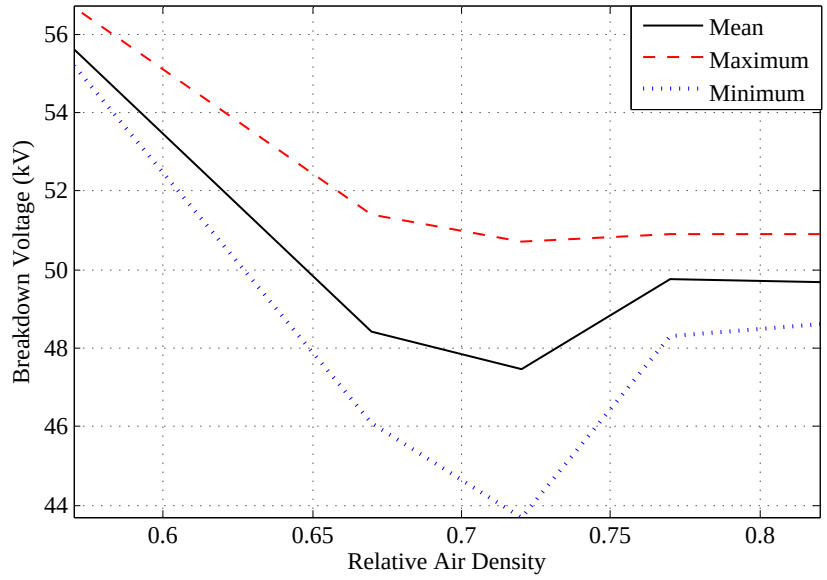


FIGURE 5.9: Variation of obtained breakdown voltages from the mean for 0.1 m gap

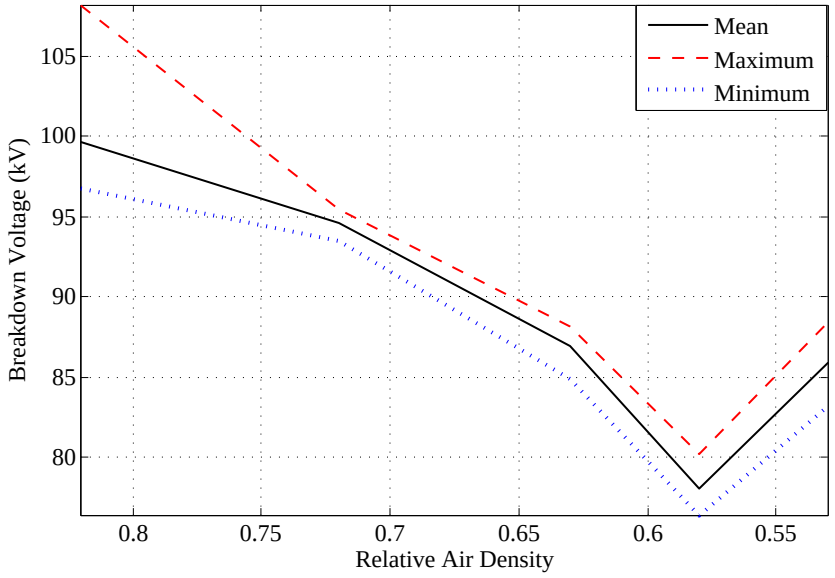


FIGURE 5.10: Variation of obtained breakdown voltages from the mean for 0.2 m gap

The maximum variation from the mean for the 0.1 m set of results is 7.9% at $\delta$=0.72, 8.6% at $\delta$=0.82 for the 0.2 m air gap and 9.8% at $\delta$=0.82 for the 0.3 m air gap length. These errors are particularly large and are mainly caused by an anomalous datum point

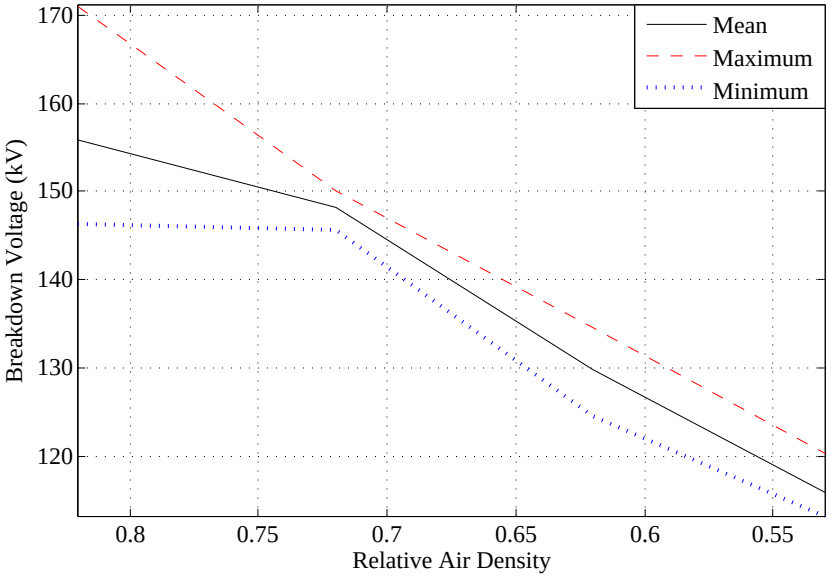


FIGURE 5.11: Variation of obtained breakdown voltages from the mean for 0.3 m gap

from the 5 points collected for that gap length at that voltage. These irregularities can be attributed to the presence of space charge in the chamber that can distort the electric field in an unexpected detrimental way. The average errors over the set of results are 3.9% for the 0.1 m air gap, 3.3% for the 0.2 m and 4.7% for the 0.3 m air gap. Therefore the results are deemed reasonably accurate as they fall within the acceptable error of 5% and therefore worthy to be used for the following analysis.

For the 0.1 m air gap, breakdown in air densities greater than 0.72 was not precursed by any visible corona on the electrode. However, lower than 0.72 relative air density, a bluish film glow was observed to ignite around the tip of the rod electrode. The blue glow would extinguish and replenish as the voltage was increased. It was at this stage that the breakdown voltage of the air gap began to deviate from the usual trend of getting smaller with a decrease in relative air density. The frequency of the extinguishing and ignition of the blue glow increased as the the air gap approached breakdown then erratic breakdown arcs would occur.

When conducting the same experiment on the 0.2 m gap, corona was observed along with a blue film glow identical to that observed in the 0.1 m air gap. The blue film glow became more prevalent as pressure was decreased until a point whereby a pressure threshold was met and instead of the breakdown voltage decreasing as per norm, the

breakdown voltage began to increase. The same behaviour was noticed during the experiment with the 0.3 m air gap, however, the pressure threshold whereby the voltage trend starts increasing with decrease in air density was not met due to the aforementioned chamber dimension constraints. From the results of the 0.1 m and 0.2 m air gaps, the threshold point occurred at a lower relative air density as the gap length is increased. Therefore, given a stronger vacuum pump and a bigger chamber, it would be expected that the 0.3 m air gap would behave similar the 0.1 m and 0.2 m air gaps.

### 5.2.1 Why Breakdown Voltage Initially Decreased But Started Increasing With Further Decrease In Pressure

In general, it is expected that as pressure decreases, the voltage required to break down an air gap also decreases. However, the results of the pressure vessel experiment showed an interesting trend in that the expected trend was true only up to a certain threshold beyond which the breakdown voltage would begin increasing with further reduction of pressure. This threshold pressure seems to be related to the size of the air gap under test. That is, as the gap length increased, then a lower pressure threshold would be required for the breakdown voltage to start increasing.

A search in literature provided two possible explanations for the increase in voltage as pressure decreased. One explanation is from the classical theory of breakdown mechanisms and the other explanation is based on the observed corona activity before breakdown occurred.

#### 5.2.1.1 Classical Theory of Breakdown Mechanisms

In the classical theory of breakdown mechanisms in a gas, the mean free path between molecules in a gas plays a significant role in the breakdown process. It has been already established that the mean free path is a function of pressure according to equation 5.5.

$$\lambda \ \alpha \ \frac{1}{p} \tag{5.5}$$

where $\lambda$ is the mean free path between molecules and $p$ is the pressure the molecules are subject to. The relationship in equation (5.5) implies that the higher the pressure, the smaller the mean free path between the molecules. A small mean free path limits

the ability of molecules to gain enough energy to be able to cause ionisation and initiate the breakdown process. Therefore, in order to breakdown the air under high pressure, a higher voltage is required for electrons to initiate the ionisation, thus implying that the probability of ionisation is low for gases under high pressure. But, as the pressure decreases, the mean free path increases and less voltage can be applied to initiate breakdown. Therefore the expected trend of the breakdown voltage of an air gap to decrease with and increase in altitude.

However, there is a point whereby the pressure is very low and the mean free path so large that the probability of ionisation becomes very low. That is, considering a closed system, the molecules available for ionisation will be fewer and far apart. All this follows Figure 5.12(Adapted from [29]) derived from equation (5.6) [28, 29]

$$\alpha = Ape^{\frac{-Bp}{E}} \tag{5.6}$$

where $\alpha$ is Townsend's first ionisation coefficient, $A$ and $B$ are constants that depend on the gas type and temperature, $p$ is the gas pressure and $E$ is the electric field. The

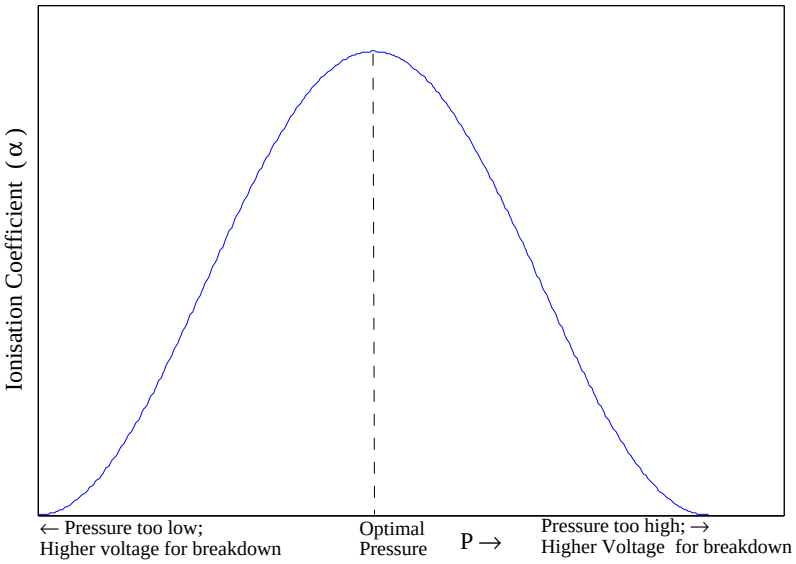


FIGURE 5.12: Probability of ionisation vs Pressure

variation of the pressure threshold as the air gaps get bigger can be attributed to the electric field the air was subjected to. Therefore, as the gap length increased, the electric field within the chamber also increased moving the threshold pressure lower.

#### 5.2.1.2 Corona Theory Under DC Stress

Another explanation for the observed increase in voltage as pressure decreases is the involvement of ion space charge during corona and breakdown. As observed in all three gaps, the presence of a blue film glow at lower relative air densities corresponded to an increase in breakdown voltage instead of the expected trend of decrease in breakdown voltage. This is similar to the positive glow mode of corona discharge [27]. The theory on positive corona discharge states that there are three modes of positive corona discharge under DC voltage stress. These modes listed according to increasing field intensity for their onset are [27]:

1. Burst corona
2. Onset streamer
3. Positive glow

Brief explanations for each of the modes are as follows.

**Burst Corona**

Burst corona is a result of ionisation occurring on the anode surface due to the electron avalanches from the cathode losing its energy as they neutralise at the anode [27]. As a result, positive ions are built up around the area where neutralisation occurred therefore creating a local positive space charge, which eventually kills the discharge at that point. Available free electrons are then neutralised at a different point on the anode while the positive space charge earlier developed fades away[27].

**Onset Streamer**

As the voltage (and electric field) is increased, the local space charge around the anode leads to field enhancement and attraction of the subsequent electron avalanches [27]. Due to the attraction of the subsequent electron avalanches to the positive space charge field, streamers are developed and extend farther into the areas of low electric field within the air gap thereby creating more positive ions (positive space charge) within

the low electric field region in the air gap. The overall effect of the subsequent electron avalanches, the free electrons being absorbed at the anode and low positive ion mobility leads to a net positive space charge being developed in front of the anode [27]. The electric field gradient in front of the anode therefore drops below the critical field (due to the positive space charge) required to sustain ionisation and the developed streamer is suppressed. The presence of an applied field, due to the voltage source, removes the created positive ion space charge and restores the initial field conditions and the process restarts. This ultimately leads to pulsating discharges occurring around the anode [27].

The attributes of the onset streamer were observed prior to breakdown during tests on the 0.1 m and 0.2 m air gaps at RADs of and below 0.77 and 0.57 (the knee points) respectively. Breakdown of the 0.1 m air gap at RAD 0.77 occurred soon after the presence of the onset streamer and no other corona mode was observed. The same occurred for the 0.2 m air gap between RADs of 0.72 and 0.62.

### Positive Glow

A continual increase in electric field increases the discharge and ionisation activities over the anode surface. Within the region of the intense ionisation activity, a luminous layer is created [27]. The positive glow is developed due to the applied electric field being strong enough to quickly repel the positive ion space charge from around the anode, therefore promoting ionisation activity on the anode surface. However, the field intensity is not strong enough to develop radial discharges that lead to the formation of streamers [27]. This leaves the surface of the anode with high intensity ionisation activity and the luminous glow is developed. The development and presence of the positive glow causes a significant increase in breakdown voltage [27].

During the experiments carried out in the lab, a faint blue luminous glow was observed at low RAD values. As the RAD values became lower, the blue luminous glow became brighter and that is when an increase in breakdown voltage was observed for the 0.1 m and 0.2 m air gaps. The blue luminous glow was also observed during the experiment with the 0.3 m air gap but breakdown occurred when the glow was not as bright as observed in the 0.1 m and 0.2 m experiments. The visual observations and the behaviour of the breakdown voltage suggests that the blue luminous glow observed was indeed a positive glow and signalled a change in the breakdown mechanisms. This observation

suggests that when improved correction factors are determined, they should include a factor that corresponds to the change in breakdown mechanisms for the air gap under test at the appropriate altitude.

### 5.2.2 Atmospheric Correction Factors on Pressure Vessel Test Results

#### 5.2.2.1 IEC 60060-1

IEC 60060-1 is the most common standard being used for atmospheric correction of air gaps and some high voltage equipment, like insulator strings. Despite the fact that the standard application is limited to a minimum relative air density of 0.8 [3] ( ≈2 000 m altitude), the correction factors were applied to the pressure vessel tests to find out whether indeed the IEC standard was not applicable to altitudes above 2 000 m.

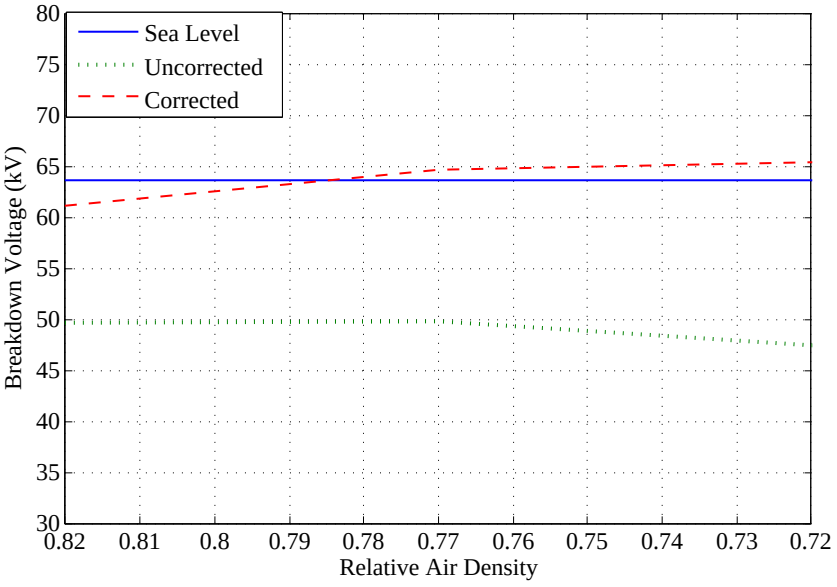


FIGURE 5.13: IEC 60060-1 correction of 0.1 m air gap results

The data of the three air gap sizes were corrected according to IEC 60060-1(2010) and the plots of the obtained data are shown in Figures 5.13 to 5.15. Data points beyond the knee point were removed from the correction as the data belongs to another regime of breakdown mechanisms. These data points are for the 0.1 m air gap where RAD is below 0.72 and for the 0.2 m air gap where RAD is below 0.58.

Figure 5.13 shows that the IEC 60060-1 standard corrects reasonably well for very small gaps, in this case, 0.1 m air gap. The correction applied to the data according to IEC

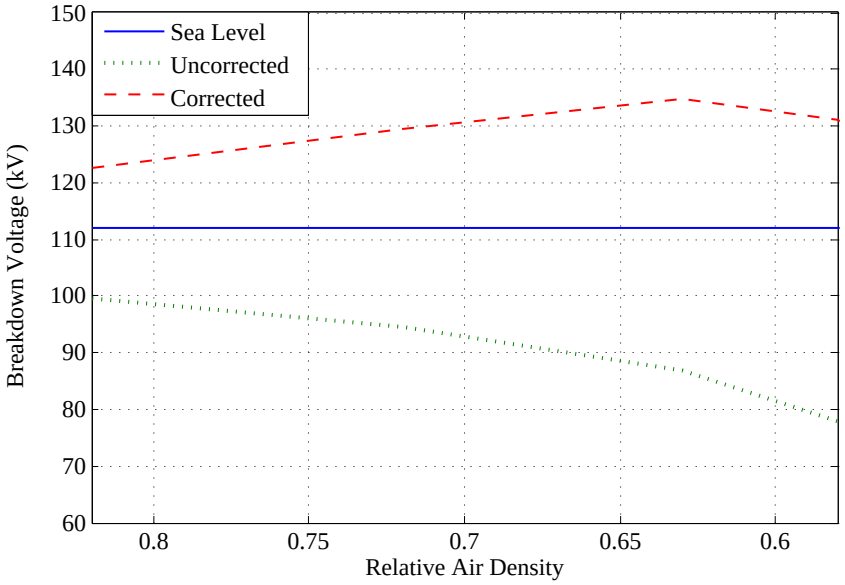


FIGURE 5.14: IEC 60060-1 correction of 0.2 m air gap results

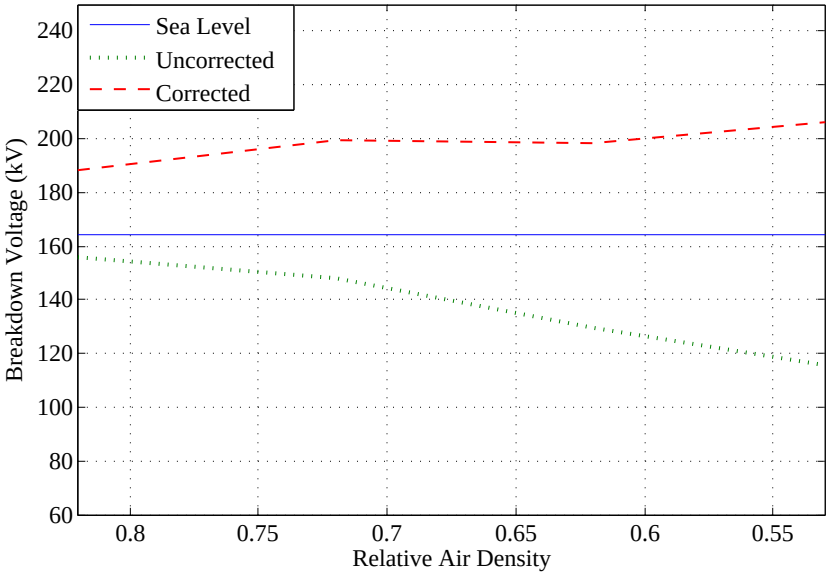


FIGURE 5.15: IEC 60060-1 correction of 0.3 m air gap results

60060-1 had an average 3% deviation from the expected sea level breakdown voltage. As was also observed in Figure 5.7, the IEC correction of the smallest gap size (0.1 m) is the most accurate despite the altitude. Figures 5.14 and 5.15 also confirm the trend shown by the low altitude and high altitude data in that as the gap length increases, the correction becomes more inaccurate. The average deviation from the sea level breakdown voltages for the 0.2 m and 0.3 m air gaps was 15.5% and 20.75% respectively. These deviations are large compared to the low altitude and high altitude data from the open

air experiments (5.6% and 7.1% respectively), thereby confirming that the IEC standard is indeed unsuitable for data obtained from RAD less than 0.8. The observed data also suggests that for very small gaps (in the order of 0.1 m and less), IEC 60060-1 is suitable when RAD is as small as 0.72.

The trend of the corrected voltages seem to suggest that the IEC 60060-1 has a mathematical flaw that does not allow it to correct appropriately for small relative air densities, or that there is change in breakdown mechanisms as RAD reduces. According to [30], the average breakdown electric field at time of breakdown is determined by equation 5.7 and can be used to determine the mechanism that caused the breakdown.

$$E_{Breakdown} = \frac{V_{breakdown}}{d_{breakdown}} \tag{5.7}$$

An electric field of approximately 500 kV/m implies a streamer dominated breakdown mechanism. This is because 500 kV/m has been adopted as the mean electric field for streamer propagation under standard atmospheric conditions [11]. By calculating the average electric fields of the obtained results using equation 5.7, the calculated electric fields imply streamer breakdown in all three air gaps. The calculated electric fields are shown in Table 5.10.

TABLE 5.10: Table showing the average electric fields during breakdown

| **Gap Length (m)** | **RAD** | **$E_{breakdown}$(KV/m)** |
|---|---|---|
| 0.1 | 0.82 | 497.00 |
| | 0.77 | 497.60 |
| | 0.72 | 474.60 |
| | 0.67 | 484.20 |
| | 0.57 | 556.00 |
| 0.2 | 0.82 | 498.20 |
| | 0.72 | 472.90 |
| | 0.63 | 434.40 |
| | 0.58 | 390.00 |
| | 0.53 | 429.30 |
| 0.3 | 0.82 | 519.67 |
| | 0.72 | 493.87 |
| | 0.62 | 432.80 |
| | 0.53 | 386.00 |

However, it is expected that electric field required for positive streamer propagation should be proportional to air density [11]. This is to imply that if the breakdown of

the air gaps was dominated by positive streamers, it would have been expected that the electric field also decrease with a decrease in relative air density for all three gap lengths, but this is not so for the 0.1 m air gap. The air gap seems to be displaying varying electric fields as the relative air density decreases.

The Cigré brochure [11] states that the parameter **g** (calculated from equation 5.8 where L is the discharge length and $k$ is a parameter for the voltage type used) is used to give an estimate of the similarity of the discharge to that of a pure positive streamer.

$$g = \frac{U_{50}}{500\delta Lk} \tag{5.8}$$

The brochure states that [11]:

- **g**≈1 implies a positive streamer discharge process. This is when the dielectric strength is expected to be proportional to the relative air density
- **g**<1 implies a streamer and leader dominated discharge with the dielectric strength is not as influenced by the relative air density
- 1<**g**<2 implies a positive and negative streamer dominated discharge process and the situation is deemed "very complicated"
- **g**>2 implies a uniform air gap and the breakdown is corona dominated.

To be able to determine the breakdown mechanisms of the air gaps, the parameter **g** was calculated for each air gap and shown in Table 5.11. The calculated **g** parameters were all found to be between 1 and 2, implying both negative and positive streamer dominated discharge thus presenting a "complicated"scenario.

From the principles used to derive the IEC 60060-1 standard, the relationship in equation 5.9 was established

$$\delta^m = \frac{U_b}{500d} \tag{5.9}$$

where $m$ is a parameter that covered the influence of the environmental conditions, the waveform applied and the parameters of the insulation under test [30]. When the breakdown process of an air gap is streamer dominated, then $m$=1 [30]. According to IEC 60060-1, $m$=1 when 1<**g**<2, which is when the positive and negative streamers dominate the discharge process. For the collected data, the calculated $m$ values according

TABLE 5.11: Table showing the calculated g-factors

| **Gap Length (m)** | $\delta$ | **g** |
|---|---|---|
| 0.1 | 0.82 | 1.22 |
| | 0.77 | 1.30 |
| | 0.72 | 1.33 |
| | 0.67 | 1.45 |
| | 0.57 | 1.96 |
| 0.2 | 0.82 | 1.23 |
| | 0.72 | 1.32 |
| | 0.63 | 1.39 |
| | 0.58 | 1.37 |
| | 0.53 | 1.63 |
| 0.3 | 0.82 | 1.25 |
| | 0.72 | 1.35 |
| | 0.62 | 1.37 |
| | 0.53 | 1.42 |

the equation 5.9 were mostly negative. This scenario shows a problem with the IEC 60060-1 whereby the same $m$ value is used to correct voltages governed by different environmental, waveform and insulation material parameters. This concern was also shared by [22]. Therefore, there is a need for a more refined method to determine the $m$ parameter in order to obtain accurate corrections.

#### 5.2.2.2 Calva's Method Applied For Comparison With Pressure Vessel Tests

The results of the experiment were compared to the procedure proposed by Calva et al [9] according to equations 5.1 to 5.3. The comparison of the test results to the Calva prediction are found in Table 5.12 and in Figure 5.16 to Figure 5.18. The plots show that the proposed method by Calva does not cater for the increase in voltage with the further decrease in pressure, but it does provide some form of trend that agrees with the experimental data.

The trend in the results shows that the Calva prediction method can be modified to fit the experimental data.

TABLE 5.12: Pressure Vessel Test Results Compared to Calva Prediction

| **Gap Length (m)** | **RAD** | **Average Breakdown (kV)** | **Calva Prediction (kV)** | **Error (%)** |
|---|---|---|---|---|
| 0.1 | 0.82 | 49.7 | 45.9 | 8 |
| | 0.77 | 49.8 | 41.7 | 16 |
| | 0.72 | 47.5 | 37.6 | 21 |
| 0.2 | 0.82 | 99.6 | 85.3 | 14 |
| | 0.72 | 94.6 | 69.9 | 26 |
| | 0.63 | 86.9 | 56.7 | 35 |
| | 0.58 | 78.0 | 47.8 | 39 |
| 0.3 | 0.82 | 155.9 | 126.1 | 19 |
| | 0.72 | 148.2 | 105.1 | 29 |
| | 0.62 | 129.8 | 85.4 | 34 |
| | 0.53 | 115.8 | 68.4 | 41 |

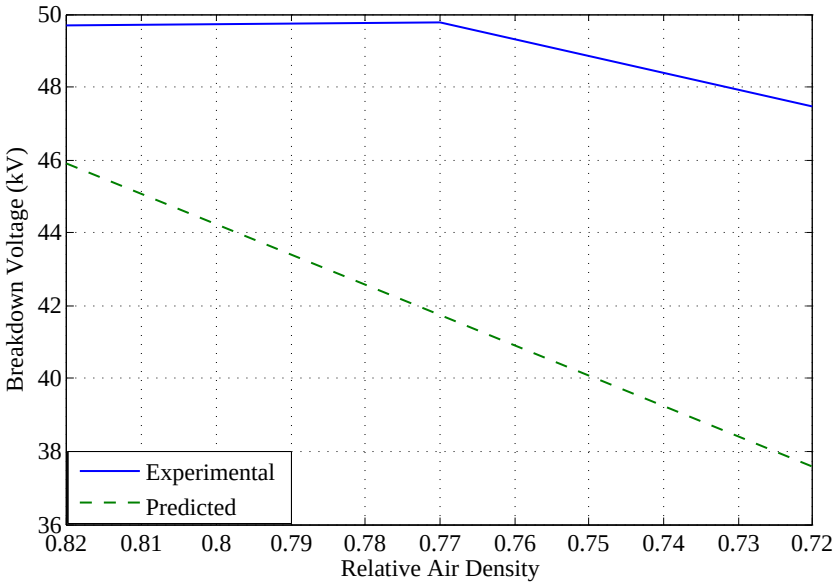


FIGURE 5.16: Comparison of experimental results with Calva's prediction method for 0.1 m air gap

#### 5.2.2.3 Mapping of Calva's Prediction Method to the Experimental Data

In order to map the Calva predicted results to the experimental data, a difference function was derived and added to the Calva prediction function. By so doing, the Calva prediction function was therefore scaled in gradient and mapped upwards to fit the experimental data. This method was done considering that a linear trend was observed in the results and therefore a linear function was deemed suitable for the mapping. The data points where the breakdown voltage began to increase due to the corona were not considered.

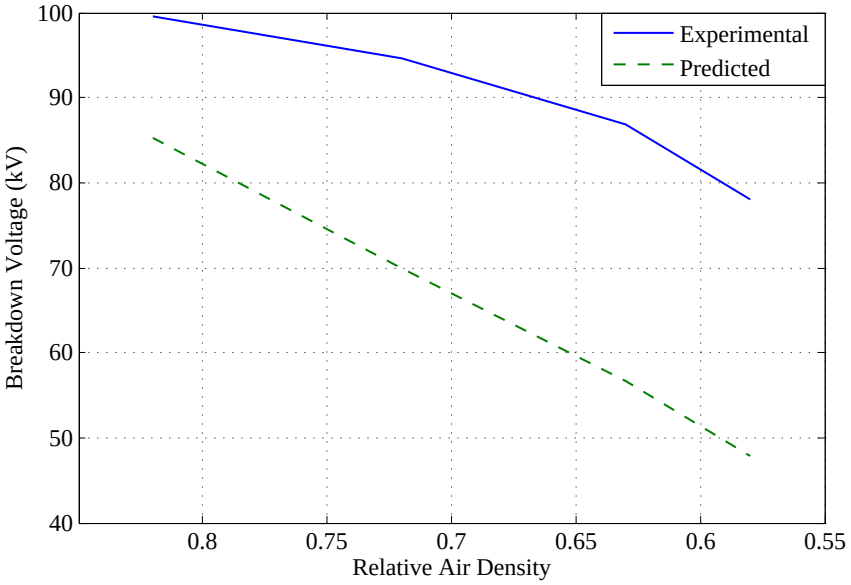


FIGURE 5.17: Comparison of experimental results with Calva's prediction method for 0.2 m air gap

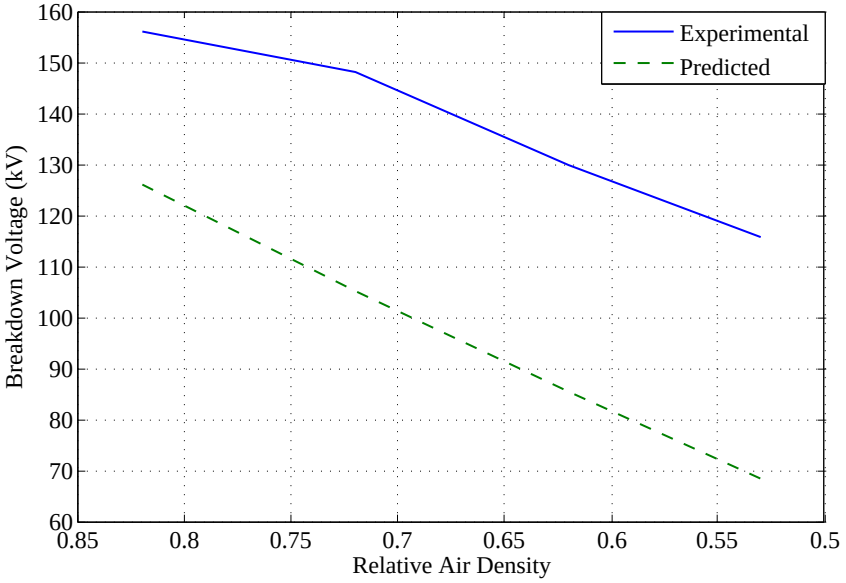


FIGURE 5.18: Comparison of experimental results with Calva's prediction method for 0.3 m air gap

Consider the pressure vessel experiment for the 0.1 m gap size with information in Table 5.13.

The difference between the experimental breakdown voltage ($U_b$) and the Calva predicted breakdown voltage ($U_{b(predicted)}$) is calculated and plotted against the relative air density ($\delta$) as shown in Figure 5.19. A line of best fit was then determined to create

TABLE 5.13: Pressure vessel 0.1 m gap test information

| $\delta$ | $\mathbf{U_b}$**(kV)** | $\mathbf{U_{b(predicted)}}$**(kV)** | $\mathbf{U_b}$-$\mathbf{U_{b(predicted)}}$ | **Calva+Difference function** |
|---|---|---|---|---|
| 0.82 | 49.7 | 45.92 | 3.78 | 49.90 |
| 0.77 | 49.76 | 41.74 | 8.02 | 48.77 |
| 0.72 | 47.46 | 37.59 | 9.87 | 47.76 |

the difference equation (equation (5.10)) which would be added to the Calva prediction function.

$$U_{diff} = -61\delta + 54 \tag{5.10}$$

The resulting function, shown in equation 5.12, where $U_{diff}$ is defined in equation 5.10 and the other terms are as previously defined. Equation 5.12 shows the adjusted prediction method for the 0.1 m air gap tests and it is plotted to compare how accurate it is in relation to the experimental data in Figure 5.20.

$$V_b = [500d(k_1 + k_2)S] + U_{diff} \tag{5.11}$$

$$V_b = [500d(k_1 + k_2)S] - 61\delta + 54 \tag{5.12}$$

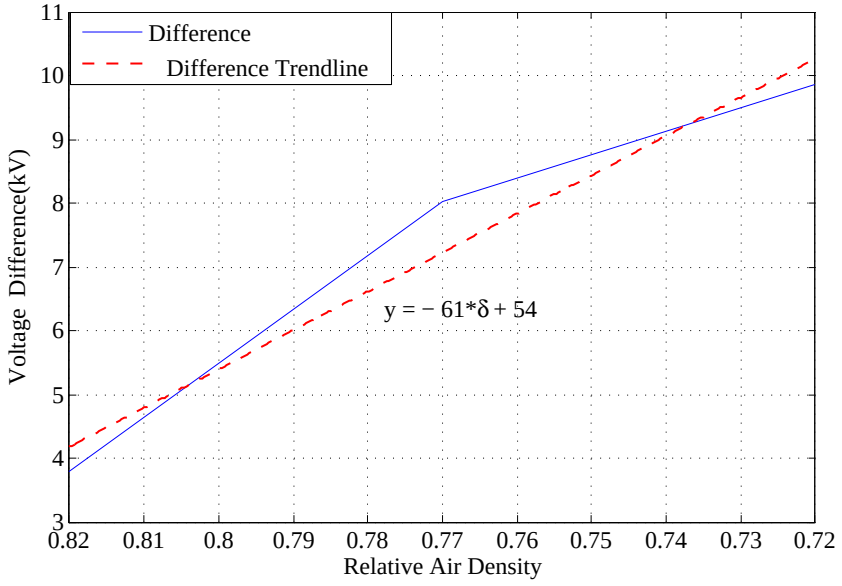


FIGURE 5.19: Difference function for 0.1 m pressure vessel experiment

The application of the difference method to the 0.1 m gap pressure vessel experiments produced a result with absolute errors shown in Table 5.14 of each reading taken.

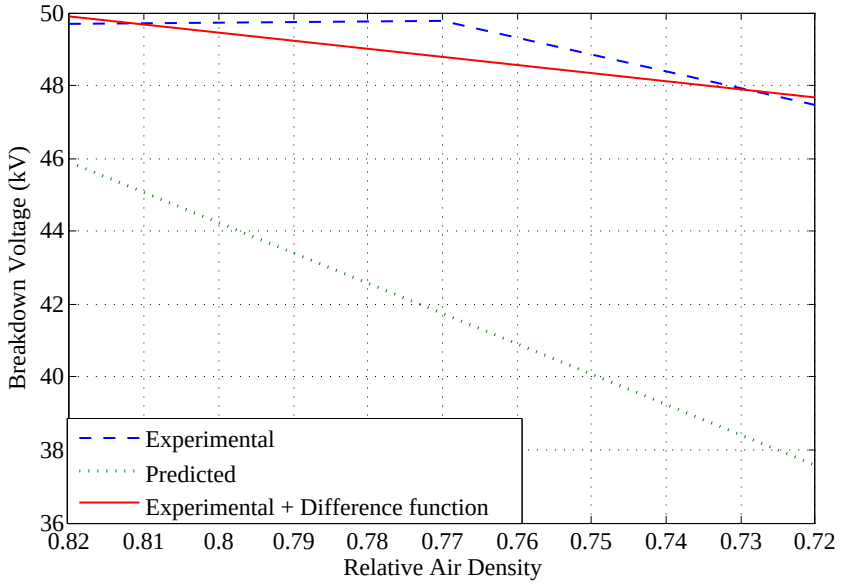


FIGURE 5.20: Comparison of prediction including difference method for 0.1 m gap length

TABLE 5.14: Error of mapped data to experimental data for 0.1 m air gap

| $\delta$ | $\mathbf{U_b(kV)}$ | $\mathbf{U_{b(mapped)}(kV)}$ | **Absolute Error (%)** |
|---|---|---|---|
| 0.82 | 49.70 | 49.90 | 0.40 |
| 0.77 | 49.76 | 48.77 | 2.03 |
| 0.72 | 47.46 | 47.67 | 0.44 |

The error of the mapping for the 0.1 m gap size is within the acceptable statistical variation 5%. The same procedure was repeated for the 0.2 m and 0.3 m air gap sizes. The difference functions to be added to the Calva prediction method, as done in equation 5.12, for the 0.2 m and 0.3 m air gaps are shown in equations 5.13 and 5.14 respectively.

$$U_{diff} = -68\delta + 72 \tag{5.13}$$

$$U_{diff} = -57\delta + 79 \tag{5.14}$$

Similar plots to Figure 5.20 were done for the 0.2 m and 0.3 m gaps and are shown in Figure 5.21 and Figure 5.22 respectively.

Tables 5.15 and 5.16 show the errors of the mapping for each gap length. The tables show that the mapping applied reduced the error in experimental and predicted results to within 5%.

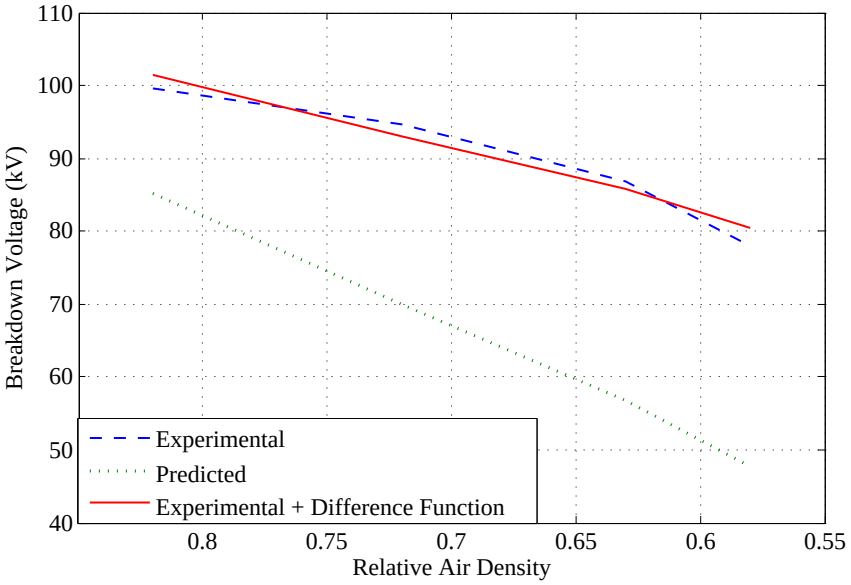


FIGURE 5.21: Comparison of prediction including difference method for 0.2 m gap length

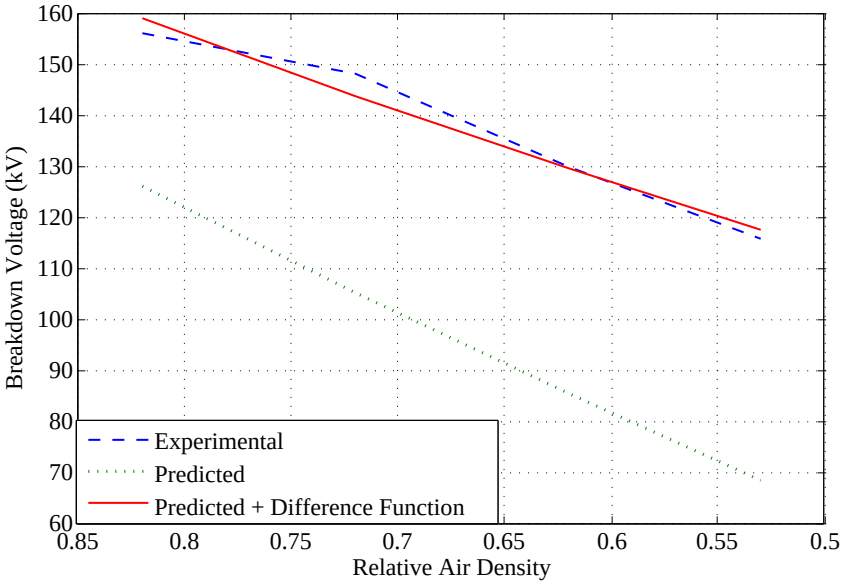


FIGURE 5.22: Comparison of prediction including difference method for 0.3 m gap length

TABLE 5.15: Error of mapped data to experimental data for 0.2 m air gap

| $\delta$ | $\mathbf{U_b(kV)}$ | $\mathbf{U_{b(mapped)}(kV)}$ | **Absolute Error (%)** |
|---|---|---|---|
| 0.82 | 99.64 | 101.49 | 1.86 |
| 0.72 | 94.58 | 92.96 | 1.71 |
| 0.63 | 86.88 | 85.84 | 1.20 |
| 0.58 | 78.00 | 80.36 | 3.03 |

TABLE 5.16: Error of mapped data to experimental data for 0.3 m air gap

| $\delta$ | $\mathbf{U_b}$**(kV)** | $\mathbf{U_{b(mapped)}}$**(kV)** | **Absolute Error (%)** |
|---|---|---|---|
| 0.82 | 155.90 | 158.99 | 1.98 |
| 0.72 | 148.16 | 143.59 | 3.09 |
| 0.62 | 129.84 | 129.50 | 0.26 |
| 0.53 | 115.80 | 117.60 | 1.55 |

Tables 5.14 to 5.16 show that the prediction method proposed by Calva is viable for predicting the breakdown voltage of small air gaps at low relative air densities when modified by adding equations 5.10 to 5.14 to the Calva prediction method for air gaps of sizes 0.1 m - 0.3 m respectively in order to attain accuracy within 5%. Due to limitations in supply voltage, pressure vessel size and pump drawing ability, more data could not be collected for a wider range of relative air density and gap size. Therefore, the adjustments made to the Calva prediction method for the respective gap sizes are specifically for the mentioned gap sizes and relative air density range.

Due to the lack of a large data set and the number of variables involved in the breakdown process of air (relative air density, humidity, rod geometry etc), the difference equations could not be generalized into a single function to be added to the Calva prediction method so that it applies to any gap length and this could be an interesting extension of this work in the future. Also, by collecting more data, the difference equation may change in order to fit all the possible RAD ranges and also increase the accuracy of the function.

---

*Closing Summary In Answering the Research Question Of This Dissertation*

---

Tests were conducted and it has been shown that the atmospheric correction procedure in the IEC 60060-1 (2010) is more suitable for use when applied to low altitude data. When applied to high altitude data (1 740 m), the procedure has been found to introduce errors as the gap length increases. The Calva prediction method has proved to be accurate when applied to data below 1 740 m in altitude. Despite the IEC 60060-1 (2010) stating that the atmospheric procedure is inapplicable when RAD is less than 0.8, corrected data from the pressure vessel suggests that the procedure is accurate for very small air gaps (0.1 m and below) up to RAD 0.72. The results from the other air gap sizes tested (0.2 m and 0.3 m) agree with the claim by IEC 60060-1 (2010) in the standards

inability to obtain accurate atmospheric correction factors when RAD is lower than 0.8. Calva's prediction method was inaccurate when applied to the pressure chamber conditions, but the prediction methods results followed the trend of the experimental results. Factors were derived to add to the Calva prediction method for the method to fit the experimental data.

The experiment conducted in the pressure vessel showed that as pressure decreases, the breakdown voltage of the same gap length decreases until a threshold whereby the voltage begins to increase. This behaviour was explained by means of the classical breakdown theory and the corona mechanisms under HVDC stress.

Therefore, the altitude correction method stated in IEC 60060-1 (2010) and the Calva prediction method are both applicable and accurate when applied to low altitude data. Calva's model has an advantage in that it can predict the breakdown voltage of an air gap by considering the environmental conditions and the air gap length only. Whereas, the IEC 60060-1 (2010) standard requires more parameters. Both IEC 60060-1 (2010) standard and the Calva prediction method are not applicable for a wide altitude range. However, the Calva prediction method can be modified so as to increase the accuracy. The method is therefore recommended for further modification.

# Chapter 6

# Conclusions and Recommendations

## 6.1 Conclusions

The following are the important findings and conclusions of the research:

### Open Air Tests (0 m - 1 740m asl)

1. IEC 60060-1 altitude correction factors' accuracy improves with reduction in altitude.
2. IEC altitude correction factors confirmed to be applicable for altitudes below 1 800 m asl. However, the increase in error is apparent as the altitude and air gap length increases.
3. The Calva prediction method accurately predicts the DC breakdown voltage for air gaps within the 5% acceptable error at altitudes up to 1 740 m asl.

**Pressure Vessel Tests Simulating High Altitudes (1 740 m - 5 200 m asl)**

1. At simulated altitudes higher than 1 740 m, IEC 60060-1 correction factors are inaccurate (resulting in errors greater than 5%). This confirms that the standard does not apply for altitudes above 1 740 m asl.

2. Each gap size breakdown voltage as a function of altitude has a knee point threshold where the trend changes from decrease of breakdown voltage with decrease in pressure to an increase in voltage with further decrease in pressure.

3. For each gap length, the Calva prediction method can be modified to accurately predict the breakdown voltage at high altitude.

## 6.2 Recommendations For Future Work

The following recommendations have been suggested to further the current research:

- It is imperative that tests be done at sea level to obtain baseline breakdown voltages. These tests should be done at the standard temperature of $20^0$C and can be taken as the standard breakdown voltage of the tested gap sizes. All proposed atmospheric correction methods applied should produce results that compare to the standard voltages obtained.

- The work conducted in this work was done using positive polarity HVDC. It is recommended that the work be redone using negative polarity so that it can be compared whether the gaps perform in a similar mechanism to that of the positive polarity. That is, to test whether a significant increase in breakdown voltage is observed at lower pressures and if the Calva prediction method does produce similar results to those experimentally obtained.

- Tests results for the same gap sizes are required for altitudes with RADs of 0.77, 0.72, 0.62 and 0.53. These results can be used to compare with those obtained in the pressure vessel.

- The work can repeated for increased gap sizes. This would imply a bigger pressure vessel and higher voltages and would pose the problem of a bushing. Therefore a new pressure vessel that could meet the given requirements should be designed.

- It is recommended that more results be obtained for various gap sizes at various RADs. This is to increase the data available to accurately derive the appropriate function to add to the Calva prediction method. Overall, it would be desired that a general function be derived for adding to the Calva prediction method instead of different functions specific to an air gap as done in this work.

- In order to obtain photographic evidence of the breakdown mechanism that occur during the breakdown process, it is recommended that a high speed camera be acquired.

# References


[1] P. Tuson. HVDC Strengthening in Southern Africa. In *Power Engineering Society Conference and Exposition in Africa, 2007. PowerAfrica '07. IEEE*, pages 1–6, July 2007. doi: 10.1109/PESAFR.2007.4498096.

[2] Marco Glastra. Drakensberg-mafadi peak. URL http://www.footprint.co.za/drakensberg_mafadi.htm. Last accessed: 25 February 2016.

[3] SANS 60060-1. High-voltage test techniques. part 1: General definitions and test requirements, 2011.

[4] T. Britten, L. Pillay, P. Naidoo, F F. Bologna, D. Muftic, and N. Ijumba. Eskom's proposed strategic research into hvdc transmission. *IEEE Power and Energy Magazine*, pages 28–32, July 2005.

[5] N. Parus, I R. Jandrell, N. Mahatho, T. Govender, and H A. Roets. Live work under hvdc voltage: An investigation into altitude effects of flashover voltage for rod-plane air gaps. In *Proceedings of the Eighteenth International Symposium on High Voltage Engineering*, Seoul, South Korea, August 2013.

[6] F.W. Peek. Effect of altitude on the spark-over voltages of bushings, leads and insulators. *Transactions of the American Institute of Electrical Engineers*, XXXIII(2):1721–1730, June 1914. ISSN 0096-3860. doi: 10.1109/T-AIEE.1914.4765197.

[7] T. Udo and Yasuo Watanabe. Dc high-voltage sparkover characteristics of gaps and insulator strings. *IEEE Transactions on Power Apparatus and Systems,*, PAS-87(1):266–270, Jan 1968. ISSN 0018-9510. doi: 10.1109/TPAS.1968.291998.

[8] N.L. Allen, M. Boutlendj, and H.A. Lightfoot. Dielectric breakdown in nonuniform field air gaps. *IEEE Transactions on Electrical Insulation,*, 28(2):183–191, Apr 1993. ISSN 0018-9367. doi: 10.1109/14.212243.

[9] P.A. Calva, V. del Moral, M.G. Marquez, and G.P. Cabrera. In *Conference on Electrical Insulation and Dielectric Phenomena, 2003. Annual Report.*

[10] N.L. Allen. Correction procedures for high-voltage measurements under a variable air density. *IEEE Proceedings on Science, Measurement and Technology*, 153(5):194–200, September 2006. ISSN 1350-2344. doi: 10.1049/ip-smt:20050040.

[11] WG 33-07. Guidelines for the evaluation of the dielectric strength of external insulation, 1992.

[12] A. Robledo-Martinez and P A. Calva. Dc breakdown characteristics of rod-rod and rod-plane gaps in reduced-density air. In *Proceedings of the Sixth International Symposium on High Voltage Engineering*, volume 3, New Orleans, USA, 1989.

[13] M. Boutlendj and N L. Allen. Assessment of air-density correction for practical electrode systems. *European Transactions on Electrical Power*, 6(4):267–274, July 1996.

[14] IEEE standard for high-voltage testing techniques. *IEEE Std 4-2013 (Revision of IEEE Std 4-1995)*, pages 1–213, May 2013. doi: 10.1109/IEEESTD.2013.6515981.

[15] H J. Geldenhuys. The breakdown voltage of air in a 50 cm rod-plane gap over a practical range of air density and humidity. *$5^{th}$ International Symposium on High Voltage Engineering*, 1987.

[16] A. Pigini, G. Sartorio, M. Moreno, M. Ramirez, R. Cortina, E. Garbagnati, A.C. Britten, and K.J. Sadurski. Influence of air density on the impulse strength of external insulation. *IEEE Transactions on Power Apparatus and Systems*, PAS-104(10):2888–2900, Oct 1985. ISSN 0018-9510. doi: 10.1109/TPAS.1985.319134.

[17] SANS 60060-1. High-voltage test techniques. part 1: General definitions and test requirements, 1989.

[18] M. Ramirez, M. Moreno, A. Pigini, G. Rizzi, and E. Garbagnati. Air density influence on the strength of external insulation under positive impulses: Experimental investigation up to an altitude of 3000m a.s.l. *IEEE Transactions on Power Delivery*, 5(2):730–737, April 1990.

[19] K. Feser and J. Schmid. Temperature effect on the streamer breakdown of air. In *Proceedings of the Sixth International Symposium on High Voltage Engineering*, volume 3, New Orleans, USA, August 1989.

[20] IEC 60071-2. Insulation co-ordination- part 2: Application guide, 1996.

[21] I. Gutman, A. Pigini, J. Rickmann, J. Fan, D. Wu, and E. Gockenbach. Atmospheric and altitude correction of air gaps, clean and polluted insulators: state-of-the-art within Cigré and IEC. Number D1-213, France, August 2014.

[22] J. Rickmann et al. Analysis and comparison of atmospheric and altitude correction methods for air gaps and clean insulators. In *Proceedings of the Eighteenth International Symposium on High Voltage Engineering*, number OC2-03, pages 542–547, Seoul, South Korea, August 2013.

[23] H. Isa, Y. Sonoi, and M. Hayashi. Breakdown process of a rod-to-plane gap in atmospheric air under dc voltage stress. *IEEE Transaction on Electrical Insulation*, 26(2), April 1991.

[24] T. Suzuki, K. Miyake, and T. Hara. Breakdown process in rod-to-plane gaps with dc voltages. *IEEE Transactions on Industry Applications*, IA-21(1), January/February 1985.

[25] T. Christen, H.Bohme, A. Pedersen, and A. Blaszczyk. Streamer line modeling. In *Scientific Computing in Electrical Engineering*, volume 16 of *Mathematics in Industry*. Springer-Verlag, New York, 2012.

[26] M.S. Naidu and V. Kamaraju. *High Voltage Engineering*. Tata McGraw Hill Education Private Limited, 2009. ISBN 9780070669284.

[27] F.A.M. Rizk and G.N. Trinh. *High Voltage Engineering*. Taylor & Francis, 2014. ISBN 9781466513761.

[28] E. Kuffel, W.S. Zaengl, and J. Kuffel. *High Voltage Engineering: Fundamentals*. Applied Electricity and Electronics. Butterworth-Heinemann, 2000. ISBN 9780750636346.

[29] F.H. Kreuger. *Industrial High Voltage 1, 2, 3*. Delft University Press, Delft, Netherlands, 1991.

[30] D. Wu and J. Rickmann. Challenges in developing a unified method for atmospheric correction. Cigré SCD1 Colloquium, Cigré, Rio de Janeiro, Brazil, 2015.

# Appendix A

# Experimental Data And Results

Table A.1: Low Altitude Experimental Data

| **Gap Length(m)** | **0.10** | **0.15** | **0.20** | **0.25** | **0.30** | **0.35** | **0.40** |
|---|---|---|---|---|---|---|---|
| **Temperature($^0$C)** | 27.6 | 26.2 | 27.8 | 26.5 | 27.2 | 21.9 | 25.5 |
| **Pressure (mbar)** | 987.8 | 986.3 | 986.1 | 985.4 | 985.2 | 985.8 | 985.5 |
| **Rel. Humidity (%)** | 48.6 | 56.0 | 51.8 | 54.8 | 54.9 | 56.0 | 46.0 |
| **Test 1(kV)** | 57.4 | 81.8 | 107.6 | 131.7 | 157.3 | 174.8 | 197.0 |
| **Test 2(kV)** | 55.6 | 81.6 | 107.8 | 131.6 | 156.5 | 174.9 | 196.9 |
| **Test 3(kV)** | 57.4 | 83.0 | 107.3 | 131.6 | 156.8 | 174.7 | 196.3 |
| **Test 4(kV)** | 56.9 | 82.6 | 107.6 | 131.3 | 157.6 | 174.8 | 197.0 |
| **Test 5(kV)** | 57.3 | 82.2 | 107.8 | 131.2 | 157.3 | 175.4 | 196.6 |
| **Ave. Breakdown Voltage (kV)** | 56.92 | 82.24 | 107.62 | 131.48 | 157.1 | 174.92 | 196.76 |

Table A.2: High Altitude Experimental Data

| **Gap Length(m)** | **0.10** | **0.15** | **0.20** | **0.25** | **0.30** | **0.35** | **0.40** |
|---|---|---|---|---|---|---|---|
| **Temperature(0C)** | 15.3 | 14.4 | 15.4 | 14.9 | 15.1 | 15.8 | 14.8 |
| **Pressure (mbar)** | 844.7 | 841.7 | 840.2 | 841.1 | 842.3 | 839.7 | 842.3 |
| **Rel. Humidity (%)** | 41 | 45 | 34 | 42 | 46 | 33 | 47 |
| **Test 1(kV)** | 54.2 | 68.2 | 81.1 | 100.8 | 118.8 | 129.4 | 156.8 |
| **Test 2(kV)** | 52.5 | 66.3 | 80.9 | 99.7 | 119.0 | 130.0 | 157.2 |
| **Test 3(kV)** | 52.4 | 68.3 | 81.1 | 100.2 | 118.4 | 129.6 | 156.2 |
| **Test 4(kV)** | 51.2 | 68.1 | 81.4 | 100.0 | 116.6 | 130.0 | 157.2 |
| **Test 5(kV)** | 52.2 | 67.9 | 81.5 | 100.1 | 118.2 | 130.6 | 156.6 |
| **Ave. Breakdown Voltage (kV)** | 52.50 | 67.75 | 81.18 | 100.15 | 118.20 | 129.92 | 156.80 |

TABLE A.3: Sea Level Results

| **Gap length (m)** | **0.10** | **0.15** | **0.20** | **0.25** | **0.30** | **0.40** |
|---|---|---|---|---|---|---|
| **Temperature** | 23.6 | 23.5 | 23.4 | 23.4 | 23.3 | 23.3 |
| **Pressure (mbar)** | 1012.4 | 1012.4 | 1012.5 | 1012.6 | 1012.8 | 1012.7 |
| **Rel. Humidity (%)** | 89 | 89 | 90 | 90 | 92 | 92 |
| **Test 1 (kV)** | 64.0 | 87.0 | 112.0 | 140.0 | 164.0 | 218.0 |
| **Test 2 (kV)** | 64.0 | 87.0 | 112.0 | 140.0 | 164.0 | 218.0 |
| **Test 3 (kV)** | 63.0 | 88.0 | 113.0 | 140.0 | 164.0 | 216.0 |
| **Test 4 (kV)** | 63.0 | 88.0 | 111.0 | 140.0 | 165.0 | 220.0 |
| **Test 5 (kV)** | 64.0 | 87.0 | 112.0 | 139.0 | 164.0 | 218.0 |
| **Ave. Breakdown Voltage (kV)** | 63.6 | 87.4 | 112.0 | 139.8 | 164.2 | 218.0 |

TABLE A.4: Pressure Vessel Test Experimental Data

| **Gap Length (m)** | **0.1** | | | | | **0.2** | | | | | **0.3** | | | |
|---|---|---|---|---|---|---|---|---|---|---|---|---|---|---|
| **Ambient Pressure(mbar)** | 835.9 | 835.6 | 834.7 | 835.1 | 831.5 | 831.5 | 834.4 | 837.2 | 837.4 | 837.1 | 838.8 | 838.4 | 837.9 | 837.5 |
| **Test Pressure(mbar)** | 835.9 | 785.6 | 734.7 | 685.1 | 581.5 | 831.5 | 734.4 | 637.2 | 587.4 | 537.1 | 838.8 | 738.4 | 637.9 | 537.5 |
| **Temperature($^0$C)** | 23.2 | 23.2 | 23.1 | 23.2 | 23.2 | 20.4 | 20.2 | 20.3 | 20.3 | 20.2 | 22.1 | 22.3 | 22.5 | 23.1 |
| **Rel. Humidity(%)** | 42 | 42 | 42 | 43 | 44 | 48 | 49 | 49 | 45 | 49 | 49 | 50 | 50 | 49 |
| $\delta$ | 0.82 | 0.77 | 0.72 | 0.67 | 0.57 | 0.82 | 0.72 | 0.63 | 0.58 | 0.53 | 0.82 | 0.72 | 0.62 | 0.53 |
| **Test 1 (kV)** | 48.6 | 50.9 | 44.5 | 47.3 | 56.7 | 98.1 | 94.9 | 87.2 | 76.7 | 83.2 | 171.1 | 145.7 | 124.5 | 113.7 |
| **Test 2 (kV)** | 50.3 | 49.6 | 49.2 | 51.4 | 55.6 | 98.2 | 95.3 | 88.0 | 80.1 | 86.5 | 146.3 | 149.9 | 126.7 | 114.0 |
| **Test 3 (kV)** | 49.0 | 50.0 | 50.7 | 49.3 | 55.2 | 97.0 | 93.8 | 86.2 | 76.4 | 86.2 | 150.3 | 147.9 | 132.2 | 117.8 |
| **Test 4 (kV)** | 49.7 | 48.3 | 43.7 | 48.0 | 55.3 | 96.7 | 93.5 | 88.1 | 76.6 | 88.4 | - | 147.2 | 134.6 | 120.3 |
| **Test 5 (kV)** | 50.9 | 50.0 | 49.2 | 46.1 | 55.2 | 108.2 | 95.4 | 84.9 | 80.2 | 85.0 | - | 150.1 | 131.2 | 113.2 |
| **Ave. Breakdown Voltage(kV)** | 49.7 | 49.8 | 47.5 | 48.4 | 55.6 | 99.6 | 94.6 | 86.9 | 78.0 | 85.9 | 155.9 | 148.2 | 129.8 | 115.8 |

# Appendix B

# SAUPEC 2015 Discussion Paper

This appendix contains a discussion paper handed in to the South African Universities Power Engineering Conference in 2015.

# A CRITICAL ANALYSIS OF THE CURRENT HIGH VOLTAGE ALTITUDE CORRECTION METHODS

**T. Gora and Dr. C. Nyamupangedengu***

* *Faculty of Engineering and the Built Environment, Private Bag 3, Wits 2050, South Africa E-mail: tatenda.gora@students.wits.ac.za cuthbert.nyamupangedengu@wits.ac.za*

**Abstract:** Altitude correction factors are a critical component in the design of high voltage systems at high altitudes. Unfortunately, the common standards currently used for altitude correction are mostly valid for altitudes of 1 800 m and have been proven to be unreliable for altitudes higher than this. This paper critically analyses and discusses the discrepancies in three popular standards used for altitude correction. The research work on altitude correction being done at Wits University is highlighted in the context of the worldwide efforts in this knowledge area.

**Key words:** Altitude, DC, Correction Factor

## 1. INTRODUCTION

The desire to meet electricity demands, especially in emerging economies, has led power utilities to embark on projects that involve the transmission of power from sources that are far away from the load centres. The number of High Voltage Direct Current (HVDC) schemes around Europe and Asia and the lengths of the transmission lines show the extent at which HVDC is being used to connect the load centres to remote generation sources [1]. In China, the Xiangjiaba-Shanghai HVDC link connects the load centre from the generation source which is approximately 4 000 km away. The Xiangjiaba-Shanghai link passes through the Tibet region which is quite mountainous, resulting in the line passing through altitudes above 4 000 m. Research is still being done on insulator performance at such high altitudes [2]. In Africa, Eskom is considering possibilities of importing power from the Congo. This project will involve the transmission of power over distances of approximately 4 000 km. For this project to be economically viable, the power will have to be transmitted using high voltage direct current (HVDC) technology. However, the available standards for altitude correction have discrepancies that can hinder the design of a reliable system at high altitudes.

This paper highlights the evolution of the altitude correction factors being applied and discusses the discrepancies in the common standards used in the world. A brief discussion on current work being done to solve the problem of unreliable altitude correction factors is also given.

## 2. BACKGROUND

As altitude increases, air density decreases and air breakdown mechanisms change. The IEC 60060-1 (2010) standard has been found to cover only a limited altitude range [3, 4, 5]. Some models that can possibly extend the altitude correction factors to cover a higher altitude range have been suggested in literature but are not yet incorporated into the standards. Further verification of the proposed models is required, especially for DC voltages.

*EVOLUTION HISTORY OF THE ALTITUDE CORRECTION FACTORS*

### *2.1* ***Peek Model***

The effect of altitude on the breakdown voltage of insulators was noted as early as 1914 by Peek [6], and a lot of work has been done since then with regard to air density effects on the breakdown voltage of air gaps and external insulation, and more recently air gaps under DC voltage stress [3, 4, 7, 8, 9, 10, 11, 12]. Peek [6] investigated the effect of altitude on the spark-over voltages of bushings, leads and insulators by placing them in a cask and varying the pressure. Pressure was varied to obtain relative air densities between 0.5 and 1.0 while the temperature variations due to the pressure changes were recorded. In his research, Peek [6] was able to produce tables of correction factors to be used on specific insulators by reading off the relative air density. Therefore, the correction factors for insulators were different from those of bushings and leads under the same relative air density [6]. Peek attributed these to the uniformity of the field suggesting that the flashover voltage for a uniform field decreases directly with $\delta$, whereas for non-uniform fields, the flashover voltage decreases at a lesser rate than $\delta$ [6]. This means that given that the flashover voltage of an insulator at sea level ($\delta$=1) is $v_1$, then the breakdown voltage $v$ at $\delta$=$x$ was given by

$$v = xv_1 \tag{1}$$

where $\delta$ is the relative air density at a specific altitude and read from the tables derived by Peek [6]. This therefore implied that the breakdown voltage was directly proportional to the air density. Peek also concluded that the effects of the change in $\delta$ due to pressure changes and constant temperature were the same as the change in $\delta$ due to temperature changes and constant pressure [6].

### 2.2 *IEC 60-1*

In 1973, the IEC 60-1 was amended. In the 1973 version of IEC 60-1, it was stated that the breakdown voltage of an air gap or insulator at relative air density δ, $u_\delta$ is related to the breakdown voltage of the same air gap or insulator under standard conditions, $u_0$ by [13]

$$u_\delta = k_d u_0 \tag{2}$$

where $k_d$ is the air density correction factor defined as

$$k_d = (\frac{P}{P_0})^m (\frac{T_0}{T})^n \tag{3}$$

where $P$ and $P_0$ are the pressure and standard pressure respectively while $T$ and $T_0$ are the temperature and standard temperature respectively. The exponents $m$ and $n$ are the variations of pressure and temperature respectively that are supposed to be determined before $k_d$ is evaluated. Since the air density is dependent on pressure, the determination of the exponent $m$ became the area of concern regarding atmospheric corrections and was defined in IEC 60-1 (1973) as

$$m = -0.12d + 1.12 \tag{4}$$

where $d$ is the air gap length between 1 m and 6 m. For d≤1 m, $m$=1.0 and $m$=0.4 for d≥6 m. The factor $m$ in this standard was therefore independent of the type of voltage used and the relative air density being corrected for. This therefore implied that the variation of pressure was only dependent on the length of the air gap. Compared to the model proposed by Peek, the model in the IEC 60-1 does not give a linear relationship between the flashover voltage and the relative air density. For DC and impulse voltages of either polarity, the standard specifies that $m$ and $n$ can be considered equal.

### 2.3 *Pigini Model(IEC 60060-1)*

During his research, Geldenhuys [14], was able to derive the approximate expression of the average electric field required for positive streamer propagation as given in equation (5).

$$E_s^+ = 425\delta^{1.5} + (4 + 5\delta)H \tag{5}$$

where $H$ is the humidity and δ is the relative air density. By varying the humidity, the average electric field required for streamer propagation under standard conditions was determined to be 500 kV/m. The breakthrough achieved by Geldenhuys [14] gave way for the determination of the breakdown voltage, by taking reference of the final jump that leads to breakdown, of an air gap in terms of the electric field of the leader zone of the discharge ($E_l$), the length of the leader ($l_l$), the electric field of the streamer zone ($E_s$) and the length of the streamer ($l_s$) to be given by equation (6) [15].

$$U = E_l l_l + E_s l_s \tag{6}$$

If breakdown occurs purely due to the streamer mechanisms (without any leader formation), the leader terms $E$ and $l$ are set to zero leaving the breakdown voltage to be dependent on only the streamer field $E_s$ and streamer length $l_s$. With this information, Pigini et al [15] were able to derive a factor $G$ to be used to determine the index of the relative air density correction factor by incorporating the discharge mechanism used and the relative air density. To correct the voltage, a similar expression to equation (2) was used but modified as follows,

$$U_{50} = U_{50(std)}(\delta.K)^n \tag{7}$$

where $K$ is the humidity correction factor, $n$ is the air density correction factor and $U_{50}$ is the breakdown voltage under non-standard conditions. The factor G was determined on the assumption that the major process during the breakdown of the gap was streamers [15]. G was defined as

$$G = \frac{U_{50}}{500\delta kd} \tag{8}$$

where $d$ is the length of the discharge gap and $k$ is a factor dependent on the type of voltage used and δ is defined as:

$$\delta = \frac{P}{P_0}\frac{273 + t_0}{273 + t} \tag{9}$$

To determine $n$ in equation (7), the G factor, equation (8), was used and $n$ took the following values [15] depending on the range of values of G

$$n = \frac{G_0(G_0 - 0.2)}{0.8} \tag{10}$$

$$n = \frac{3 - G_0}{2G_0} \tag{11}$$

where $G_0$ is the G factor under standard conditions (δ and $k$=1). Equation (10) was valid for 0.3≤G≤1 and equation (11) was valid for 1≤G≤2. These results by [15] were incorporated into the IEC 60060-1 (1989), including the graphs of equation (10) and equation (11) as the air density correction factors [16]. The results still play a major role in the recent IEC 60060-1(2010) which, instead of using graphs for determining G as in IEC 60060-1(1989), uses equations that are quite similar to equations (10) and (11) [17]. It is important to note that the model derived by Pigini et al takes into account the voltage type through the factor $k$ in equation (8) whereas IEC 60-1 (1973) did not include any factor that took into account the type of voltage used. Since the standard was produced from the work conducted by Pigini et al, the standard is limited to an altitude of 1 800 m. Given that the only difference in the altitude correction procedures highlighted in the current version of IEC 60060-1 (2010) with those of IEC 60060-1 (1989) is the use of equations to determine the index $n$ instead of graphs, it therefore holds that the current version of IEC 60060-1 is also limited to an altitude of 1 800 m.

### 2.4 *Ramirez Model*

A year after IEC 60060-1 (1989) was published, Ramirez and his counterparts [18] proposed a model claimed to be more accurate than the one incorporated in IEC 60060-1(1989) and takes account of the influence of air density on rod-plane gaps. The model is expressed in equation (12)

$$\frac{U}{U_0} = \frac{0.8[1+T(1-\delta)](\delta - 0.2G_0')}{(1-0.2G_0')} + 0.2 \tag{12}$$

where $\delta$ is the relative air density calculated by equation (9) and

$$T = 1.4\frac{1-0.8G_0'}{1-0.2G_0'} \tag{13}$$

with $G_0$ defined as

$$G_0' = \frac{U_0}{500[\frac{1+(F_0-1)}{3}D]} \tag{14}$$

where $F_0$ is the gap factor. This proposed model satisfies corrections for altitude up to 3000 m [18].

### 2.5 *Calva Model*

Calva et al [9] proposed a model to use for altitude correction for gaps under DC voltage stress. This model determines the breakdown voltage $V_b$ as

$$V_b = E_{so}d[k_1 + k_2]S \tag{15}$$

where $k_1$ is the air density correction factor

$$k_1 = \delta^m \tag{16}$$

and $m$=1.4 for positive polarity and 0.44 for negative polarity. $k_2$ is the humidity correction factor

$$k_2 = 1.3\delta^{-0.83}\frac{h-11}{100} \tag{17}$$

and S is the gap factor. $E_{so}$ is the electric field required for streamer propagation and considered to be 500 kV/m for positive polarity and for negative polarity is given by equation (18)

$$E_{so} = 1476.4 \times 1121.91d \tag{18}$$

The models presented by Ramirez et al [18] and Calva et al [9] were not considered as inputs to the latest version of the IEC 60060-1(2010) and it would therefore be of interest to compare these models. It is now generally agreed that there are shortfalls in IEC 60060-1 with regard to altitude correction factors. In that regard, a Cigre work group (WG D1.50) "Atmospheric and altitude correction factors for air gaps and clean insulators" has been established to coordinate further studies and investigation on altitude correction. It has also been proven by [3] that the IEC 60060-1 is still inconsistent in its calculated results compared to the experimental results obtained as altitude increases for air gaps under DC voltage stress and that the model proposed by Calva et al yields more accurate results than the IEC 60060-1(2010).

It has been observed that when the models by Ramirez, Pigini and Calva were derived, there were inconsistencies in the type of voltage used. It is suspected that the inconsistency in the voltage type used to derive the models could be among the causes of the variations in the models. The variation in the types of voltages used for the models is as follows:

- IEC 60060-1(2010) has input from empirical results conducted with switching impulses [14, 19] and lightning impulses [14, 19, 15]
- The model presented by Ramirez was derived under impulse voltage conditions [18]
- The model by Cavlva et al is purely under DC voltage conditions [4, 9]

Therefore work to determine the validity of these models using the same voltage type is required.

## 3. IRREGULARITIES IN THE COMMONLY USED STANDARDS

There is a fair number of standards used internationally that involve atmospheric correction voltages. The three notable standards used are the IEC 60060-1(2010) [17], IEC 60071-2 (1996) [20] and IEEE Std 4 (2013) on high voltage testing techniques [21]. However, these standards have notable irregularities regarding atmospheric correction that can bring to question which correction method is reliable. The atmospheric correction discrepancies in the three above mentioned standards are highlighted in this section.

### *3.1 IEC 60060-1 (2010)*

This is the standard derived from the work done by Pigini et at [15] and is the most commonly used standard. This standard defines two methods of atmospheric correction namely:

1. The standard procedure- This procedure is used to correct voltages from non-standard conditions to standard conditions using the relationship

$$U_0 = \frac{U}{K_t} \tag{19}$$

where $U_0$ is the disruptive-discharge voltage under standard conditions, $U$ is the measured disruptive-discharge voltage under non-standard conditions and $K_t$ is the atmospheric correction factor [17].

2. The converse procedure- This is an iterative method used to correct voltages from standard conditions to non-standard conditions using the relationship stated in equation (19) with $U$ as the subject of the formula.

The determination of $K_t$ in [17] involves the calculation of the g-factor to determine the exponents $m$ and $w$. The function that relates $m$ to the g-factor is derived from a curve that averages the results obtained during the work done by [15] of different gap geometries and positive polarities of different impulse shapes [22]. This gives rise to the possibility of over-correction or under-correction the voltage [22]. With regards to negative polarity impulses, the value $m$=1 was assumed by [15] and incorporated into the standard. This implies that the value of $m$ for negative impulses is independent of the air density. Since the variation of air density has an effect on the breakdown voltage, the assumption of a constant value of $m$ is an approximation that cannot be considered accurate.
The relationship between $m$, $w$ and $g$ in [17] is only valid when $\delta$ x k $\approx$ 1 [5]. This condition is valid for high voltage laboratories located at altitudes near sea level. Laboratories at much higher altitudes have the relationship $\delta$ x k $<$ 1 [5] implying that the application of the correction method in [17] becomes invalid for results obtained in such laboratories.
For one to be able to use the g-factor, the $U_{50}$ of the apparatus/gap is assumed to be known. However, for high voltage apparatus, the type test withstand voltage is the one known and cannot be assumed to be the $U_{50}$ of the apparatus [5]. This implies that the g-factor calculated using the type test withstand voltage is invalid. Also, as earlier mentioned, the g-factor incorporates the average electric field strength required for streamer propagation (500 kV/mm), therefore implying that it is more accurate for streamer dominated discharges. Otherwise, the expression given for the g-factor cannot be taken as an accurate approximation.
These irregularities make the IEC 60060-1 standard quite unreliable for correction of voltages at altitudes greater than the maximum altitude at which the tests were conducted (1 800 m) and for discharges that are not streamer dominated.

### *3.2 IEC 60071-2 (1996)*

This standard was based on the same data used to develop IEC 60060-1. This therefore makes the standard to be valid only up to 1 800 m, but is assumed to be applicable for higher altitudes. The relationship between the required withstand voltage ($U_{rw}$) and the co-ordination withstand voltage ($U_{cw}$) is given by equation (20)

$$U_{rw} = U_{cw} \times K_a \tag{20}$$

where $K_a$ is the atmospheric correction factor given by equation (21)

$$K_a = e^{m(\frac{H}{8150})} \tag{21}$$

where H is the altitude in m. In this standard, the value of $m$ is defined as 1 for lightning impulses and short duration AC voltage tests. For switching impulses, the value of $m$ is taken from a plot of curves that relate $m$ to ($U_{cw}$). However,($U_{cw}$) is defined as the 10% probability breakdown voltage therefore, when designing insulation for a lower breakdown voltage probability, the value of ($U_{cw}$) cannot be used [5]. The curves relating $m$ and ($U_{cw}$) in the standard are for phase-to-earth insulation, longitudinal insulation, phase-to-phase insulation and rod-plane gap. These cannot fully describe the dielectric strength and and discharge characteristics of different gap configurations, rod-to-rod for instance. Also, a value for $m$ to be used for AC voltages is recommended but no recommendation is given for DC voltage.
Even though this standard is assumed to be able to correct for altitudes greater than 1 800 m, there are irregularities in the determination of $m$ and no recommendation for DC voltages is given.

### *3.3 IEEE Std 4*

This standard has two methods for atmospheric correction [21].

1. Method 1- This method uses the factor $K$ and is the same as the one used in IEC 60060-1
2. Method 2- This method uses the factors $k_d$ (air density correction factor) and $k_h$ (humidity correction factor) for correction and is applicable to gaps less than 1 m.

Since Method 1 is similar to the one mentioned in IEC 60060-1, it will not be discussed again in this section. Method 2 stated that the following relationship,

$$U = \frac{k_d}{k_h} U_0 \tag{22}$$

where $U_0$ and $U$ have the same definition as mentioned in Section 3.1.
The values of $m$ and $n$ used for evaluating $k_d$ are assumed to be the same for all electrode configurations for DC voltages and lightning impulse voltages despite the air density that the configuration is set. For other electrode configurations and voltage types, the values of $m$, $n$ and $w$ are determined from a graph that relates the three variables to the gap length [21]. The values of $m$, $n$ and $w$ will also be the same for the same gap length, configuration. This does not agree with the variation of the air density correction factor with the type of discharge that governs breakdown in the air gap.

## 4. ONGOING WORK TO RESOLVE THE DISCREPANCIES IN CURRENT ALTITUDE CORRECTION METHODS

Due to the discrepancies in altitude corrections methods, a Cigre work group (WG D1.50) “Atmospheric and altitude correction factors for air gaps and clean insulators ”has been established to develop appropriate correction factors that can be used. This group involves members from Australia, Brazil, China, Germany, Italy, Japan, South Africa, Sweden and the USA. Among the work being done by this group, they are looking at deriving a method that uses a single value of $m$ over the $g$ curve for various electrode arrangements. Work is also being done in South

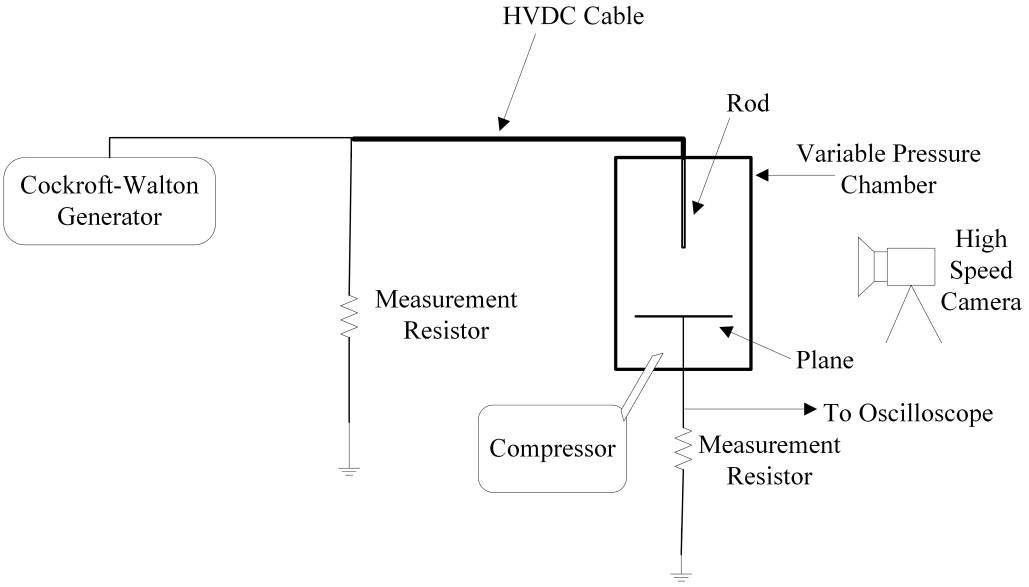


Figure 1: Conceptual set up of experiment

Africa, in collaboration with the Chinese to produce data to be used by the Cigre group.
At Wits University, there is ongoing work to simulate altitude conditions by varying the air pressure in a chamber and doing rod-plane breakdown tests under DC voltages. This project looks to add information, especially for DC voltages, to compliment other efforts being done to develop much more accurate correction factors. Currently, the variable pressure chamber to house the set up is is under construction. The gap sizes will be limited to approximately 0.8 m due to voltages supply limitations. A conceptual diagram of the experimental set up is shown in Figure 1. The results of the experiment will also be used to validate the models mentioned in the background section for DC voltage stress as they were mostly developed from data for lightning and switching impulse tests. The major steps to be conducted during the experiment are highlighted below:

- The first experiment will be conducted under standard pressure. Once the breakdown voltages of the different gap lengths up to 1 m are recorded, a graph will be plotted of breakdown voltage versus gap length.
- The breakdown voltages recorded in the first experiment will then be corrected to different altitudes up to 4 500 m using the IEC 60060-1 (2010), the Ramirez model and the Calva model. The breakdown voltages at the different altitudes will be plotted against the gap lengths.
- Experiments will be conducted again at the pressure levels that correspond to the air densities of the altitudes used to correct the voltages as mentioned in the previous bullet point.
- The breakdown voltages are then plotted versus gap length and then compared to the ones obtained from the three models to be verified.
- Using statistical methods, the model that corrects the voltages to the closest experimental value obtained will be justified.
- Using the recordings of the breakdown processes during the experiment, the model that yields the best results will also be analysed and justified.

A major challenge on how to bring in 300 kV HVDC into the metallic walled pressure chamber is being faced. The bushings required for DC voltages around 300 kV are very large, exceeding lengths of 2 m, and may cause structural problems on the chamber. Besides the structural problem, acquiring an already made bushing can also be very expensive and very difficult as the bushings are hard to find. To counter this problem, an HVDC cable can be used. Alternatively, a bushing fit enough to use only for the experiments can be constructed in the high voltage laboratory. This option is currently under rigorous investigation.

## 5. CONCLUSION

The use of HVDC transmission technology in developing countries is on the rise. This has seen transmission lines being set up in areas reaching altitudes of 4 500 m. However, it has been established that the altitude correction factors have discrepancies when applied to altitudes higher than 1 800 m. Further discrepancies in the current altitude correction methods have been laid out and further work is required to determine the appropriate correction factors. A Cigre working group has been set up to work towards resolving this issue and a lot of input

is still required. Some research efforts at Wits University aim at contributing to the knowledge in that regard.

## 6. ACKNOWLEDGEMENTS

The authors would like to acknowledge with gratitude Eskom for their support of the High Voltage Engineering Research Group through TESP. They would also like to express gratitude to the Department of Trade and Industry (DTI) for THRIP funding and to thank the National Research Foundation (NRF) for direct funding.

## REFERENCES

[1] *HVDC Power Transmission Part 1: Basic Principles, Planning and Converter Technology*, vol. 9 of *Eskom Power Series*. Crown Publications, 2012.

[2] D. Yujian, L. Weiming, S. Zhiyi, L. Qingfeng, G. U. Chen, and S. Zhaoying. "Switching Impulse Voltage Flashover Characteristics of Air Gaps in ±800 kV UHV DC Transmission Tower and Altitude Correction." *Cigre A3-104*, 2012.

[3] N. Parus, I. R. Jandrell, N. Mahatho, T. Govender, and H. A. Roets. "Live work under HVDC voltage: An investigation into altitude effects of flashover voltage for rod-plane air gaps." submitted for publication.

[4] P. A. Calva and F. P. Espino. "Correction Factors for Positive DC Voltages." *IEEE Transactions on Dielectrics and Electrical Insulation*, vol. 5, no. 4, pp. 541–544, August 1998.

[5] J. Rickmann et al. "Analysis and comparison of atmospheric and altitude correction methods for air gaps and clean insulators." *18$^{th}$ International Symposium on High Voltage Engineering*, , no. OC2-03, pp. 542–547, August 2013.

[6] F. W. Peek(Jr). "Effect of altitude on the spark-over voltages of bushings, leads and insulators." *AIEE transactions*, vol. 33, pp. 1721–1730, December 1914.

[7] T. Udo and Y. Watanabe. "DC High-voltage Sparkover Characteristics of Gaps and Insulator Strings." *IEEE Transactions on Power Apparatus and Systems*, vol. pas-87, no. 1, pp. 266–270, January 1968.

[8] N. L. Allen, M. Boutlendj, and H. A. Lightfoot. "Dielectric Breakdown In Nonuniform Field Air Gaps: Ranges of Applicability to dc Voltage Measurement." *IEEE Transaction on Electrical Insulation*, vol. 28, no. 2, pp. 183–191, April 1993.

[9] P. A. Calva, V. del Moral, M. G. M*á*rquez, and G. P. Cabrera. "New Proposal of Correction Factors for DC Voltages." *Conference on Electrical Insulation and Dielectric Phenomena*, pp. 455–458, 2003.

[10] N. L. Allen. "Correction procedures for High voltage measurements under variable air density." *IEE Proceedings on Science, Measurement and Technology*, vol. 153, no. 5, pp. 194–200, September 2006.

[11] M. Moreno, A. Pigini, and F. Rizk. "Influence of air density on the dielectric strength of external insulation." *Guidelines for the evaluation of dielectric strength for external insulation*, 1993. CIGR*É* Working Group 33.07.

[12] A. Robledo-Martinez and P. A. Calva. "DC Breakdown Characteristics of Rod-Rod and Rod-Plane Gaps in Reduced-Density Air." In *Sixth International Symposium on High Voltage Engineering*, vol. 3. New Orleans, USA, 1989.

[13] M. Boutlendj and N. L. Allen. "Assessment of Air-Density Correction for Practical Electrode Systems." *European Transactions on Electrical Power*, vol. 6, no. 4, pp. 267–274, July/August 1996.

[14] H. J. Geldenhuys. "The breakdown voltage of air in a 50 cm rod-plane gap over a practical range of air density and humidity." *5$^{th}$ International Symposium on High Voltage Engineering*, 1987.

[15] A. Pigini et al. "Influence of air density on the impulse strength of external insulation." *IEEE Transactions on Power Apparatus and Systems*, vol. PAS-104, no. 10, pp. 2888–2900, October 1985.

[16] SANS 60060-1. "High-voltage test techniques. Part 1: General definitions and test requirements.", 1989.

[17] SANS 60060-1. "High-voltage test techniques. Part 1: General definitions and test requirements.", 2011.

[18] M. Ramirez, M. Moreno, A. Pigini, G. Rizzi, and E. Garbagnati. "Air density influence on the strength of external insulation under positive impulses: Experimental investigation up to an altitude of 3000m a.s.l." *IEEE Transactions on Power Delivery*, vol. 5, no. 2, pp. 730–737, April 1990.

[19] K. Feser and J. Schmid. "Temperature effect on the streamer breakdown of air." *6$^{th}$ International Symposium on High Voltage Engineering*, vol. 3, August/September 1989.

[20] IEC 60071-2. "Insulation co-ordination- Part 2: Application Guide.", 1996.

[21] IEEE Std 4-2013. "IEEE Standard for High-Voltage Testing Techniques.", 2013.

[22] I. Gutman et al. "Atmospheric and altitude correction of air gaps, clean and polluted insulators: state-of-the-art within CIGR*É* and IEC." *CIGR*É, , no. D1-213, August 2014.

# Appendix C

# ISH 2015 Publication

This appendix contains a publication handed in to the $19^{th}$ International Symposium on High Voltage Engineering in 2015.

# Investigating the Effects of Altitude (Air Density) on the HVDC Breakdown Voltage of Rod-Plane Air Gaps

T. Gora* and C. Nyamupangedengu and I.R. Jandrell
University of the Witwatersrand, 1 Jan Smuts Ave, Braamfontein, Johannesburg, South Africa
*Email: <tatenda.gora@students.wits.ac.za>

**Abstract:** This paper is on a study of altitude correction factors on short air gap DC breakdown voltage. Tests were conducted on small rod-plane air gaps in a pressure vessel. The air gaps used varied between 100 mm and 300 mm in length and pressure was drawn in the pressure vessel to give relative air densities as low as 0.53. The pressure was drawn from an ambient pressure of about 835 mbar. The range of pressures used made it possible to simulate relative air densities corresponding to altitudes of 1700 m to 4500 m. The results obtained showed a decrease in breakdown voltage as pressure decreased, but only up to a threshold point beyond which an increase in breakdown voltage at very low pressures was observed. The results were corrected using IEC 60060-1 and were also compared to predicted breakdown voltages proposed by Calva et al. The corrected results according to the IEC 60060-1 standard did not resemble the trend of a decrease in breakdown voltage as relative air density decreases. When compared to the predicted breakdown voltages according to the method by Calva et al, the experimentally obtained results did relate to the predicted breakdown voltages. Even though the predicted flashover voltages were higher, the trend in the breakdown voltage agreed with the ones obtained using Calva et al but only until the pressure threshold was reached. A potential exists for the method proposed by Calva to be improved for small air gaps.

## 1 INTRODUCTION

The desire to meet electricity demands, especially in emerging economies, has led power utilities to embark on projects that involve the transmission of power from sources that are far away from the load centres. The number of High Voltage Direct Current (HVDC) schemes around Europe and Asia and the lengths of the transmission lines show the extent at which HVDC is being used to connect the load centres to remote generation sources [1]. In China, the Xiangjiaba-Shanghai HVDC link connects the load centre from the generation source which is approximately 4 000 km away. The Xiangjiaba-Shanghai link passes through the Tibet region which is quite mountainous, resulting in the line passing through altitudes above 4 000 m. Research is still being done on insulator performance at such high altitudes [2]. In Africa, Eskom is considering possibilities of importing power from the Congo. This project will involve the transmission of power over distances of approximately 4 000 km. For this project to be economically viable, the power will have to be transmitted using high voltage direct current (HVDC) technology. It has, however, been generally agreed that the available standards for altitude correction have discrepancies that can hinder the design of a reliable system at high altitudes.

It is generally agreed that there is need to develop altitude correction methods applicable to altitudes beyond 1800 m. In that regard, there is a Cigré working group (D1.50) that is currently working towards the development of such a standard. At the University of the Witwatersrand, Johannesburg, ongoing work is being done to contribute towards reviewing the altitude correction methods. This paper presents some of the results obtained so far.
Before presenting the results, this paper starts with a review of the evolution of the altitude correction methods.

## 2 EVOLUTION OF ALTITUDE CORRECTION METHODS: A CRITICAL REVIEW

This section discusses proposed models of altitude correction factors.

### 2.1 Peek Model

Peek [3] investigated the effect of altitude on the sparkover voltages of bushings, leads and insulators by placing them in a cask and varying the pressure. Pressure was varied to obtain relative air densities between 0.5 and 1.0 while the temperature variations due to the pressure changes were recorded. In his research, Peek [3] was able to produce tables of correction factors to be used on specific insulators by reading off the relative air density. Therefore, the correction factors for insulators were different from those of bushings and leads under the same relative air density [3]. Peek attributed these to the uniformity of the field suggesting that the flashover voltage for a uniform field decreases directly with $\delta$, whereas for non-uniform fields, the flashover voltage decreases at a lesser rate than $\delta$ [3]. This means that given that the flashover voltage of an insulator at sea level ($\delta$=1) is $v_1$, then the breakdown voltage $v$ at

$\delta$=$x$ was given by

$$v = xv_1 \tag{1}$$

where $\delta$ is the relative air density at a specific altitude and read from the tables derived by Peek [3]. This therefore implied that the breakdown voltage was directly proportional to the air density.

### 2.2 IEC 60-1

In 1973, the IEC 60-1 was amended. In the 1973 version of IEC 60-1, it was stated that the breakdown voltage of an air gap or insulator at relative air density $\delta$, $u_\delta$ is related to the breakdown voltage of the same air gap or insulator under standard conditions, $u_0$ by [4]

$$u_\delta = k_d u_0 \tag{2}$$

where $k_d$ is the air density correction factor defined as

$$k_d = (\frac{P}{P_0})^m (\frac{T_0}{T})^n \tag{3}$$

where $P$ and $P_0$ are the pressure and standard pressure respectively while $T$ and $T_0$ are the temperature and standard temperature respectively. The exponents $m$ and $n$ are the variations of pressure and temperature respectively that are supposed to be determined before $k_d$ is evaluated. Since the air density is dependent on pressure, the determination of the exponent $m$ became the area of concern regarding atmospheric corrections and was defined in IEC 60-1 (1973) as

$$m = -0.12d + 1.12 \tag{4}$$

where $d$ is the air gap length between 1 m and 6 m. For d$\leq$1 m, $m$=1.0 and $m$=0.4 for d$\geq$6 m. The factor $m$ in this standard was therefore independent of the type of voltage used and the relative air density being corrected for. This therefore implied that the variation of pressure was only dependent on the length of the air gap. Compared to the model proposed by Peek, the model in the IEC 60-1 does not give a linear relationship between the flashover voltage and the relative air density. For DC and impulse voltages of either polarity, the standard specifies that $m$ and $n$ can be considered equal.

### 2.3 IEC 60060-1(Pigini Model)

The IEC 60060-1 (1989) standard stated that

$$U_{50} = U_{50(std)}(\delta.K)^n \tag{5}$$

where $K$ is the humidity correction factor, $n$ is the air density correction factor and $U_{50}$ is the breakdown voltage under non-standard conditions. A new factor, G, was introduced into this correction. G was determined on the assumption that the major process during the breakdown of the gap was streamers [5]. G was defined as

$$G = \frac{U_{50}}{500\delta kd} \tag{6}$$

where $d$ is the length of the discharge gap and $k$ is a factor dependent on the type of voltage used and $\delta$ is defined as:

$$\delta = \frac{P}{P_0}\frac{273 + t_0}{273 + t} \tag{7}$$

To determine $n$ in equation (5), the G factor, equation (6), was used and $n$ took the following values [5] depending on the range of values of G

$$n = \frac{G_0(G_0 - 0.2)}{0.8} \tag{8}$$

$$n = \frac{3 - G_0}{2G_0} \tag{9}$$

where $G_0$ is the G factor under standard conditions ($\delta$ and $k$=1). Equation (8) was valid for 0.3$\leq$G$\leq$1 and equation (9) was valid for 1$\leq$G$\leq$2. These results by [5] were incorporated into the IEC 60060-1 (1989), including the graphs of equation (8) and equation (9) as the air density correction factors [6]. The results still play a major role in the recent IEC 60060-1(2010) which, instead of using graphs for determining G as in IEC 60060-1(1989), uses equations that are quite similar to equations (8) and (9) [7]. It is important to note that the model derived by Pigini et al takes into account the voltage type through the factor $k$ in equation (6) whereas IEC 60-1 (1973) did not include any factor that took into account the type of voltage used. Since the standard was produced from the work conducted by Pigini et al, the standard is limited to an altitude of 1 800 m. Given that the only difference in the altitude correction procedures highlighted in the current version of IEC 60060-1 (2010) with those of IEC 60060-1 (1989) is the use of equations to determine the index $n$ instead of graphs, it therefore holds that the current version of IEC 60060-1 is also limited to an altitude of 1 800 m.

### 2.4 Ramirez Model

A year after IEC 60060-1 (1989) was published, Ramirez and his counterparts [8] proposed a model claimed to be more accurate than the one incorporated in IEC 60060-1(1989) and takes account of the influence of air density on rod-plane gaps. The model is expressed in equation (10)

$$\frac{U}{U_0} = \frac{0.8[1 + T(1 - \delta)](\delta - 0.2G_0')}{(1 - 0.2G_0')} + 0.2 \tag{10}$$

where $\delta$ is the relative air density calculated by equation (7) and

$$T = 1.4\frac{1 - 0.8G_0'}{1 - 0.2G_0'} \tag{11}$$

with $G_0$ defined as

$$G_0' = \frac{U_0}{500[\frac{1+(F_0-1)}{3}D]} \tag{12}$$

where $F_0$ is the gap factor. This proposed model satisfies corrections for altitude up to 3000 m [8].

### 2.5 Calva Model

Calva et al [9] proposed a method whereby one could predict the breakdown voltage of an air gap under DC stress at any relative air density. This model determines the breakdown voltage $V_b$ as

$$V_b = E_{so} d[k_1 + k_2]S \tag{13}$$

where $k_1$ is the air density correction factor

$$k_1 = \delta^m \tag{14}$$

and $m$=1.4 for positive polarity and 0.44 for negative polarity. $k_2$ is the humidity correction factor

$$k_2 = 1.3\delta^{-0.83}\frac{h-11}{100} \tag{15}$$

and S is the gap factor. $E_{so}$ is the electric field required for streamer propagation and considered to be 500 kV/m for positive polarity and for negative polarity is given by equation (16)

$$E_{so} = 1476.4 \times 1121.91d \tag{16}$$

It is apparent that the limitations of the current altitude correction methods for altitudes beyond 1800 m need to be addressed. This paper presents results for tests performed under DC voltage stress for simulated altitudes between 1700 m and 4500 m.

## 3 EXPERIMENTAL SET UP

The single line diagram of the set up of the experiment is shown in Figure 1 while Figure 2 shows a picture of experimental set up used in the laboratory. The set up consisted of a 400 kV rated Walton-Cockroft generator, a 2 MΩ current limiting resistor and the electrode set up in a test cell.

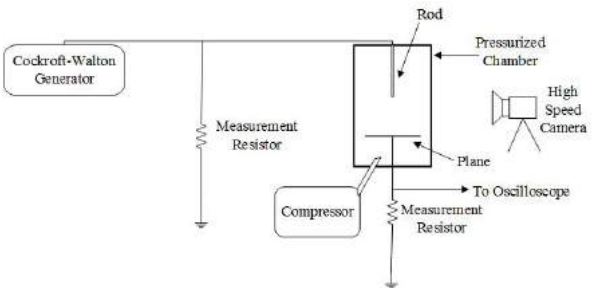


**Figure 1:** Single line diagram of experimental set up

The Walton-Cockroft generator used is equipped with an inbuilt voltage divider connected to an LED to display the voltage reading. All voltage measurements were obtained using the same voltage divider.

An aluminium electrode 700 mm long with a 15 mm diameter flat tip was connected to the resistor

**Figure 2:** Picture of experimental set up

and used as the rod electrode. The rod protruded into a 550 mm chamber with a borate glass wall with an inner diameter of 120 mm as shown in Figure 3. To adjust the distance between the rod tip and the grounded plane set at the bottom of the chamber, an adapter was machined which allowed the user to undo the rod, set the appropriate length and then hold the rod in place.

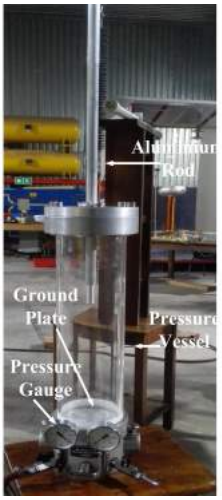


**Figure 3:** Picture of chamber and electrode set up

The chamber was equipped with two valves used to either draw a vacuum or compress air by connecting either a pump or compressor. Both valves had a gauge to show how much pressure has been drawn from the ambient atmospheric pressure or compressed above the ambient atmospheric pressure. For either a vacuum to drawn or air to be compressed, nozzles from the valves were located at the base of the chamber that allowed air to flow either way. An Edwards™vacuum pump was used and the lowest pressure achieved was 300 mbar below ambient.

## 4 THE TEST PROCEDURE

The gap length was varied between 100 mm and 300 mm. Air gaps larger than 300 mm could not be tested due space limitations in the vessel. In order to adjust the air gap length to a required value, the rod was initially set in such a manner so that the rod tip would be in contact with the ground plate. A zero point was then marked on the rod. When the rod is pulled up, the distance between the zero mark and the cap surface of the vessel would be equivalent to the length between the rod tip and the ground plate.
Once the required gap length was set, tests were first done at the ambient atmospheric pressure. Voltage was increased at a rate of approximately 2 kV/s until there was breakdown in the air gap. Pressure was then reduced by 100 mbar and the voltage was raised again until breakdown occurred. The process would then be repeated for the specific gap length until the test pressure was 300 mbar below the ambient pressure. Each breakdown test was repeated five times per gap length per pressure level.
Before increasing the voltage, the high speed camera was manually triggered to start recording and monitor any visible activities that could occur before breakdown.

## 5 RESULTS AND DISCUSSION

The five breakdown voltages obtained for each pressure level and gap size were averaged. The results of the average breakdown voltages against relative air pressure for each gap size are shown in Figure 4.

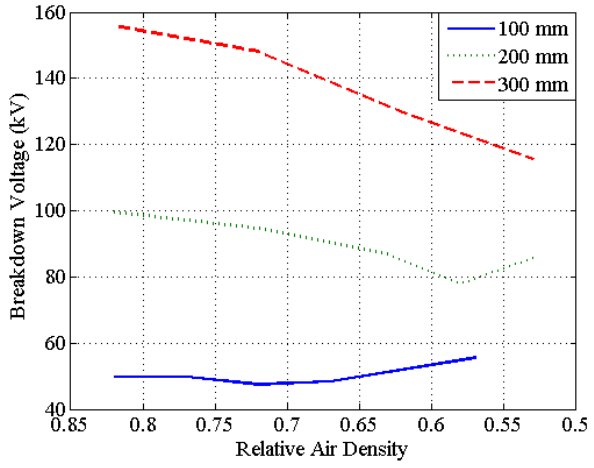


**Figure 4:** Plot of experimental DC flashover voltages

It was noted that the breakdown voltages of the air gaps decreased with a decrease in pressure (relative air density), but only to a knee point. After a threshold in pressure which seems to be related to the gap length, the breakdown voltage begins to increase with a further decrease in pressure. The pressure threshold becomes lower with an increase in gap length. It was also observed that as the pressure decreased, pre-breakdown corona became more prominent. For breakdown points beyond the knee point, the pre-breakdown corona was observed to periodically appear and disappear before the complete breakdown of the air gap.
It has already been established that the breakdown voltage of an air gap is dependent on the mean free path between the air molecules [10]. As the pressure decreases, the mean free path between the molecules increases allowing greater mobility for there to be ionisation with less energy required compared to when the mean free path is small. However, there is a point whereby the quantity of molecules present is so small, reducing the probability of ionization. This whole process is governed by Townsend's first ionization coefficient, $\alpha$, which is a function of the electric field (E) and the pressure (p) according to equation (17)

$$\alpha = Ape^{-\frac{Bp}{E}} \tag{17}$$

where A and B are constants dependent on the temperature and gas type [11]. This relationship states that at very low and very high pressures, Townsend's first ionization coefficient decreases therefore implying an increase in the breakdown voltages. It is believed that this may be the cause of the increase in the breakdown voltage as pressure continues to decrease.

When applied to altitude correction factors, the breakdown voltage trend observed may be of major concern. A factor may need to be applied to cater for the increase in voltage at very low relative air densities and small air gaps. The breakdown voltages obtained during the testing were corrected to standard conditions using IEC 60060-1 (2010) [7]. The method proposed by Calva [9] which can be used to predict the breakdown voltage of an air gap at any relative air density was also used and the results obtained were compared to the experimental results. Figure 5 to Figure 7 show the obtained results corrected using [7].

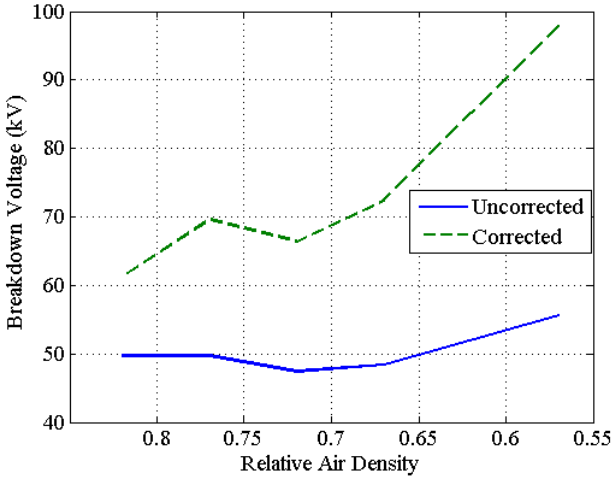


**Figure 5:** DC breakdown voltage vs relative air density for 100 mm air gap

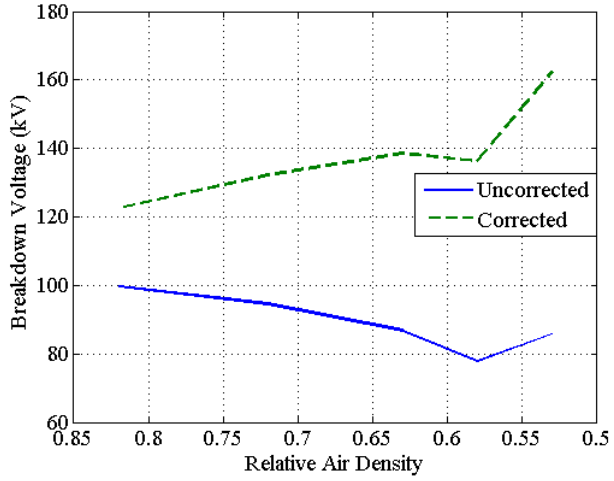


**Figure 6:** DC breakdown voltage vs relative air density for 200 mm air gap

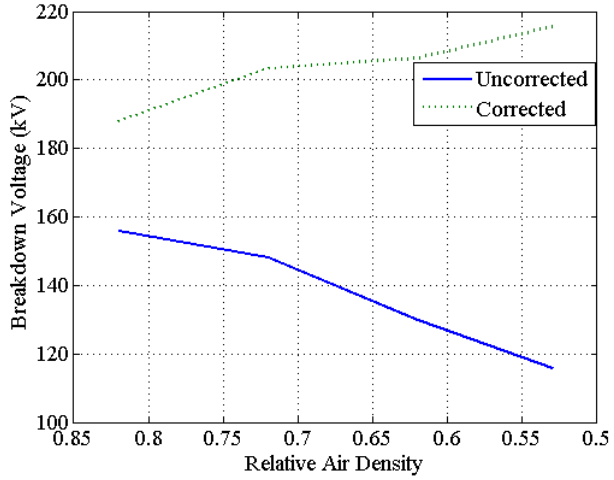


**Figure 7:** DC breakdown voltage vs relative air density for 300 mm air gap

Ideally, the correction factors applied to the experimental results were supposed to map the experimental plot to a straight horizontal line that corresponds to the actual breakdown voltage under standard conditions. However, the IEC 60060-1 correction method maps the results onto a diverging graph above the breakdown voltage under standard conditions. This confirms the limitations in the standard for results obtained for air densities less than 0.8. The same trend was observed for the 200 mm and 300 mm air gaps as shown in Figures 6 and 7. The failure of the IEC 60060-1 standard to correct at higher altitudes can be attributed to the fact that the IEC 60060-1 standard was derived empirically using data obtained at altitudes up to 1 800 m [5]. Therefore, the changes in breakdown mechanisms that occur at higher altitudes (thus lower relative air density) were not incorporated into the standards.

The method proposed by Calva [9] to determine the breakdown voltage at any relative air density was applied and the results were plotted on the same axis as the uncorrected data. The plots are shown in Figures 8 - 10.

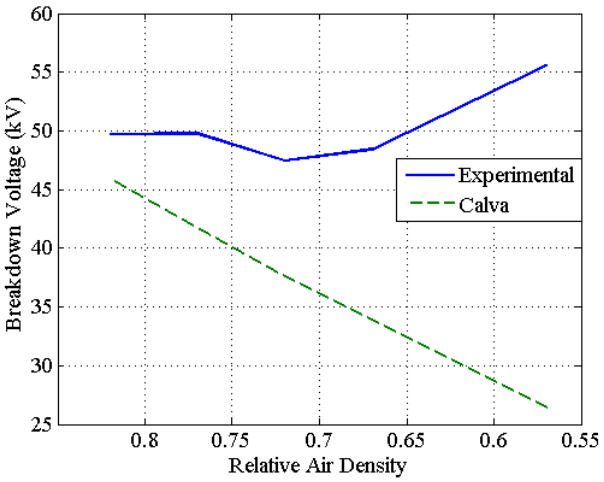


**Figure 8:** Comparison of results to method proposed by Calva for 100 mm air gap

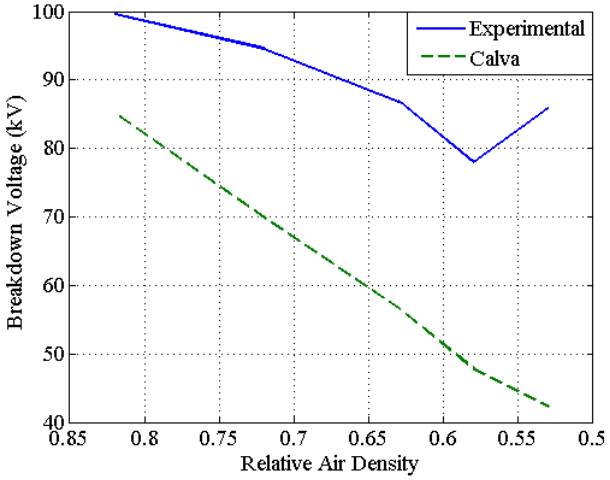


**Figure 9:** Comparison of results to method proposed by Calva for 200 mm air gap

The comparison of the experimentally obtained breakdown voltages to the predicted breakdown voltages according to the method by Calva only agree in trend that as relative air density decreases, the breakdown voltage for a specific gap length also decreases. The trend was observed to agree more as the gap length increases. This trend is only consistent up to the knee point where divergence begins. It was also observed that the method proposed by Calva predicted the voltage to be less than the experimental results. By assessing the way in which the trend agrees, there is a potential to improve Calva's method to predict the breakdown voltages for small air gaps at altitudes higher

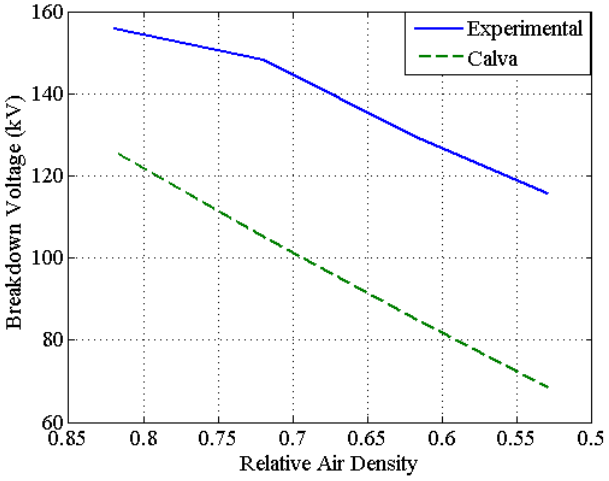


**Figure 10:** Comparison of results to method proposed by Calva for 300 mm air gap

than 1800 m by incorporating a factor that can allow the Calva method to precisely predict the breakdown voltage of a small air gap.

## 6 CONCLUSION

Laboratory experiments were conducted using a pressure vessel to simulate different relative air densities and DC breakdown tests were done in the simulated conditions. Rod-plane gaps of sizes between 100 mm and 300 mm were used. From the results, it is confirmed that the current IEC 60060-1 standard does not apply for altitudes above 1800 m. The method proposed by Calva, however, is more accurate in predicting breakdown voltages at high altitudes and as far as trend is concerned. The error in the trend becomes less with an increase in gap length.

## ACKNOWLEDGMENTS

The authors sincerely acknowledge the ISH 2009-SAIEE Postgraduate Research Scholarship in High Voltage Engineering for directly funding this research work. The authors would also like to acknowledge, with gratitude, Eskom for their support of the High Voltage Engineering Research Group through TESP. Authors would also like to express gratitude to the Department of Trade and Industry (DTI) for THRIP funding and to thank the National Research Foundation (NRF) for direct funding of the High Voltage Research Group of the University of the Witwatersrand, Johannesburg.

## REFERENCES

[1] *HVDC Power Transmission Part 1: Basic Principles, Planning and Converter Technology*, ser. Eskom Power Series. Crown Publications, 2012, vol. 9.

[2] D. Yujian, L. Weiming, S. Zhiyi, L. Qingfeng, G. U. Chen, and S. Zhaoying, "Switching impulse voltage flashover characteristics of air gaps in ±800 kv uhv dc transmission tower and altitude correction," *Cigre A3-104*, 2012.

[3] F. W. Peek(Jr), "Effect of altitude on the sparkover voltages of bushings, leads and insulators," *AIEE transactions*, vol. 33, pp. 1721–1730, December 1914.

[4] M. Boutlendj and N. L. Allen, "Assessment of air-density correction for practical electrode systems," *European Transactions on Electrical Power*, vol. 6, no. 4, pp. 267–274, July/August 1996.

[5] A. Pigini *et al.*, "Influence of air density on the impulse strength of external insulation," *IEEE Transactions on Power Apparatus and Systems*, vol. PAS-104, no. 10, pp. 2888–2900, October 1985.

[6] SANS 60060-1 , "High-voltage test techniques. part 1: General definitions and test requirements," SABS, Pretoria, South Africa, 1989.

[7] SANS 60060-1, "High-voltage test techniques. part 1: General definitions and test requirements," SABS, Pretoria, South Africa, 2011.

[8] M. Ramirez, M. Moreno, A. Pigini, G. Rizzi, and E. Garbagnati, "Air density influence on the strength of external insulation under positive impulses: Experimental investigation up to an altitude of 3000m a.s.l." *IEEE Transactions on Power Delivery*, vol. 5, no. 2, pp. 730–737, April 1990.

[9] P. A. Calva, V. del Moral, M. G. Márquez, and G. P. Cabrera, "New proposal of correction factors for dc voltages," *Conference on Electrical Insulation and Dielectric Phenomena*, pp. 455–458, 2003.

[10] E. Kuffel, W. S. Zaengl, and J. Kuffel, *High Voltage Engineering: Fundamentals*, 2nd ed. Oxford, Boston: Butterwoth-Heinemann, 2000.

[11] F. Kreuger, *Industrial High Voltage 1, 2, 3*. Delft, Netherlands: Delft University Press, 1991.

# Appendix D

# Cigré WG D1.50 Contribution

This appendix contains a contribution to the Cigré WG D1.50 Task Force on short air gaps.

# Contribution to Cigré D1:50 - short gap task group

*Prepared for Cigré D1-50 by Tatenda Gora and Cuthbert Nyamupangedengu; University of the Witwatersrand, Johannesburg, South Africa.*

## 1. Introduction

This report presents the results obtained in South Africa for short rod-plane gaps of lengths up to 0.4 m. The tests were to verify the effects of pressure (thus relative air density) on the breakdown voltage on short gaps. Two types of tests were conducted in this work:

- Open air tests - where simple rod-plane tests were conducted in laboratories situated at 1 700 m above sea level (asl) and 210 m asl for high and low altitude conditions respectively.
- Pressure vessel tests- where rod-plane tests were conducted in a vessel under reduced pressure so as to simulate different relative air densities.

Some of the results were published during the recently held ISH 2015 conference in Pilsen [1]. All the tests conducted in this work were for positive polarity HVDC.

## 2. Brief description of experimental set up and procedure

### 2.1 Open Air Laboratory Test

#### Experimental Set up

The open air laboratory tests were conducted at altitudes of 210 m and 1 700 m respectively. A diagram of the experimental set up is shown in Figure 1. A 15 mm copper rod with a fitted flat end cap was used as the rod electrode in the experiment. The same electrode was used for both high and low altitude experiments.

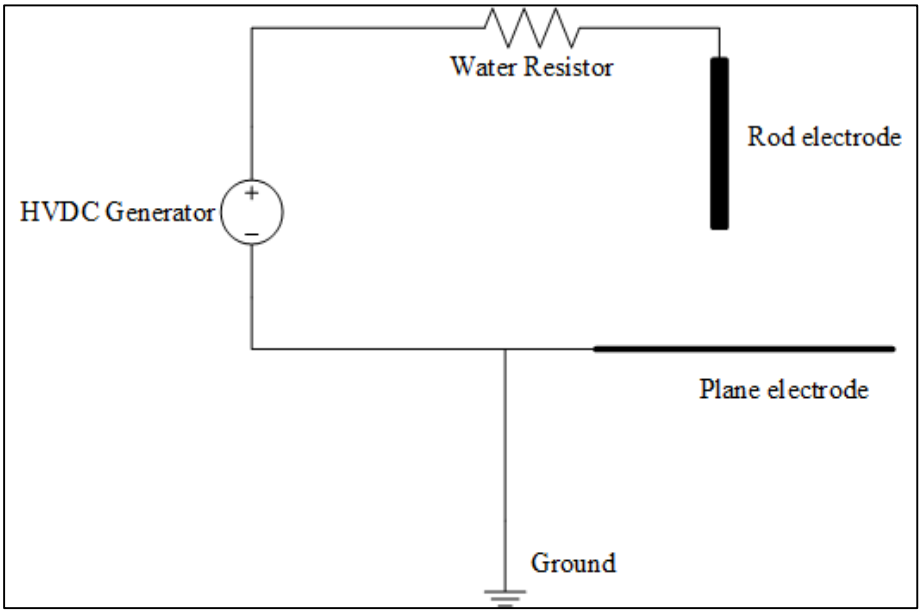


Figure 1: Diagram of open air experimental set up

Figure 2: Image of test set up at 1 700 m asl

### Experimental Procedure

The air gap length during the tests was adjusted in steps of 0.05 m from 0.10 m to 0.40 m. For every gap length, 5 breakdowns were conducted by slowly increasing the voltage. Between each breakdown, a 5 minute window was observed to allow any accumulated space charge to dissipate. The voltage divider of the HVDC generator was utilised for recording the breakdown voltages.

## 2.2 Pressure Vessel Tests

### Experimental Set Up

The pressure vessel tests were conducted in a 0.55 m cylindrical tube with a 0.12 m inner radius borate glass wall. The vessel could only vacuum pressure due to alterations made to the lid so that a rod could be fitted. An aluminium rod machined to the same tip dimensions as the copper rod used in the open air tests was used as the rod electrode. A diagram of the experimental setup is shown in Figure 3 accompanied by a picture of the laboratory setup in Figure 4.

### Experimental Procedure

Due to limitations of the pressure vessel, the maximum air gap size tested was 0.3 m. The air gap size was adjusted in 0.1 m intervals from 0.1 m to 0.3 m. The procedure was as follows:

- Set gap length and record ambient pressure, temperature and humidity
- At ambient pressure, conduct 5 breakdown experiments by and record results. Observe 10 window to allow space charge dissipation between each breakdown.
- By maintaining the gap length, draw 100 mbar pressure from the pressure vessel. Record temperature and humidity and repeat the step in the previous bullet. This was done until breakdown results at 300 mbar below ambient pressure were obtained.
- Increase gap length by 0.1 m and repeat bullets 1 to 3 until results for 0.3 m are obtained.

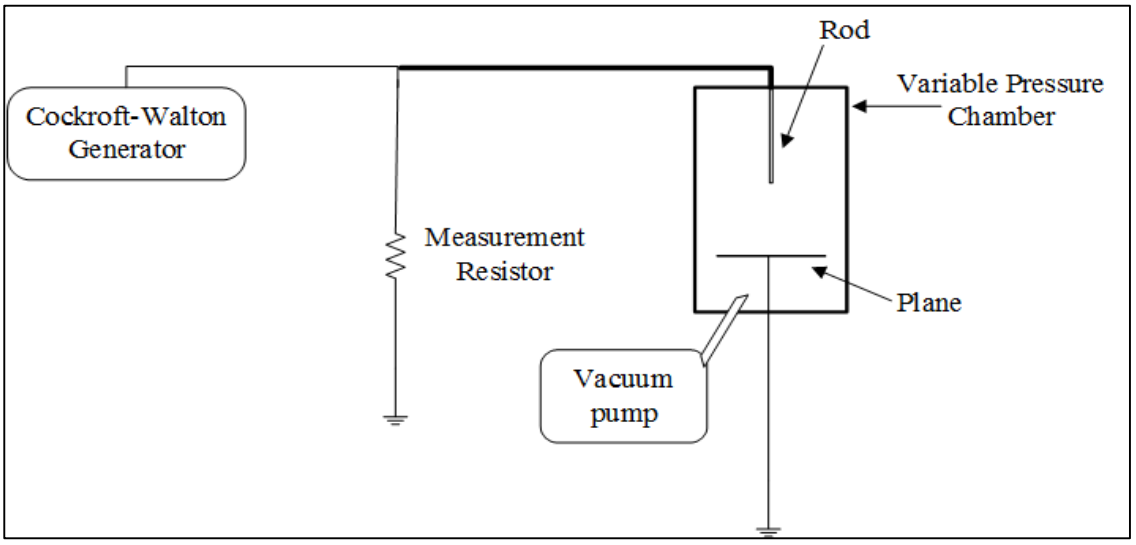


Figure 3 : Pressure vessel experimental set up

Figure 4: Pressure vessel laboratory set up

# 3. Results

## 3.1 Open air tests in laboratory

### Low altitude results (210 m asl)

Table 1 and Figure 5 show the results obtained at low altitude. There is a close relationship between the IEC corrected and uncorrected results as expected since the tests were done close sea level.

Table 1: Low altitude open air test results

| Gap Length (m) | Temperature ($^0$C) | Pressure (mbar) | Humidity (%) | Uncorrected breakdown voltage (kV) | IEC 60060-1 (2010) Corrected breakdown voltage (kV) | % Variance |
|---|---|---|---|---|---|---|
| 0.10 | 27.6 | 987.8 | 48.6 | 56.92 | 59.61 | 4.1 |
| 0.15 | 26.2 | 986.3 | 56.0 | 82.24 | 84.93 | 3.2 |
| 0.20 | 27.8 | 986.1 | 51.8 | 107.62 | 111.61 | 3.6 |
| 0.25 | 26.5 | 985.4 | 54.8 | 131.48 | 136.14 | 3.4 |
| 0.30 | 27.2 | 985.2 | 54.9 | 157.1 | 162.04 | 3.0 |
| 0.35 | 24.9 | 985.8 | 56.0 | 174.92 | 181.94 | 3.9 |
| 0.40 | 25.5 | 985.5 | 46.0 | 196.76 | 210.23 | 6.4 |

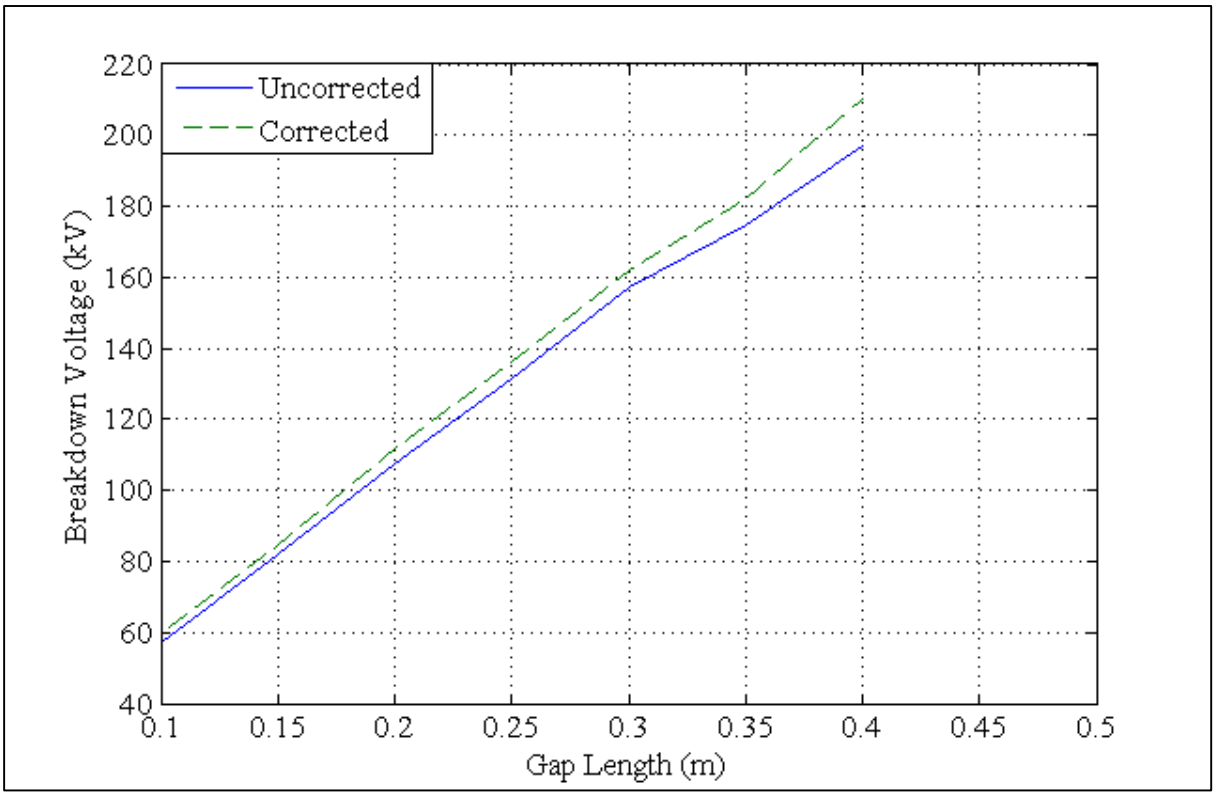


*Figure 5: Plot of IEC 60060-1(2010) corrected and uncorrected laboratory gap tests at 210 m asl*

### High altitude results (1 700 m asl)

Table 2 and Figure 6 show the results obtained for the open air tests at high altitude of 1 700 m asl. The variance between the corrected and uncorrected at high altitude is bigger than at low altitude implying that the correction factors are more accurate at lower altitudes than higher altitudes. Figure 6 also confirms the trend.

Table 2: High altitude open air test results

| Gap Length (m) | Temperature ($^0$C) | Pressure (mbar) | Humidity (%) | Uncorrected breakdown voltage (kV) | IEC 60060-1 (2010) Corrected breakdown voltage (kV) | % Variance |
|---|---|---|---|---|---|---|
| 0.10 | 15.3 | 844.7 | 41 | 52.50 | 64.43 | 18.5 |
| 0.15 | 14.4 | 841.7 | 45 | 67.75 | 82.77 | 18.1 |
| 0.20 | 15.4 | 840.2 | 34 | 81.18 | 102.81 | 21.0 |
| 0.25 | 14.9 | 841.1 | 42 | 100.15 | 122.89 | 18.5 |
| 0.30 | 15.1 | 842.3 | 46 | 118.2 | 140.33 | 15.8 |
| 0.35 | 15.8 | 839.7 | 33 | 129.92 | 163.04 | 20.3 |
| 0.40 | 14.8 | 842.3 | 47 | 156.8 | 187.09 | 16.2 |

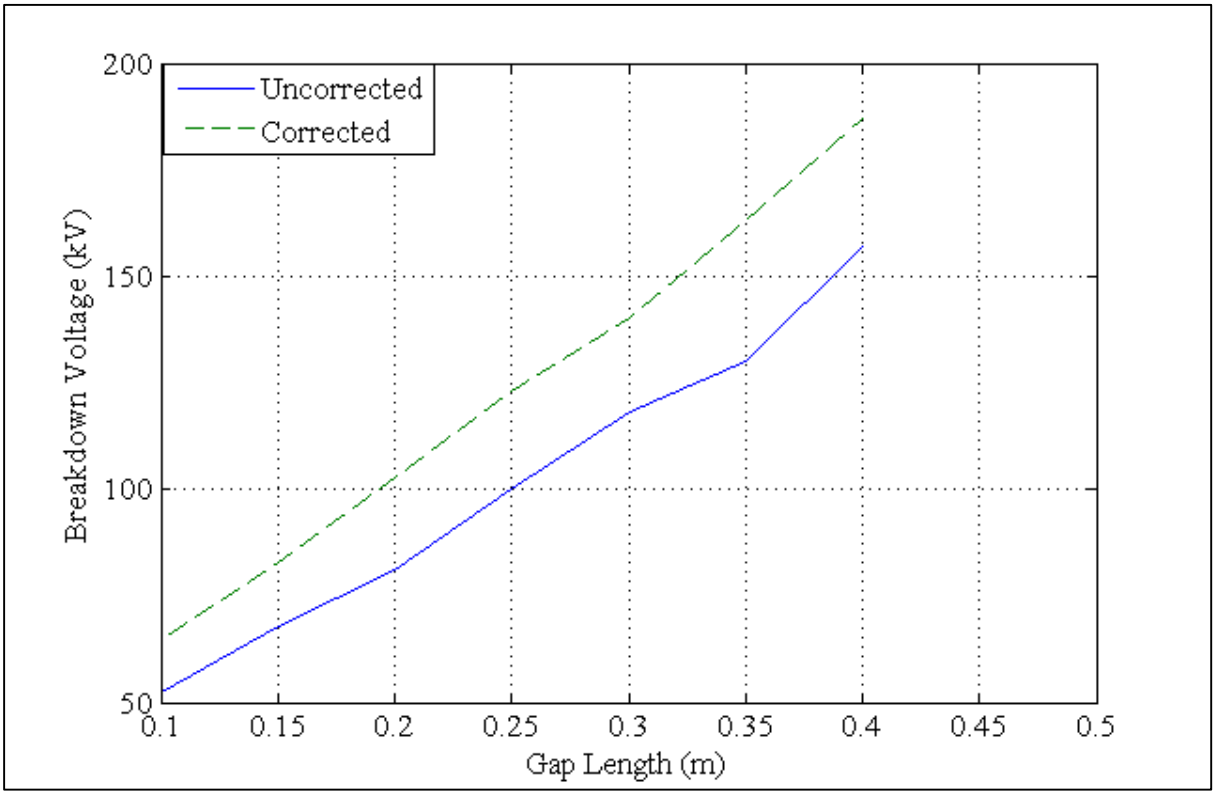


*Figure 6: Plot of IEC 60060-1(2010) corrected and uncorrected laboratory gap tests at 1700 m asl*

## Comparison of corrected low and high altitude air test results

Table 3: Comparison of High and low altitude corrected results

| Gap length (m) | High altitude corrected voltage (kV) | Low altitude corrected voltage (kV) | Percentage absolute error (%) |
|---|---|---|---|
| 0.10 | 64.43 | 59.61 | 8.09 |
| 0.15 | 82.77 | 84.93 | 2.54 |
| 0.20 | 102.81 | 111.61 | 7.88 |
| 0.25 | 122.89 | 136.14 | 9.73 |
| 0.30 | 140.33 | 162.04 | 13.40 |
| 0.35 | 163.04 | 181.94 | 10.39 |
| 0.40 | 187.09 | 210.23 | 11.01 |

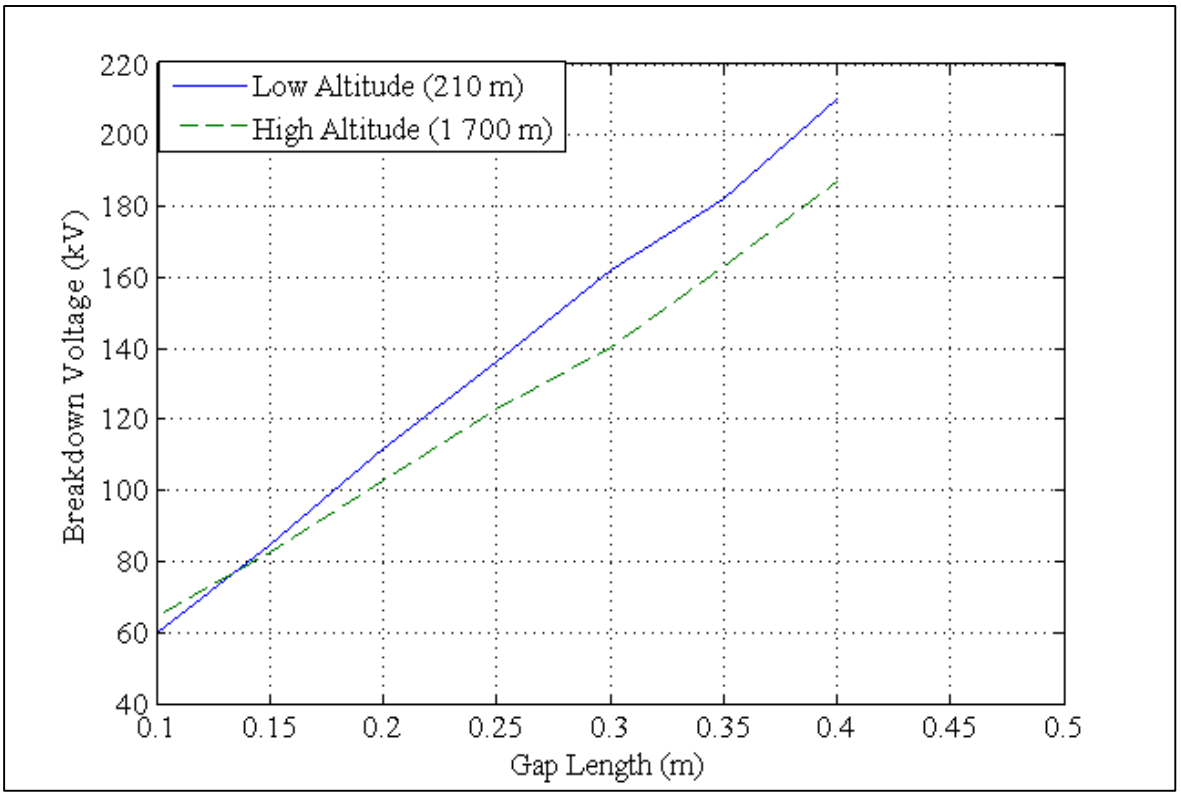


*Figure 7: Comparison of IEC 60060-1(2010) corrected results for high and low altitude*

Remarks:

- The two plots in Figure 7 are supposed to coincide, or within at least 5% error, due to the fact that they are being corrected to the same standard conditions. This is what the IEC 60060-1 (2010) correction procedure is supposed to achieve ideally.
- Trend in plot leads to speculation that the bigger the air gap, the larger the error to be observed
- There is a need for baseline results obtained at sea level (0 m asl) at standard temperature (20 $^0$C) to compare how the correction varies from the actual baseline.